

© 2015

Alessandro Venosa

ALL RIGHTS RESERVED

**Identification of Distinct Macrophage Subpopulations
During Nitrogen Mustard-Induced Lung Injury and Fibrosis:
Mechanisms of Recruitment and Activation**

By Alessandro Venosa

A dissertation submitted to the
Graduate School-New Brunswick
Rutgers, The State University of New Jersey
and
The Graduate School of Biomedical Sciences

In partial fulfillment of the requirements

For the degree of

Doctor of Philosophy

Joint Graduate Program in Toxicology

Written under the direction of

Professor Debra L Laskin

And approved by

New Brunswick, New Jersey

OCTOBER, 2015

ABSTRACT OF THE DISSERTATION

Identification of Distinct Macrophage Subpopulations
in Nitrogen Mustard-induced Lung Injury and Fibrosis:
Mechanisms of Recruitment and Activation

By ALESSANDRO VENOSA

Dissertation Director:

Professor Debra L. Laskin

Nitrogen mustard (NM) is an alkylating agent known to cause extensive pulmonary injury progressing to fibrosis. This is accompanied by a persistent infiltration of activated macrophages into the lungs which contribute to the development, progression and resolution of tissue damage. Macrophages are highly plastic cells capable of altering their activation state depending on the surrounding microenvironment. Two major phenotypically distinct subpopulations of macrophages have been identified: proinflammatory/cytotoxic M1 and antiinflammatory/wound repair M2 macrophages. Treatment of rats with NM (0.125 mg/kg) resulted in sequential infiltration of iNOS⁺ and CD11b⁺CD43⁺ M1 proinflammatory/cytotoxic macrophages into the lung 1-3 d after exposure, followed by accumulation of CD68⁺, CD163⁺, CD206⁺, YM-1⁺, ARG-1⁺ and CD11b⁺CD43⁻ M2 macrophages, which were most notable at 28 d. This correlated with acute injury and fibrogenesis. Expression of chemokine receptors involved in recruitment of M1 and M2 bone marrow (CCR2⁺ and CX₃CR1⁺, respectively) and splenic (ATR-1 α ⁺)

macrophages was also upregulated. Splenectomy resulted in increased numbers of CCR2⁺, iNOS⁺ and CD11b⁺CD43⁺ proinflammatory M1 macrophages in the lung 1-7 d post exposure. Conversely CD11b⁺CD43⁻ M2 antiinflammatory/wound repair macrophage accumulation and gene expression was blunted. These changes in macrophage in the lung correlated with heightened tissue injury and more rapid fibrosis. Early after NM exposure, miRNAs involved in regulating the inflammatory response (miR-125, miR-9) were upregulated in lung macrophages. With time, miRNAs involved in promoting proliferation and fibrosis (let7, miR-21, miR-29) were upregulated. Increased expression of HDAC, which regulate histone activity, as well as H3K9Ac and H3K4TM, were also upregulated early after NM exposure. HDAC inhibition using valproic acid resulted in reduced activation of M1proinflammatory/cytotoxic macrophages and increased activation of M2 antiinflammatory/wound repair macrophages, suggesting a pathway regulating macrophage activity in the lung after NM exposure. Identification of macrophage subpopulations participating in the inflammatory response and understanding the mechanisms regulating their activation and recruitment may lead to more targeted and effective treatment against vesicant-induced pulmonary injury.

DEDICATION

I dedicate this work to my family and friends.

Without your support I am not sure I would have got this far.

You are the people I look up to and the main reason I am here.

Thank you all for believing in me, even when I didn't.

ACKNOWLEDGEMENTS

I am pretty sure that if I begin acknowledging all the people care to me, this would require a whole chapter. This section is probably the toughest for me; I always had troubles expressing my appreciation and gratitude with the written word. Is needless to say that my parents, Milva and Salvatore, are the absolute winners of this special list. You have given me overwhelming support even when I decided to pack up and leave for graduate school, destination: the other side of the world; I know I will never be able to pay you back; you mean everything to me. And obviously my sister, Valentina; her admiration has always pushed me to do better and be better; my goal has always been to make her proud. I also want to thank my brand you brother-in-law, Andrea, for volunteering to be my sister's scape goat after I left.

The path to a PhD can only be achieved thanks to an outstanding supporting cast. For me it was the RATS. They have been there for me every time I needed it, preserving my sanity... and God knows how much a graduate student needs that. When I started I had no idea I would have bonded so much with you all. I will never be able to thank you enough for your friendship and support. I am especially grateful to the Massa Family. Chris and Kate have been much more than friends, they made me feel as part of their family. Of course I have not forgotten the two most beautiful girls in the world, my Goddaughters Anna and Emma Massa. They gave me new energies to face any adversity, I am so fortunate to be in their lives. Someday 20 years from now, whether they want it or not, I will sit down with them to tell the story of 'how I met their parents'..followed by detailed reading of my thesis.

Of course the acknowledgement section would not be complete without mentioning the component of my lab for their incommensurable help in a day by day basis. In particular, I want to thank Rama Malaviya and Angela Marie Groves. You have being the best of the best friends. You taught me everything I know; I am honored to be part of your lives.

Special recognition goes to my committee members, Drs. Jeffrey Laskin and Helmut Zarbl who have guided me to develop my project, as well as helped me growing as a scientist. I don't even know what words to use to thank Dr. Andrew Gow. In addition, to his mentorship he has been a friend to me. I know you are one of the biggest reasons for my scientific and personal maturation. Lastly, I would like to thank my advisor, Debra Laskin. You have done so much more than training me during graduate school, you believed in me from the very beginning and knew I was going to succeed. I will never forget it. Thank you for being a great advisor, a mentor, and a friend.

TABLE OF CONTENTS

ABSTRACT OF THE DISSERTATION	ii
DEDICATION	iv
ACKNOWLEDGEMENTS	v
TABLE OF CONTENTS	vii
ABBREVIATIONS	x
LIST OF FIGURES	xiii
LIST OF SUPPLEMENTAL FIGURES	xv
LIST OF TABLES	xvi
INTRODUCTION	
Respiratory Tract	1
Sulfur and Nitrogen Mustard	6
Lung Inflammation	8
Macrophage Ontogeny and Activation	9
Mechanisms Mediating Recruitment of Inflammatory Macrophages to Sites of Injury	14
Origin of Inflammatory Macrophages	15
Epigenetics and Control of Innate Immunity	17
AIMS OF THE DISSERTATION	24
MATERIALS AND METHODS	
Animals and Treatments	26
Bronchoalveolar Lavage and Total Inflammatory Cell Collection	26
Histology and Immunohistochemistry	27
Nuclear Extraction and Quantification	28
Western Blot Analysis	29
HDAC Activity Assay	29

mRNA and miRNA Isolation, Microarray and Real Time-PCR	30
Flow Cytometry and Cell Sorting	31
Statistics	32
PART I. CHARACTERIZATION OF DISTINCT MACROPHAGE SUBPOPULATIONS PARTICIPATING TO NITROGEN MUSTARD-INDUCED LUNG INJURY AND FIBROSIS	
	33
RESULTS	34
DISCUSSION	37
PART II. ROLE OF SPLEEN DERIVED MACROPHAGES IN NITROGEN MUSTARD INDUCED LUNG INFLAMMATION, INJURY AND FIBROSIS	
	43
RESULTS	44
DISCUSSION	47
PART III. ELUCIDATE EPIGENETIC MECHANISMS REGULATING LUNG MACROPHAGE ACTIVATION IN RESPONSE TO NITROGEN MUSTARD-INDUCED TOXICITY	
	53
PART IIIa. EFFECTS OF NITROGEN MUSTARD EXPOSURE ON EPIGENETIC MECHANISMS OF MACROPHAGE ACTIVATION	
RESULTS	54
DISCUSSION	56
PART IIIb. REGULATION OF NITROGEN MUSTARD-INDUCED LUNG MACROPHAGE ACTIVATION BY THE HISTONE DEACETYLASE INHIBITOR VALPROIC ACID	
RESULTS	61
DISCUSSION	63
OVERALL SUMMARY	68
CONCLUSIONS	71

FUTURE STUDIES	73
PART IV. ADDITIONAL STUDIES IN PROGRESS	
A. IN VITRO IMAGING OF NM-INDUCED LUNG INJURY	76
B. EFFECTS OF CCR2 INHIBITION ON NM-INDUCED LUNG INFLAMMATION AND INJURY	76
C. RNA SEQUENCING ANALYSIS	77
D. STUDIES ON FOAM CELL FORMATION IN THE LUNG AFTER NM EXPOSURE	78
FIGURES	79
SUPPLEMENTAL FIGURES	146
TABLES	166
REFERENCES	176

ABBREVIATIONS

5-HT	serotonin
ApoE	apolipoprotein E
ARG	arginase
ATR-1	angiotensin-2 receptor-1
BAL	bronchoalveolar lavage fluid
SM	sulfur mustard
CCL	chemokine ligand
CCR	chemokine receptor
CD	cluster of differentiation
CD11b	integrin alpha M
CD43	sialophorin/sialoadhesin
CD68	macrosialin
CD80	co-stimulatory factor/activation B7 1 antigen
CD86	co-stimulatory factor/activation B7 2 antigen
CD163	macrophage associated antigen/hemoglobin Scavenger Receptor
CD206	mannose receptor
CL	clodronate liposomes
COX-2	cyclooxygenase-2
CX ₃ CL1	fractalkine
CXCL4	platelet factor 4
CX ₃ CR1	chemokine (C-X ₃ -C motif) receptor
CYPb5	cytochrome b5
D (d)	days
DAMPS	danger-associated molecular patterns
DNMT	DNA methyltransferase

FA	fatty acid
GAPDH	glyceraldehyde 3-phosphate dehydrogenase
GdCl ₃	gadolinium chloride
GM-CSF	granulocyte-macrophage colony-stimulating factor
H	histone
HAT	histone acetyltransferase
HDAC	histone deacetylase
HMT	histone methyltransferase
IFN- γ	interferon-gamma
i.t.	intratracheal
IL-1 β	interleukin-1 beta
IL-4	interleukin-4
IL-6	interleukin-6
IL-10	interleukin-10
IL-12	interleukin-12
IL-13	interleukin-13
M-CSF	macrophage colony-stimulating factor
miRNA/miR	microRNA
MHC	major histocompatibility complex
MMP	matrix metalloproteinases
NADPH	nicotinamide adenine dinucleotide phosphate
NF- κ B	nuclear factor-kappa B
NM	nitrogen mustard
NOS	nitric oxide synthase
NRF-2	nuclear factor (erythroid-derived 2)-like 2
PAMPS	pathogen associated molecular patterns

PCNA	proliferating cell nuclear antigen
PCR	polymease chain reaction
PPAR- γ	peroxisome proliferator activated receptor-gamma
PTX	pentraxin
RNS	reactive nitrogen species
ROS	reactive oxygen species
SM	sulfur mustard
SPX	splenectomized
TGF- β	transforming growth factor-beta
TLR	toll-like receptor
TNF α	tumor necrosis factor-alpha
VPA	valproic acid
YM-1	chitinase-3-like-3
γ -H2A.X	phosphorylated histone H2A variant-X

FIGURES LIST

- Fig. 1. Nitrogen mustard structure and examples of side chain moieties.
- Fig. 2. Mechanism of nucleophilic attack of reactive mustards.
- Fig. 3. Effects of NM on CD11b and iNOS expression.
- Fig 4. Effects of NM on CD68, CD163 and CD206 expression.
- Fig 5. Effects of NM on ARG-II and YM-1 expression.
- Fig. 6. Effects of NM on lung macrophage expression of M1 and M2 genes.
- Fig. 7. Flow cytometric analysis of lung macrophages.
- Fig. 8. Effects of NM on proliferation of macrophage subpopulations.
- Fig. 9. Effects of NM on gene expression in macrophage subpopulations.
- Fig. 10. Effects of NM on macrophage chemokine/chemokine receptor expression.
- Fig. 11. Effects of NM on CCR2 and CX₃CR1 expression.
- Fig. 12. Effects of splenectomy on NM-induced CD11b and iNOS expression.
- Fig. 13. Effects of splenectomy on NM-induced expression of pro- and antiinflammatory genes.
- Fig. 14. Effects of splenectomy on NM-induced accumulation of CD68⁺ and CD163⁺ macrophages in the lung.
- Fig. 15. Effects of splenectomy on NM-induced accumulation of CD206⁺ and YM-1⁺ macrophages in the lung.
- Fig. 16. Effects of splenectomy on NM-induced expression of macrophage chemokine and chemokine receptor genes.
- Fig. 17. Effects of splenectomy on NM-induced expression of CCR2⁺, CX₃CR1⁺ and ATR-1⁺ macrophages in the lung.
- Fig. 18. Flow cytometric analysis of lung macrophages.
- Fig. 19. Effects of splenectomy on NM-induced lung pathology.
- Fig. 20. Effects of NM on expression of histone H2A.X phosphorylation.

- Fig. 21. Effects of NM on modified histone expression.
- Fig. 22. Effects of NM on H3K9Ac and H3K9TM expression.
- Fig. 23. Effects of NM on H3K36DM, H3K4MM and H3K4TM expression.
- Fig. 24. Effects of NM on p300, SIRT1 and HDAC2 expression.
- Fig. 25. Effects of NM on lung macrophage HDAC activity.
- Fig. 26. Effects of NM on miRNA expression.
- Fig. 27. Effects of valproic acid (VPA) on NM-induced HDAC2, p300 and H3K9Ac expression.
- Fig. 28. Effects of valproic acid (VPA) on NM-induced pro- and antiinflammatory expression.
- Fig. 29. Effects of valproic acid (VPA) on NM-induced macrophage gene expression.
- Fig. 30. Effects of valproic acid (VPA) on NM-induced CCR2, ATR-1 α and CX₃CR1 expression.
- Fig. 31. Flow cytometric analysis of lung macrophages.
- Fig. 32. Effects of valproic acid (VPA) on NM-induced oxidative stress, proliferation and DNA damage.
- Fig. 33. Effects of valproic acid (VPA) on NM-induced lung injury and inflammation.
- Fig. 34. Effects of valproic acid (VPA) on NM-induced lung pathology.

SUPPLEMENTAL FIGURES

Fig. 1S. MRI analysis of rats exposed to NM.

Fig.2S. Quantitation of NM-induced lung injury.

Fig. 3S. 3D tissue rendering of lung after exposure to PBS control (CTL) or NM.

Fig. 4S. Effects of CCR2 inhibition on NM-induced CCR2 expression.

Fig. 5S. Effects of CCR2 inhibition on lung injury and inflammation.

Fig. 6S. Effects of CCR2 inhibition on cellular infiltration.

Fig. 7S. Effects of CCR2 inhibition on NM-induced lung pathology.

Fig. 8S. Effects of NM oxidized-LDL uptake.

Fig. 9S. Effects of NM on macrophage lipid content.

Fig. 10S. Effects of NM on gene expression associated with lipid regulation.

TABLES

Table 1. Semi-quantitative IHC scoring

Table 2. Expression of CD43 and CD68 by lung macrophages

Table 3. Effects of splenectomy on NM-induced sorted macrophage gene expression.

Table 4. Effects of splenectomy on NM-induced lung injury and inflammation.

Table 5. Effects of splenectomy on NM-induced lung pathology

Table 6. Splenectomy semi-quantitative IHC scoring

Table 7. Effects of VPA on NM-induced lung pathology

Table 8. Valproic acid semi-quantitative IHC scoring

INTRODUCTION

Respiratory Tract

The respiratory tract includes the nose, mouth, throat and pharynx (upper); the respiratory airways, larynx, trachea, bronchi, bronchioles (middle) and the lung (lower). Structurally, the lung consists of a series of branching airways leading to the gas exchange unit, the acinus. This architectural feature is perhaps the most commonly used due to its grape-like structure. Although conceptually simple, the physiology of these structures remains quite abstracted to date due to absent or only rudimentary respiratory bronchioles in rodent models, which are hardly representative of the human anatomy. This ultimately resulted in species specific recognition of sac-like structures, identified as alveoli. Each alveolus is very closely associated with a capillary containing deoxygenated blood from the pulmonary artery. Rapid and passive exchange of oxygen between vasculature and airway is achieved via an interface between capillaries and airways. Whereas expiration is a response mediated by the natural elasticity of the lung, during inspiration, chest and diaphragmatic muscles contract in unison, creating negative pressure within the lungs resulting in influx of air through the upper and lower airways. The O_2/CO_2 interface and respiratory rate play important role in pH regulation through fine regulation of CO_2 concentration. Although this mechanism is effective for short term pH restoration, renal buffering is more effective for long term buffering.

Respiration renders the lung prone to exposure to particles mixed in the air, which accumulate in the respiratory tract based on their size (Donaldson *et al.*, 2010). While particle between 1 millimeter (mm) and 200 μm (micrometer) deposits in the bronchial tree (interception), impaction is characteristic of particles ranging from 10-200 μm (Fig. 1). Due to their size and trajectory, these particles impact or stick to a surface, hence accumulating in the nose and throat. Sedimentation is a process associated with

bronchiolar deposition of particles between 0.5-10 μm , while particles smaller than 0.5 μm move deep in the airways by "Brownian motion" and deposit in small airways and alveoli. Clearance of these particles is dependent on two major mechanisms: mucociliary escalator and macrophage phagocytosis. The former has been shown to represent the primary mechanism of clearance in the upper airways, and is a process requiring the production of mucus to capture cellular debris and larger particles which is then moved away from the airways. Airway mucus is a mixture of polypeptides, cellular debris and oligomeric mucin which lines the airways, trapping both bacteria and other airborne particles. This mixture is then brushed upwards by tiny hair-like structures called cilia, and ultimately removed by a combination of coughing and swallowing. In healthy individuals, rates of mucus secretion and clearance are balanced (Williams *et al.*, 2006). By contrast, macrophage phagocytosis, although effective in eliminating foreign bodies from the airways, is associated with development of an inflammatory response. These processes are dependent on the burden of the foreign body, leading to tissue damage when exceeding resident macrophage function. In addition to particles, pulmonary injury can be due to liquids, a process called aspiration, exposure to noxious gas and other oxidants. This in turn may lead to direct recognition and phagocytosis by the immune system, while also damaging the pulmonary epithelium and ultimately generate an inflammatory response (Colasurdo *et al.*, 1995; Janahi *et al.*, 2000).

To reproduce the human responses to toxicants and understand the mechanisms of injury pathogenesis and resolution, several rodent experimental models have been developed. This include gaseous inhalation (ozone), as well as oropharyngeal (bleomycin) and intratracheal (nitrogen mustard) techniques (Anderson *et al.*, 2009; Malaviya *et al.*, 2012; Groves *et al.*, 2012; Egger *et al.*, 2013). However, due to the anatomical differences between rodents and humans, some precautions have to be

taken. Rodents are restricted nose breathers and their nasal cavities exhibit unique structures, called turbinates, which are far more efficient in trapping chemicals and particles in the higher airways, reducing the similarities of these experimental models to the human exposures. To obviate to this issues, intratracheal and oropharyngeal exposures have been developed. These techniques can in fact delivery the toxicant of interest in a controlled manner while bypassing the turbinates. Small saline volumes are usually used to minimize physiological effects of fluid administration.

A range of techniques for visualization and quantification of pulmonary injury have been developed for analysis of humans and rodents. The most widely studied is bronchoalveolar fluid protein content analysis, an early marker of vasculature damage and leakage into the lung space (Bhalla *et al.*, 1999). With the advancement of technology, current clinical practice has been using cutting edge imaging techniques, namely magnetic resonance imaging and computed tomography, which are not invasive and allow for real time and precise analysis of injury development and extent. Recently, these techniques have been successfully scaled down for rodent analysis, allowing for improved quality of analysis of experimental models, as well as better comparison to human studies (Oakes *et al.*, 2013).

Anatomically each region of the lung is comprised of multiple specialized cell populations including alveolar epithelial type I cells, alveolar epithelial type II cells, goblet cells, fibroblasts, endothelial cells, and resident alveolar and interstitial macrophages. The majority of the respiratory surface area is covered by type I cells, which play an important role in gas exchange. Due to their wide alveolar occupancy, type I cells are especially sensitive to injury (Herzog *et al.*, 2008). Type II cells have a cuboidal morphology and are smaller than type I cells. Although they have slow mitotic rate (28-35 days), this is accelerated following injury, when they function as progenitor cells for

injured type I cells (Herzog *et al.*, 2008); they also release reactive nitrogen species (RNS), cytokines and growth factors, such as interleukin (IL)-1 β , IL-1 α , tumor necrosis factor (TNF)- α , and IL-6 (Herzog *et al.*, 2008; Punjabi *et al.*, 1994). Goblet cells are cells pivotal in production and storage of mucus. Their presence is mostly in the upper airways, where they play a role to supply mucus for the mucociliary elevator.

Interestingly, recent evidence showed that these cells play a role in tissue protection by proliferating and produce excess mucus in the lower airways, in turn reducing the shear stress during persistent inflammation (Rogers, 1994). Fibroblasts account for almost 30% of the cells in the normal lung and function predominantly as alveolar support and as extracellular matrix secretory units.

The immune systems plays pivotal role in patrolling the pulmonary parenchyma. There are several subsets of myeloid cells that have been characterized in this compartment, namely dendritic cells, resident alveolar macrophages, interstitial macrophages and pleural macrophages. Dendritic cells (DCs) can be recognize by their distinctive stellate morphology. These cells originate from bone marrow derived monocytes and have been shown to travel freely during both homeostatic and diseased state. Their exhibit dual function as they have been shown to act as professional antigen presenting cells durign immature stages, by expressing high levels of major histocompatibility complex type II (MHC-II) and the integrin CD11c. Once a pathogen is phagocytized, these cells go through a process of maturation that includes upregulation of costimulatory proteins such as CD80, CD83, CD86 and CD40, important in interaction and modulation of T cells (Colonna *et al.*, 2004). Alveolar macrophages show some redundancy in the cellular function, but have been shown to remain in the lung throughout their lifespan. These cells patrol the airways, providing immediate host defense by recognizing common microbial motifs through specific receptors (e.g., pattern recognition receptors [PRR] and Toll-like receptor [TLR]) and engulfing foreign

materials (Descamps *et al.*, 2012). They also have the ability to present antigen to lymphocytes, release pro- or anti-inflammatory cytokines and chemokines with properties that are essential for the regulation inflammatory responses, as well as recruit peripheral leukocytes (Mantovani *et al.*, 2004). This is important since turnover of alveolar macrophages is relatively slow; their half-life is 30-60 days, resulting in a long lived resident population (Maus *et al.*, 2006). An important feature of alveolar macrophages is their ability of clear the body of foreign pathogens, mainly via a respiratory burst. In this process, they release reactive oxygen and nitrogen species (ROS and RNS) which alter the oxidative burden and cellular signaling pathways. ROS and RNS are also effector molecules with microbicidal and cytotoxic properties. However, uncontrolled release of these reactive oxidants results in oxidative stress and contributes to tissue injury (Chow *et al.*, 2003). In addition to these two subsets, interstitial and pleural macrophages have been shown to play unique roles in lung homeostasis and injury, diversity that is exhibited at the morphological, phenotypic and biochemical level (Parent, 2015). In addition, interstitial and pleural macrophages are seen in very specific location in different organs. Whereas interstitial macrophages are small insize and often are not shown to exhibit great dfferences compared to alveolar macrophages. However during the inflammatory response this cells express high levels of the antiinflammatory chemokine receptor CX₃CR1 and the scavenger receptors CD163 and CD206, which are associated with an M2-like phenotype (Parent, 2015). In contrast, pleural macrophages appear to be less involved in the defense against pathogens but are still highly skilled to eprform antigen presentation (Basic *et al.*, 1979); Cailhier et al (2006) showed that these cells retain inflammatory functions as measured by TNF α and reactive species production. Furthermore, due to their location, they have been shown to funtion as aids the facilitate the movement of the parietal and visceral pleura by releasing surfactant like proteins (Lehnert *et al.*, 1992; Gjemarkaj *et al.*, 1999).

Sulfur and Nitrogen Mustard (NM)

Sulfur and nitrogen mustard are bifunctional alkylating agents developed in the 1830's and 1930's respectively. Structurally, these chemicals are closely related with only the central sulfur moiety with nitrogen. This resemblance ultimately results in analogous physical and chemical properties and reactivity. Sulfur and nitrogen mustard have both remarkable blistering capacities in mucous membranes, an observation that resulted in the stockpiling of these chemicals by Germany and America during World War II. Although there is no documented use of NM as a chemical weapon, sulfur mustard was used in the Iran-Iraq conflict and still represents a terroristic treat. Due to the ease of preparation and absence of an effective antidote/therapy several experimental models of exposure have been developed. In addition, due to the same reasons, only few centers have clearance to use sulfur mustard, while nitrogen mustard is more accessible. As a result, nitrogen mustard models have shown comparable damage to human intoxication for skin (Smith *et al.*, 1998), eye (Ghasemi *et al.*, 2008), digestive (Anilkumar *et al.*, 1992) and respiratory tract (Ghanei *et al.*, 2010), bone marrow (Smiley *et al.*, 1961). Although acute exposure to mustards is associated with extensive tissue damage, the chronic health effects are severe in nature (Ghanei and Harandi, 2007). In particular exposure of the respiratory tract has been associated with high morbidity and mortality (Weinberger *et al.*, 2011). Pulmonary exposure to NM or SM results in severe lung damage (Kehe and Szinicz, 2005). Human case studies have reported laryngeal and tracheobronchial mucosa destruction, pulmonary edema, and pulmonary emphysema, affecting alveoli and interstitium and progressing to fibrosis (Balali-Mood and Hefazi, 2006). In experimental rodent models, NM causes a similar progressive response characterized by a macrophage-rich inflammatory response and extensive tissue destruction, followed by a chronic resolution/wound phase which progresses to fibrosis (Malaviya *et al.*, 2010; Malaviya *et al.*, 2012). During the acute

phase, tissue damage includes perivascular and peribronchial edema, inflammatory leukocyte infiltration, luminal accumulation of cell debris, and extravasation of red blood cells. With time, thickening of alveolar septal walls, bronchial epithelial cell plying, metaplasia, as well as hyperplasia and hypertrophy of goblet cell are also observed (Malaviya *et al.*, 2012). Tissue destruction is also associated with bronchiolization of the alveolar epithelium, a metaplastic alteration observed in premalignant cancers, where alveolar cells transition into bronchiolar-like epithelium (Wang *et al.*, 2009). At the later stages of the exposure, lung emphysema and fibrin depositions are also prominent. **Due to their persistent accumulation during pathogenesis, progression and resolution of NM-induced pulmonary injury, it has been suggested that macrophages participate in each of these responses.** This is supported by findings that shortly after exposure of rodents to NM, macrophage expression of proinflammatory and cytotoxic proteins, such as TNF- α , cyclooxygenase-2 (COX-2) and inducible nitric oxide synthase (iNOS), as well as tissue remodeling factors like matrix metalloproteinase (MMP) are upregulated (Anderson *et al.*, 2009; Malaviya *et al.*, 2010; Malaviya *et al.*, 2012; Sunil *et al.*, 2011a; Sunil *et al.*, 2012). It has also been reported that respiratory function is impaired after vesicant exposure resulting in alterations comparable to emphysema (Sunil *et al.*, 2011b). Lung responsiveness to challenge with the bronchoconstrictor metacholine, also indicated reduced tissue resistance after NM, suggesting loss of airway tone (Sunil *et al.*, 2011b).

From the chemical stand point, mustards have been divided into HN1, HN2 and HN3 subgroups. Whereas the central nitrogen moiety and the di-ethylchloride side chains remain identical among the three types of mustards, the alkyl side chains is variable (R= methyl, chloro-ethyl, and phenylalanine) (Fig. 2, top panels). The ethylchloride represents the reactive and toxic moiety; when in water or any biological fluid, the chloride readily dissociates from the molecule leading to chemical

rearrangement that results in positively charged nitrogen and an alkyl cyclic moiety which is highly unstable and reactive. This reactive electrophilic aziridinium intermediate covalently binds to nucleophilic moieties via SN1 nucleophilic attack (Fig. 2, bottom panels) leading to functional inactivation of targets, cross-linking of biological residues and cytotoxicity. The damage is mediated by DNA strand breaks, alkylation of cellular components including proteins, membrane lipids and nucleotides, depletion of glutathione and production of ROS and RNS, respectively. Nucleotide alkylation often leads to cross-linking, a process by which two broken strands of the DNA are joined together impeding strand separation. This has been shown to result in distortions of the double helix of DNA and subsequent cytotoxicity, as this blocks DNA polymerases, inhibiting DNA replication and/or DNA transcription (Brulikova *et al.*, 2012). Mustards preferentially target the nitrogen in position 7 (N-7) of the guanine nucleoside (Kohn *et al.*, 1987), as well as nucleophilic amino acids in proteins such as cysteine, lysine and histidine inducing adducts that can blunt the catalytic activity of several proteins (Thompson and DeCaprio, 2013). Following NM-induced double strand breaks, cellular stress and dysfunction leads to inflammation, activation of the antioxidant response machinery and/or DNA repair pathways including homologous recombinational repair (HRR) and non-homologous end joining mechanism (NHEJ) (De Silva *et al.*, 2000), or cell death in case the damage cannot be repaired (Noll *et al.*, 2006)..

Lung Inflammation

Inflammation is the response of the immune system to injurious or infectious agents. The four cardinal signs of inflammation are swelling, redness, heat, and pain. These processes are regulated by inflammatory mediators released at the site of injury. One of the early steps in the inflammatory process is increased vascular permeability. This results in fluid and protein leakage into the damaged tissue, as well as leukocyte emigration to the affected area. The first cells accumulating at the site of inflammation

are polymorphonuclear neutrophils (PMN) due to their rapid mobility. Although PMN are capable of strong antimicrobial activity, their role in inflammation is limited by their short half-life (Geering and Simon, 2011). However, they are important in recruiting other immune cells to sites of inflammation, in particular long-lived macrophages which are important determinants of the outcome of inflammation (Zhang *et al.*, 2008a).

Inflammation can be considered as consisting of two main phases: an early pathogenic phase, which is associated with increased expression and release of proinflammatory/cytotoxic mediators, and a late resolution phase, which is characterized by the release of antiinflammatory/wound healing mediators after elimination of the insult/stimulus. Mechanisms that regulate the transition from the early to late phase appear to involve both epithelial cells and leukocytes, via the release antiinflammatory cytokines and proresolution lipids (Alessandri *et al.*, 2013; Buckley *et al.*, 2014; Maskrey *et al.*, 2011). Macrophages participate in both phases of inflammation, as they are known to modify their phenotype and release pro- or antiinflammatory mediators (Murray and Wynn, 2011) and eicosanoids in response to distinct environmental cues (Stout *et al.*, 2005; Stout and Suttles, 2004). However, whereas short term damage signals promptly re-establish homeostasis, chronic inflammatory responses are associated with dysregulated resolution, which can result in extensive parenchymal destruction.

Macrophage Ontogeny and Activation

For more than half a century we collected evidence that macrophages are mononuclear myeloid cells originating from bone marrow precursors (van Furth *et al.*, 1972). More recently, however, this notion has been updated based on developmental data showing macrophages subsets parting ways in the yolk sac during gestational hematopoiesis. In these early prenatal phases, bone marrow and tissue resident macrophages constitute the only white blood cell population, which matures into tissue

resident macrophages independently from blood monocyte infiltration (Samokhvalov, 2014). It has also been established that immune lineage hematopoietic stem cells (HSCs) emerge later during gestational life and they migrate to the fetal liver; conversely, bone marrow precursors represent the main site of hematopoiesis beginning after birth (Orkin and Zon, 2008). Phenotypically, bone marrow stem cells differ from yolk-sac-derived progenitors based on their responsiveness to the transcription factor MYB (Schulz *et al.*, 2012) and their expression of CX₃CR1 and F4/80; thus, in contrast to bone marrow derived macrophages, yolk-sac-derived macrophages lack MYB (Schulz *et al.*, 2012; Hashimoto *et al.*, 2013; Epelman *et al.*, 2014) and exhibit an antiinflammatory (CX₃CR1⁺) mature (F4/80⁺) phenotype. This observation led to a reconsideration of previous notions regarding renewal of macrophage pools, as well as their recruitment, phenotype and immune function. It now appears that in homeostatic conditions bone marrow derived monocytes minimally contribute to adult resident tissue macrophage pools and that embryonic-derived resident tissue macrophages remain in the tissue in large numbers post-natally (Guilliams *et al.*, 2013). In addition, although incompletely studied, embryonic macrophages appear to be equipped with the genetic repertoire to deal with pathogens that are only marginally different from the adult counterparts; this is consistent with evidence that infections during early development are rarely surmountable (Rae *et al.*, 2007). Functionally, embryonic macrophage populations have been shown to be capable of producing extracellular matrix during development, as well as regulating their phenotype and interactions with other cells (Guilliams *et al.*, 2013).

During both developmental and adult life, macrophages have been characterized as highly plastic cells developing specialized phenotypes and functions in response to signals they encounter in their microenvironment (Porcheray *et al.*, 2005; Stout, *et al.*, 2005). They have been broadly classified into two distinct functional subpopulations: classically activated pro-inflammatory M1 macrophages and

alternatively activated anti-inflammatory/wound repair M2 macrophages (Martinez and Gordon, 2014). M1 macrophages develop in response to stimulation by interferon gamma (IFN- γ) and either pathogen associated molecular patterns (PAMPS) such as lipopolysaccharide (LPS), the proinflammatory cytokine TNF α , or granulocyte macrophage colony stimulating factor (GM-CSF) (Mantovani *et al.*, 2004). These cells are highly phagocytic and have strong microbicidal capacity (Sindrilaru *et al.*, 2011). In addition, they generate cytotoxic effector molecules such as ROS and RNS, and pro-inflammatory cytokines including TNF α , IL-6, IL-12, and IL-1 (Martinez and Gordon, 2014). M2 macrophages are important in down regulating inflammation and inducing tissue repair and remodeling. These cells have been further categorized into M2a, M2b, and M2c subgroups (Mosser and Edwards, 2008). M2a cells promote fibrogenesis, tissue repair, and proliferation. They are also important antigen presenting cells and express mannose receptor and major histocompatibility complex II (MHCII) molecules. M2a macrophages respond to IL-4 and IL-13 which antagonize the actions of interferon (IFN)- γ . The M2b phenotype exerts immunoregulatory functions and promotes type II inflammatory responses. Phenotypically these cells exhibit a very unique signature, characterized by both pro- and antiinflammatory activity, releasing IL-10, as well as TNF α , IL-1 and IL-6, but not the prototypical M1 cytokine, IL-12. This mixed phenotype could be a result of the activating stimuli, which include immune complexes and toll-like receptor (TLR) triggering. M2c macrophages are induced by IL-10, transforming growth factor- β (TGF- β), and glucocorticoids. They inhibit the production of proinflammatory cytokines, down regulating inflammation and promoting tissue repair and regeneration (Gordon, 2003; Mantovani *et al.*, 2004). In addition to these established subsets, recent reports in models of atherosclerosis have identified other subsets of M2 macrophages based on their function. These include M2_{hem} macrophages, which exhibit increased heme scavenger receptor (CD163) expression and ability to accumulate iron; and M2_{ox}

macrophages, which display prominent antioxidant capacity (Chinetti-Gbaguidi *et al.*, 2015). CXCL4-induced M4 macrophages have also been identified, which exhibit low phagocytic capacity due to blunted expression of scavenger receptors, but high proinflammatory activity (Gleissner, 2012).

One of the most established functional differences between M1 and M2 macrophages is based on their metabolism of L-arginine. While in response to pathogens/foreign bodies, M1 macrophages utilize arginine to generate the cytotoxic mediator nitric oxide (NO) via iNOS with citrulline as byproduct, M2 macrophages metabolize arginine via arginase to produce urea and ornithine, a precursor for polyamines and proline. Arginase is important in restoration/wound repair as it regulates cell proliferation and collagen production. Since the production of NO and ornithine depends on the availability of arginine, these activities can be reciprocally regulated in macrophages by cytokines that influence macrophage phenotype. Thus, it has been shown that the M1 cytokines IFN- γ and TNF α induce iNOS and the synthesis of NO, whereas the M2 cytokines IL-4, IL-13 and IL-10 induce arginase (Mills and Ley, 2014; Munder, 2009; Wu and Morris, 1998). Although these findings support the existence of distinctively polarized macrophage subsets *in vitro* (Mantovani, Sica, Sozzani, Allavena, Vecchi and Locati, 2004), more recent evidence is conflicting in this regard in an *in vivo* setting, rather suggesting their existence as a continuum of polarized states (Mosser and Edwards, 2008), without distinctive phenotypic signatures (Hume and Freeman, 2014). This notion is supported by recent studies demonstrating a dichotomy in the metabolic activity of macrophage subsets (Galvan-Pena and O'Neill, 2014). Thus, proinflammatory M1 macrophages appear to favor aerobic glycolysis, characterized by increased glucose uptake and the conversion of pyruvate to lactate. As the main function of these cells is the production of reactive species, these cells have reduced mitochondrial activity; the pentose phosphate pathway (PPP), which is the main NADPH production pathway is als

reduced, resulting in greater ROS and RNS levels. In contrast, STAT6 is thought to mediate M2 macrophage shift from glucose utilization, in favor of fatty acids (FA) as main source of energy, via activation of the peroxisome proliferator-activated receptor(PPAR) γ -coactivator-1b (PGC-1b). This results in increased mitochondrial respiration, mitochondrial biogenesis, and transcription of FA β -oxidation (Shao *et al.*, 2010). M2 metabolism is also associated with reduced PPP utilization, as well as reduced conversion of pyruvate into lactic acid in favor of the Krebs cycle (Odegaard and Chawla, 2011). Findings that blocking oxidative metabolism in M2 macrophages results in an M2 to M1 shift, while promoting FA oxidation effectively shifts M1 macrophages to an antiinflammatory M2 phenotype provide support for the idea that macrophages can be classified according to metabolic differences (Rodríguez-Prados *et al.*, 2010; Vats *et al.*, 2006). Romero *et al.* (2015) recently showed that in response to bleomycin, radiation or silica exposure, lung macrophages take up large amounts of oxidized fatty acids, in particular phosphatidylcholine, leading to foam cell formation. In addition, clinical evidence and experimental models have shown that lipid-laden macrophages exhibit altered polarization towards an M2-like phenotype which favors fibrogenesis (van Tits *et al.*, 2006). Additionally, when discussing macrophage phenotypes there are at least two more subsets of macrophages that have been shown to significantly impact tissue response in chronic inflammation and cancer, namely myeloid derived suppressor cells (MDSCs) and tumor associated macrophages (TAMs) (Ostrand-Rosenberg and Sinha, 2009; Quatromoni and Eruslanov, 2012). MDSCs play important role in controlling the inflammatory response and lymphocyte activation. This functions as a mechanism to limit excessive activation of the immune system after injury. Evidence in autoimmune disease models supports this notion, as MDSCs have been shown to be decreased in numbers in patients with autoimmune conditions; this in turn results in excessive lymphocyte activation and tissue destruction (Cripps and Gorham,

2011). Similarly, TAMs have been shown to be strongly associated with cancer. These cells exhibit elongated morphology that resembles macrophages M2 polarized macrophages, and they exhibit an M2-like (IL-10^{high} IL-12^{low}) immunosuppressive and proangiogenic phenotype that favors tumor growth. Lau et al. (2004) showed that their predominant expression in tumor regions is a characteristic of late stage tumor disease progression and poor prognosis. Several attempts to reprogram these cells towards a proinflammatory/cytotoxic phenotype have been attempted in clinical trials, however the results have been somewhat inconclusive due to the poor vascularization of the tumor areas and the difficulties in maintaining a microenvironment that favors their shift (Biswas and Mantovani, 2010).

Mechanisms Mediating Recruitment of Inflammatory Macrophages to Sites of Injury

In response to inflammatory stimuli, macrophages are recruited from hematopoietic tissues to sites of injury. This is mediated by two complementary processes: the release of chemoattractants from resident leukocytes and injured parenchymal cells, and upregulation of specific receptors on monocytic precursors. Depending on the chemoattractant released, specific leukocyte subsets are recruited (Chou *et al.*, 2010; Mantovani *et al.*, 2004; Oo *et al.*, 2010). Chemokines have been subdivided into CC, CXC, or CX₃C groups, depending on the amino acid residues present between the first two cysteines. Binding of chemokines to chemokine receptors has been shown to occur before the first and fourth cysteine residue (Olson and Ley, 2002). The NH₂ terminus is pivotal in determining the affinity of chemokines to their receptors. CXC chemokines expressing the tripeptide motif glutamic acid-leucine-arginine is associated with myeloid cell recruitment, while its absence indiscriminately recruits leukocytes. Among chemokine receptors, CXCR4 is the most investigated; it has been shown to be widely expressed by T cells, B cells, monocytes, neutrophils, and

blood-derived dendritic cells. Although CXCR1 and CXCR2 are also expressed by many leukocytes, they are physiologically important in neutrophil and monocyte activation and recruitment (Murphy *et al.*, 2000). Interestingly, while the CC chemokine family (CCR1, CCR2, and CCR4-CCR10) is expressed mainly on lymphocytes and monocytes, evidence using CCR5 knock-out mice showed altered neutrophil migration (Vilela *et al.*, 2013), suggesting at least indirect crosstalk between chemokine receptors. In contrast, CCR3 is uniquely expressed on eosinophils, mast cells, basophils, and Th2 lymphocytes. These observations indicate that chemokine receptor expression is dependent on the environmental milieu, as suggested by findings that T cell expression of CCR1, CCR2, and CXCR3 is dependent on IL-2, whereas CXCR4 is repressed by IFN- γ (Annunziato *et al.*, 1999). Leukocyte maturation also appears to regulate chemokine receptor expression, as evidenced by findings that monocytes increase homing chemokine receptors during their maturation (Sallusto *et al.*, 1999).

Origin of Inflammatory Macrophages

Bone Marrow. The bone marrow is a key organ involved in hematopoiesis and myeloid precursor development. Within the bone marrow there are several niches of progenitor and immature cells which are regulated via its unique microenvironment of cytokines and growth factors which provide signals for self-renewal, differentiation, homing and quiescence. These cellular niches, which exhibit unique surface marker expression, are localized adjacent to blood vessels, favoring egression of hemoatopietic cells in response to inflammatory signals (Mercier *et al.*, 2012). Two major chemokine receptors have been identified on bone marrow precursors that direct migration of macrophages to sites of injury or infection: CCR2 and CX₃CR1 (Tacke *et al.*, 2007). Whereas CCR2 is key to directing M1 proinflammatory macrophage trafficking (Boring *et al.*, 1997; Ishikawa *et al.*, 2014; Tsou *et al.*, 2007), CX₃CR1 appears to be important in M2 antiinflammatory macrophage migration, although this is somewhat controversial

(Arai *et al.*, 2013; Jacquelin *et al.*, 2013; Tighe *et al.*, 2011). Mice models have been pivotal in characterizing monocytes/macrophages activation and egress from the bone marrow. Monocytes exit the bone marrow as Ly6C⁺CCR2⁺ proinflammatory cells; once in the blood their fate depends on the presence of tissue injury or infection. Thus, under homeostatic conditions, these cells gradually lose inflammatory markers, eventually entering tissues and maturing into resident macrophages. In contrast, during inflammation these cells retain their proinflammatory M1 phenotype, localize at sites of injury or infection, and participate in the clearance of pathogens and debris (Gordon and Taylor, 2005). This observation adds evidence to the notion that macrophage are highly plastic cells, capable to alter their phenotype in response to stimuli. The other physiological condition where this has been observed is represented by inflammation termination, where the proinflammatory infiltrating macrophages return to a quiescent M2-like state (Arnold *et al.*, 2007; Davies *et al.*, 2013a; Liu *et al.*, 2011b; Lumeng, 2007).

Blood. Under homeostatic conditions, monocytes are released from the bone marrow at constant rates. In humans three subsets of monocytes have been identified: CD14⁺ CD16⁺CCR2^{low}CX₃CR1^{high} non-classical patrolling monocytes, an intermediate proinflammatory CD14⁺CD16⁺CCR2^{mid}CX₃CR1^{high}CCR5⁺ subpopulation and classic CD14⁺CD16⁻CCR2^{high}CX₃CR1^{low} population. These correlate with three murine subsets: CD11b⁺CD115⁺Ly6C^{low}CCR2^{low}CX₃CR1^{high} patrolling/tissue repair monocytes, intermediate CD11b⁺CD115⁺Ly6C^{mid}CCR2^{high}CX₃CR1^{low} monocytes and proinflammatory CD11b⁺CD115⁺Ly6C^{high}CCR2^{high}CX₃CR1^{low} monocytes (Yang *et al.*, 2014). Whereas nonclassical patrolling monocytes consist of the main population during homeostasis acting by removing debris and favor resolution/wound healing, the classical CCR2^{high}Ly6C⁺ monocytes are particularly abundant during the inflammatory disease. In the context of organ inflammation, depending on the timing of injury, evidence suggests

that classical monocytes are the first cells to migrate to the site of injury, while non-classical Ly6C^{low} monocytes accumulate at a later phase and aid resolution of inflammation. Mechanistically, there is also evidence that classical to non-classical phenotype conversion occurs in both bone marrow and liver in an IL-4 and IL-10 dependent fashion (Yang *et al.*, 2014).

Spleen. Although most progenitor cells are found in the bone marrow, evidence suggests that there are extramedullary sites of hematopoiesis. Among these, the spleen has been identified as a major reservoir of progenitor and mature monocytes, ready to proliferate and be deployed following injury or infection (Swirski *et al.*, 2009). Monocytes originating from bone marrow and spleen are distinct. Thus, bone marrow derived monocytes have been shown to be less mature when compared to their splenic counterparts, as evident from their high responsiveness to the growth factor M-CSF and marked ability to reach full differentiation following in vitro stimulation (Wang *et al.*, 2013). In this regard, while injection of M2 ex vivo programmed splenic macrophages has been reported to successfully ameliorate adriamycin-induced nephropathy, bone marrow programmed macrophages were ineffective, likely due to the stem cell-like nature of these cells and high proliferative activity (Cao *et al.*, 2014; Wang *et al.*, 2007). Phenotypically, spleen derived monocytes are characterized by high expression of the co-stimulatory molecule CD80 and MHC-II, which is characteristic of a fully functional and mature phenotype (Wang *et al.*, 2013). Whereas bone marrow cells egress in response to CCL2/CX3CL1, splenic monocytes/macrophages recruitment is mediated by angiotensin-II binding to angiotensin-2 receptor-1 α (ATR-1 α) (Ingersoll *et al.*, 2011).

Epigenetics and Control of Innate Immunity

Epigenetics is defined as heritable changes in gene activity and expression that occur without alteration in DNA. Epigenetic alterations are regulated by three major pathways: chemical modifications of cytosine residues in DNA (i.e. DNA methylation),

histone protein alterations (i.e. histone acetylation and methylation) and miRNA expression (i.e. miR125) (Goldberg *et al.*, 2007). Functionally, these epigenetic modifications serve to reshape chromatin structure and regulate the genetic machinery at the transcriptional and translational level. These regulatory mechanisms function not only during homeostatic conditions, but also during acute and chronic injury and inflammation (Bayarsaihan, 2011). Notably, recent findings have shown that epigenetic alterations play an important role in macrophage phenotypic switching in response to inflammatory signals following chemical injury and infection (Iliopoulos *et al.*, 2009; Kittan *et al.*, 2013; Yang *et al.*, 2014). Epigenetic dysregulation leads to altered macrophage activation, expression of genes involved in the development and resolution of the inflammatory response, and imbalanced release of cytokines and extracellular matrix proteins. In this regard, DNA methylation has been reported to be globally reduced in rheumatoid arthritis (RA) patients (Liu *et al.*, 2011a). A similar study showed that RA subjects exhibit hypomethylated CpG promoter region of IL-6 compared to healthy controls, resulting in altered gene expression and function (Nile *et al.*, 2008). Epigenetic regulation is also fundamental to leukocyte functioning, as shown in T cells, where the promoter region of the IL-2 gene is demethylated shortly after cellular activation, to favor IL-2 production (Bruniquel and Schwartz, 2003). Histone modifications are also prominent in leukocytes; naive CD4 T cells differentiation into T_h-2 cells is characterized by rapid H3 acetylation at the IL4/13 gene promoter (Williams *et al.*, 2004). The inflammatory response of macrophages to lipopolysaccharide (LPS) has also been shown to be epigenetically controlled, as these cells become tolerant upon subsequent stimulation. Foster *et al.* (2007) showed two distinct patterns of histone modifications occurring during this hyporesponsive state: one group of genes responsible for inflammatory mediator (i.e., TNF α and IL-6) production is transient,

whereas a second group of genes, which includes various antimicrobial effectors, remains primed for activation (Foster *et al.*, 2007).

DNA methylation: DNA methylation is an important mechanism of chromatin remodeling. It involves the addition of a methyl group on position 5' of cytosine in the CpG region of the DNA. Mechanistically, DNA methylation is mediated via cytosine-5-methyltransferase. The process has been shown to be partially reversible following enzymatic oxidation by TET1 (Zhao and Chen, 2013), resulting in oxidation of 5-methylcytosine (5-mc) to 5-hydroxymethylcytosine (5-hmc) (Liutkeviciute *et al.*, 2009). DNA methylation is controlled by DNA methyl transferases (DNMT1, DNMT3) and DNA demethylases. DNMT3a and DNMT3b establish the initial CpG methylation pattern *de novo*, while DNMT1 maintains this pattern during chromosome replication and repair following injury. Mechanistically, DNMT1 is driven by a Michael addition mechanism, which allows for C-5 activation on the cytosine followed by enzymatic covalent linkage with C-6 of cytosine, rendering the moiety reactive for transfer of the methyl group. Functionally, promoter region hypermethylation leads to silencing of the gene (Baylin, 2005). This is fundamental for cellular commitment during fetal stages, as well as silencing of dispensable genes in mature cells under specific conditions such as inflammation.

This highly conserved modification results in silencing of the promoter region of the target gene, and plays central role in immune cell development and regulation of molecular pathways in immune-mediated diseases (Falvo *et al.*, 2013). Macrophages release of inflammatory mediators is known to be key in disease outcome and it is controlled in part by DNA methylation status. DNA hypomethylation of TLR-2 drives hyper-responsiveness of macrophages towards bacterial peptidoglycans in cystic fibrosis patients (Shuto *et al.*, 2006). Similarly, after infection of the host, protozoa

methylyate specific regions of macrophage chromatin rendering them hyporesponsive (Marr *et al.*, 2014).

Histone modification: Chromatin remodeling is also accomplished by histone modification. This is important in regulating binding of transcription factors to the transcription starting site (TSS) of gene promoters. Histones are proteins composed by 8 subunits: 2 H2A, 2 H2B, 2 H3, and 2 H4 subunits. Each histone permits winding of about 150 bp of DNA. Depending on the modifications (methylation, acetylation, phosphorylation, SUMOylation, ubiquitination) on the different amino acid residues (especially lysine, arginine, tyrosine) present on the histone tails, the chromatin reaches a tighter or looser condensation status called euchromatin and heterochromatin, respectively. Due to the multiplicity of modifications that can occur at each histone in the promoter region of genes (Wang *et al.*, 2008), this highly refined mechanism of gene regulation has been termed the “histone code”. Modifying histone tails on the promoter of inflammatory genes has been shown to be important in rapid and transient gene expression/repression in macrophages during inflammatory responses (Heintzman *et al.*, 2009). Histone H3 and H4 have been shown to be particularly active in response to cell stimulation. Trimethylation of a lysine residue on histone H3 is associated with higher gene transcription if present on lysine-4 (H3K4) and K36, while the same modification can lead to transcriptional repression when present on lysine-9 and -27. Histone phosphorylation and acetylation (i.e. H3K9, H4K5, 10, and 16) signal heterochromatin (Rossetto *et al.*, 2012; Tsaprouni *et al.*, 2011). Heterochromatin allows for interaction of transcription factors with the promoter regions of genes leading to transcriptional initiation. Return to homeostasis is accompanied by further histone changes, mediated by acetyltransferases (HAT), histone deacetylases (HDAC), dephosphorylases and histone methyltransferases. Evidence indicates that transcriptionally active genes have a histone signature consisting of distinct modifications which include H3K4 trimethylation,

H3K9/14 acetylation, and H3K36 trimethylation (Guenther *et al.*, 2007). It has also been shown that certain histone modifications act together with DNA methylation to achieve gene silencing (Vaissiere *et al.*, 2008), indicating the complexity of these mechanisms in regulating gene expression and activity.

miRNA: Epigenetic control of gene expression is also accomplished via miRNAs. In contrast to DNA methylation and histone modifications, miRNAs do not act directly on the chromatin and are mostly active in the cytoplasm. However, their impact on inflammation is equally significant, due to their ability to modulate both translation of newly synthesized inflammatory proteins, and translation of the enzymes involved in DNA methylation (DNMTs) and histone modification (HDAC, HAT) (Pandi *et al.*, 2013). miRNAs were first recognized in the early 1990s. They are small RNAs (21-28 bp) capable of inhibiting translation of target mRNAs via negative feedback by binding to the untranslated region (both 3'- and 5'-ends) of the transcript (Orom *et al.*, 2008). miRNAs are generated via inter-genic (canonical pathway) or intra-genic path (non-canonical pathway). Their baseline expression is dependent on expression of the coding sequence of the gene they originate from. Following synthesis and initial maturation, miRNAs are exported from the nucleus to the cytoplasm by exportin-5, where there is additional cropping by the enzyme complex called Dicer leading to formation of the mature miRNA. The double stranded RNA is eventually inserted in the RNA-induced silencing complex (RISC), where one of the two strands is lost while the other one remains bound to the multi-protein (Kawahara and Mieda-Sato, 2012). The principle of miRNA-mRNA binding is based on complementarity and the strength of these bonds determines the mRNA destiny. Strong binding leads to mRNA degradation, while intermediate binding leads to mRNA inhibition and deportation to the P-body, the locus of the cell where mRNAs are stored. miRNAs not only act on the cells that produce them, but they also function extracellularly to control communication and expression of

surrounding cells when released in exosomes (Hulsmans and Holvoet, 2013). A unique feature of miRNAs is their expression in a lineage specific manner. miR-16 and miR-142 are highly expressed in all native cell lineages, while miR-451 expression predominates in reticulocytes, miR-223 in platelets, granulocytes and monocytes, and miR-150 in B- and T-lymphocytes (Merkerova *et al.*, 2008; Rosa *et al.*, 2007). In addition to their role in control of lineage commitment, miRNAs tightly regulate phenotype, inflammatory response, and cellular transformation by regulating transcription factors that control these processes (Kittan *et al.*, 2013; Kumar *et al.*, 2007). One example of miRNA associated with phenotypic switching is miR-133, which acts predominantly on vascular smooth muscle cells in cardiac tissue (Torella *et al.*, 2011). In addition to controlling cell commitment, miRNAs are centrally involved in regulating inflammatory circuits; this is mediated, in part, by their promiscuity that favors their interaction with targets that are closely related in function. In these circuits, inflammatory mediators elicited following injury, are regulated by miRNAs and these inflammatory mediators feedback and act themselves as miRNA regulators (Iliopoulos, Hirsch and Struhl, 2009). The interplay between miRNA and inflammation has been widely studied; these ncRNAs represent a potential therapeutic target. Eicosanoids are well known to initiate, amplify, and perpetuate inflammatory responses (Martin *et al.*, 1984). The generation of these lipid products from arachidonic acid is mediated by COX-2, an enzyme rapidly upregulated following injury. miR199a and miR101a have been shown to act as anti-inflammatory regulators by inhibiting COX-2 translation (Chakrabarty *et al.*, 2007). Iliopoulos *et al.* (2009; 2010) have demonstrated a link between inflammation and cancer via a feedback circuit between the inflammatory transcription factor NF- κ B, IL-6 and the miRNAs Lin28 and let-7 (Iliopoulos *et al.*, 2009; Iliopoulos *et al.*, 2010). Models of prolonged inflammation, also suggest an involvement of miR21 and miR199-5 in promoting tissue remodeling and fibrosis in the lung (Lino Cardenas *et al.*, 2013; Liu *et al.*, 2010). In this

regard, hypoxia-sensitive miR200b has been associated with regulation of cellular redox state through NADPH oxidase (Roy and Sen, 2012). These findings indicate that miRNAs represent a complex network actively involved in controlling pathogenesis, progression and resolution of the inflammatory response.

AIMS OF THE DISSERTATION

NM (mechlorethamine hydrochloride) is a highly toxic vesicant known to target the lung. Toxicity is due to alkylation of DNA and proteins and oxidative stress. Exposure to NM results in rapid structural changes in the respiratory tract, including perivascular edema and thickening of the alveolar wall, followed by bronchiolization of the epithelium which progresses to lung fibrosis. This is accompanied by an accumulation of activated macrophages in the tissue and up-regulation of inflammatory proteins implicated in the pathological processes. Macrophage activation and inflammatory protein expression are regulated at the transcriptional and translational level via chromatin remodeling and miRNAs. We hypothesize that distinct activated macrophage subpopulations contribute to lung injury and fibrosis induced by NM and that these cells are derived from bone marrow and spleen; moreover, their activation state is regulated, in part by epigenetic pathways. To test this hypothesis three specific aims were proposed:

SPECIFIC AIM 1: Characterize macrophage populations in the lung following exposure of rats to NM. Techniques in immunohistochemistry and flow cytometry/cell sorting were used to assess the phenotype and activity of macrophage subpopulations accumulating in the lung 1-28 d after exposure. Injury, fibrosis and inflammation were analyzed in bronchoalveolar lavage fluid and histological sections.

SPECIFIC AIM 2: Analyze the origin of macrophages accumulating in the lung following NM exposure. We hypothesize that bone marrow and spleen contribute to the macrophage pools accumulating in the lung after NM. The bone marrow origin of lung macrophages was assessed using an inhibitor of CCR-2, which plays an essential role in monocyte egress from the bone marrow. To evaluate the role of the spleen as an extramedullary source of lung macrophages, splenectomized (SPX) rats were used.

SPECIFIC AIM 3: Elucidate epigenetic mechanisms regulating macrophage activation following NM exposure. Transcriptional and translational regulation via histone modifications and miRNAs, respectively, are important mechanisms underlying macrophage activation and pro- and anti-inflammatory gene expression. Techniques in immunohistochemistry and western blotting were used to assess expression of histone variants and alterations in histones; miRNA PCR based arrays were used to assess translational regulation. The HDAC inhibitor, valproic acid was used to evaluate the role of histone deacetylases in NM-induced macrophage activation following NM exposure.

MATERIALS AND METHODS

Animals and Treatments

Naïve, SPX and sham operated (control) male Wistar rats (225–250 g) were purchased from Harlan Laboratories (Indianapolis, IN) and maintained in an AALAC approved animal care facility. Animals were housed in filter top microisolation cages and provided food and water *ad libitum*. Animals received humane care in compliance with the guidelines outlined in the Guide for the Care and Use of Laboratory Animals, published by the National Institutes of Health. Animals were anesthetized with 2.5% isoflurane, and then administered PBS or NM (0.125 mg/kg, mechlorethamine hydrochloride, Sigma-Aldrich, St. Louis, MO) intratracheally, as previously described (Sunil *et al.*, 2011b). All instillations were performed by David Reimer, D.V.M., Laboratory Animal Services, Rutgers University. NM was prepared immediately before administration in a designated room under a chemical hood following Rutgers University Environmental Health and Safety guidelines. In some experiments, naïve animals were treated (i.p.) with valproic acid (300 mg/kg, Sigma-Aldrich, St. Louis, MO) or vehicle control (PBS) once a day beginning 30 min after administration of NM or PBS control.

Bronchoalveolar Lavage and Inflammatory Cell Collection

Animals were euthanized by i.p. injection of Sleepaway (sodium pentobarbital, 50 mg/kg, Fort Dodge Animal Health, Fort Dodge, IA) 1 d, 3 d, 7 d or 28 d after administration of PBS or NM. Bronchoalveolar lavage (BAL) was collected by slowly instilling and withdrawing 10 ml of ice cold (4°C) PBS into the lung through a cannula inserted into the trachea. BAL was centrifuged (300xg, 8 min) and cell pellets resuspended in 1 ml of PBS for differential analysis and viable cell counts using a hemocytometer with trypan blue dye exclusion. Cell-free supernatants were assayed for protein content using a BCA protein assay kit (Pierce Biotechnologies Inc., Rockford, IL) with bovine serum albumin as the standard. The lung was then removed and 10 ml of ice cold PBS slowly instilled

and withdrawn through the cannula, while gently massaging the tissue; this procedure was repeated 4 times. The lavage fluid was combined with the initial BAL cell suspension, centrifuged (300xg, 8 min), resuspended in 10 ml PBS and cells enumerated.

Histology and Immunohistochemistry

Following BAL collection, the lung was removed, fixed with 2% paraformaldehyde and paraffin-embedded. Sections (5 μ m) were prepared and stained with hematoxylin and eosin or Gomori's Trichrome. Histopathological changes were assessed blindly by a veterinary pathologist (LeRoy Hall, DVM, PhD) as previously described (Malaviya, Venosa, Hall, Gow, Sinko, Laskin and Laskin, 2012). Semiquantitative grades (0 to 4) were assigned to histological sections, with grade 0 indicating no changes; grade 1, minimal or small changes; grade 2, medium changes; grade 3, moderate to extensive changes, and grade 4, extensive changes, relative to PBS controls. For immunostaining, tissue sections (5 μ m) were deparaffinized with xylene followed by decreasing concentrations of ethanol (100% - 50%) and then water. After antigen retrieval using citrate buffer (10.2 mM sodium citrate, 0.05% Tween 20, pH 6.0, 10 min) and quenching of endogenous peroxidase with 3% hydrogen peroxide in methanol (30 min), sections were incubated for 2 h at room temperature with 10% serum to block nonspecific binding. This was followed by overnight incubation at 4°C in a humidified chamber with rabbit monoclonal anti-CD11b (1:500, Abcam, Cambridge, MA), rabbit monoclonal anti-iNOS (1:800, Abcam), mouse monoclonal anti-CD68 (1:400, AbD Serotec, Raleigh, NC), rabbit polyclonal anti-mannose receptor (CD206, 1:400, Abcam), mouse monoclonal anti-CD163 (1:1000, AbD Serotec), rabbit polyclonal anti-YM-1 (1:800, Stem Cell Technologies, Vancouver, Canada), rabbit monoclonal anti-CCR2 (1:400, Abcam), rabbit polyclonal anti-CX₃CR1 (1:500, Abcam) or rabbit monoclonal anti-ATR-1 α (1:150, Abcam), rabbit polyclonal anti-histone deacetylase 2 (HDAC2, 1:150, Santa Cruz

Biotechnologies, Dallas, TX), rabbit monoclonal anti-acetylated H3K9 (H3K9Ac, 1:350, Cell Signaling Technology, Danvers, MA), mouse monoclonal anti-p300 (1/150, Abcam), rabbit polyclonal anti-histone deacetylase 2 (HDAC2, 1:150, Santa Cruz Biotechnologies, Dallas, TX), mouse monoclonal anti-p300 (1:200, Abcam, Cambridge, MA), mouse monoclonal anti-sirtuin 1 (SIRT1, 1:250, EMD Millipore, Billerica, MA), rabbit monoclonal anti-phospho histone2A.X (γ H2A.X., 1:400, Abcam), mouse monoclonal anti-trimethylated H3K9 (H3K9TM, 1:400, Cell Signaling), rabbit monoclonal anti-monomethylated H3K4 (H3K4MM, 1:25, Cell Signaling), rabbit monoclonal anti-trimethylated H3K4 (H3K4TM, 1:250, Cell Signaling), or rabbit monoclonal anti-dimethylated H3K36 (H3K36DM, 1:150, Cell Signaling), rabbit monoclonal anti-cytochrome b5 (CYPb5, 1:1500, Abcam), rabbit polyclonal anti-proliferating cell nuclear antigen (PCNA, 1/800, Abcam), or primary antibodies or the appropriate serum/IgG controls diluted in blocking buffer. Sections were then washed and incubated at room temperature for 30 min with biotinylated secondary antibody (Vectastain Elite ABC kit, Vector Labs, Burlingame, CA). Binding was visualized using a Peroxidase Substrate Kit DAB (Vectastain). Random sections from at least 3 rats/group were analyzed.

Nuclear Extraction and Quantification

Lung cells ($8-10 \times 10^6$) were processed using EpiQuik Nuclear Extraction kit according to manufacturer's protocol (Epigentek Group Inc, Farmingdale, NY). Briefly, cells were incubated for 15 min with lysate buffer, followed by centrifugation ($300g \times 10\text{min}$). Cytoplasmic enriched supernatants were collected for quantification; nuclear/membrane fractions were resuspended in nuclear extraction buffer, incubated for 15 min in ice, and then centrifuged ($1500g \times 15\text{ min}$). Nuclear enriched supernatants were collected and frozen for further analysis (-80°C). Cytoplasmic and nuclear extracts were quantified using BCA protein assay kit (Pierce Biotechnologies Inc., Rockford, IL) with bovine serum albumin as standard. All samples were assayed in triplicate.

Western Blot Analysis

Nuclear extracts (3 µg) were fractioned using NuPAGE 4-12% Bis-Tris gels (Life Sciences, San Diego, CA) and transferred to PVDF membranes. Nonspecific binding was blocked by incubation of the blots with 5% bovine serum albumin in Tris-buffered saline/Tween-20 (TBST) for 1 h. Blots were then incubated overnight (4°C) with rabbit monoclonal anti-tri-methyl-histone H3 (Lys4), rabbit anti-mono-methyl-histone H3 (Lys4), rabbit anti-acetyl-histone H3 (Lys9), rabbit anti-tri-methyl-histone H3 (Lys27), rabbit anti-di-methyl-histone H3 (Lys36), rabbit anti-histone H3 and mouse monoclonal anti-di/tri-methyl-histone H3 (Lys9) (Cell Signaling, Dancers, MA) primary antibodies in TBST buffer. Blots were then washed three times with TBST and incubated for 1 h at RT with HRP-conjugated secondary antibody, in 5% BSA. Immunoreactive bands were visualized using ECL-Prime detection system (GE Healthcare Biosciences, Piscataway, NJ). All primary antibodies were used in concentrations ranging from 1/1000-1/10000.

HDAC Activity Assay

HDAC activity was measured in nuclear extracts using a fluorimetric EpiQuick HDAC assay (Epigentek Group Inc., Farmingdale, NY). Briefly, nuclear extracts (4 µg) were incubated with HDAC substrate buffer or substrate mixed with the HDAC inhibitor, TSA, for 60 min. This was followed by washing 3 times for 5 min. Samples were then sequentially incubated with a capture antibody (60 min, 4°C) and a detection antibody (30 min, RT). After washing (3x, 5 min), developing solution was added; Deacetylated histone was quantified fluorimetrically on a spectrophotometer at 530 nm using a Spectra Max M2e (Molecular Devices, Sunnyvale CA) reader 2 min later. HDAC activity was expressed as nanograms of deacetylated substrate per minute per microgram of extract. Each sample was assayed three times in duplicate.

mRNA and miRNA Isolation, Microarray and Real Time PCR

Total RNA was isolated from lung cells ($6-8 \times 10^6$) via chloroform extraction followed by isolation of enriched mRNA and miRNA portion using Qiagen RNeasy Min Elute Cleanup kit (QIAGEN Inc., Valencia, CA). mRNA was reversed transcribed using a High Capacity cDNA Reverse Transcription kit (Applied Biosystems, Grand Island, NY) according to the manufacturer's protocol and frozen at -80°C . Standard curves were generated using serial dilutions from pooled cDNA samples. Real time PCR was performed using SYBR Green PCR Master Mix (Applied Biosystems) with glyceraldehyde 3-phosphate dehydrogenase (GAPDH) as an endogenous control. Full-length coding sequences were obtained from NCBI Gene Bank. Primers were designed using Primer Express 3.0 software (Applied Biosystems). The following forward and reverse primers were used: GAPDH, CCTGGAGAAACCTGCCAAGTAT and CTCGGCCGCCTGCTT; iNOS, TGGTGAAAGCGGTGTTCTTTG and ACGCGGGAAGCCATGA; cyclooxygenase-2 (COX2), TGCTCACTTTGTTGAGTAGTCATTAC and CATTCCTTCCCCCAGCAA; IL-12 α , GCACACTGGAGGCCTGCTT and TTAGTAGCCAGGCAACTCTCATTCT; IL-12 β , CAGAAAGGTGCGTTCCTCGTA and GCCCCTTTGCATTGG; matrix metalloproteinase-9 (MMP-9), ATTCTCGGTGGACCAATGACGTG and AATGTCCATGTTAACGGG; IL-10, CCCAGAAATCAAGGAGCATTTG and CAGCTGTATCCAGAGGGTCTTCA; apolipoproteinE (ApoE), TCCATTGCCTCCACCACAGT and GGCGTAGGTGAGGGATGATC; pentraxin-2 (PTX-2), TCCGGGCACAAGAGATCATC and GATGTTTCCAGGCATGTTCGT; PTX-3, GGCCAAAAGTCACCCTGTTC and CCATTCTTTTCTTGCCATCT; serotonin receptor 7 (5-HT7) CGTACCCGGTGAGGCAAA and AGAGCAGCCAGACCGACAGA; HT2 α TGCACACCCCGGCTAACTAC and GATGGACACGAGCAGGTCAGT; ATR-1 α ,

CCATTGTCCACCCGATGAA and TGA CTTTGGCCACCAGCAT; CX₃CR1, GGAGCAGGCAGGACAGCAT and CCCTCTCCCTCGCTTGTGTA; CCR2, TGACAGAGACTCTTGAATGACACA and CTCACCAACAAAGGCATAAATGAT; CCL2, CCACTCACCTGCTGCTACTCAT and TCTCCAGCCGACTCATTGG; CCR5, CCTGTTCAACCTGGCCATCT and GCCCAGAATGGGAGTGTGA; CCL5, CTCCAACCTTGCAAGTCGTCTT and TCTGGGTGGCACACACTTG. Purified miRNA fraction was converted to cDNA using QuantiTect Reverse Transcription kit (Qiagen) and a thermal cycler. Microarray polymerase chain reaction amplification and analysis were performed using miScript SYBR Green kit (Qiagen) using SNORD96A or RNU6 as an endogenous control for microarray and validation analysis, respectively. Analyses were performed on an Applied Biosystems 7300HT real time PCR system. Fold change in mRNA and miRNA analyses was calculated using $^{-\Delta\Delta C_t}$ method.

Flow Cytometry and Cell Sorting

Cells were suspended in staining buffer (PBS+2% FBS and 0.1% sodium azide) at a concentration of 3×10^6 /mL and incubated with anti-rat-FcRII/III antibody (Fc block, BD Biosciences, Franklin Lakes, NJ) for 10 min at 4°C to block nonspecific binding. This was followed by 30 min incubation with AlexaFluor 488 (AF488)-conjugated anti-CD11b, AF647-conjugated anti-CD43 or anti-CD68 antibodies or appropriate isotype controls (0.25 - $1.5 \mu\text{g}/10^6$ cells, Biolegend, San Diego, CA), and then with eFluor780-conjugated viability dye (eBioscience, San Diego, CA) for 30 min. Cells were first incubated with permeabilization/fixation buffer (eBioscience) for 30 min, followed by eFluo450-conjugated anti-Ki67 antibody. Cells were fixed in 2% paraformaldehyde and analyzed using a Beckman Coulter Gallios flow cytometer (Brea, CA); data were analyzed using Kaluza software. Macrophages were identified by forward and side scatter followed by doublet discrimination of viable cells. For sorting, cells were incubated with anti-rat-FcRII/III antibody, and then with AF488-conjugated anti-CD11b and AF647-conjugated

anti-CD43 antibodies as described above. DAPI was added to the cell suspension immediately before analysis to exclude dead cells. Viable cells were sorted into CD11b⁻/CD43⁻, CD11b⁺/CD43⁺ and CD11b⁺/CD43⁻ subpopulations using a Beckman Coulter MoFlo XDP cell sorter and processed immediately for RNA isolation.

Statistical Analysis

Experimental treatment groups consisted of a minimum of 3–4 animals/group. All experiments were repeated at least two times. BAL fluid and PCR data were analyzed using one-way and two-way ANOVA, with unpaired Student's t-test or Brown-Forsythe post hoc tests. Histopathology scores were analyzed using Kruskal-Wallis one-way ANOVA and Mann-Whitney Rank Sum post-hoc test. A p value ≤ 0.05 was considered statistically significant.

PART I. CHARACTERIZATION OF MACROPHAGE SUBPOPULATIONS ACCUMULATING IN THE LUNG IN RESPONSE TO NITROGEN MUSTARD

INTRODUCTION

SM and the related analog, NM, are highly toxic vesicants originally developed as chemical warfare agents (Dacre and Goldman, 1996; Ghabili *et al.*, 2011). Pulmonary exposure to these vesicants results in extensive tissue damage and persistent bronchiolitis, which progresses to fibrosis (Ghanei *et al.*, 2010; Weinberger *et al.*, 2011). Mortality and long-term morbidity following exposure to mustards are a consequence of alkylation and crosslinking of critical nucleophilic sites in target tissues including DNA and proteins. This combination of protein and DNA modification, along with direct oxidative action leads to cytotoxicity and inflammation, which contribute to tissue injury (Weinberger *et al.*, 2011).

Lung injury induced by mustards is associated with an accumulation of activated macrophages in the tissue (Malaviya *et al.*, 2010; Malaviya *et al.*, 2012; Sunil *et al.*, 2014). These cells are known to play a role in both acute and chronic pulmonary pathologies including cytotoxicity and fibrosis (Laskin *et al.*, 2011; Murray and Wynn, 2011). Evidence suggests that these activities are mediated by distinct populations of macrophages, which develop in response to inflammatory signals they encounter in the tissue microenvironment (Martinez *et al.*, 2008; Mosser and Edwards, 2008). Two phenotypically distinct populations of macrophages have been identified: proinflammatory/cytotoxic M1 macrophages and antiinflammatory/wound repair M2 macrophages (Martinez and Gordon, 2014). Whereas early in the pathogenic response to toxicants M1 macrophages release mediators aimed at eliminating foreign materials and debris, subsequently M2 macrophages appear in the tissue releasing mediators that promote the resolution of injury and wound repair (Sica and Mantovani, 2012).

Excessive release of mediators by M1 and/or M2 macrophage can contribute to tissue injury and disease pathogenesis, and to the development of fibrosis. The key to an effective inflammatory response to an insult appears to be a balanced activation of the two macrophage phenotypes. In this series of studies we used techniques in immunohistochemistry and flow cytometry to characterize activated macrophage populations accumulating in the lung following exposure of rats to vesicants, using NM as a model. Our findings that M1 and M2 macrophages appear sequentially in the lung following NM exposure, and that this correlated with the development of acute injury and fibrosis, provide support for a role of these phenotypically distinct populations in the pathogenesis of lung injury.

RESULTS

Macrophages accumulating in the lung after NM were initially characterized *in situ* by immunohistochemistry. CD11b is a beta-2 integrin expressed on phagocytic leukocytes infiltrating into areas of tissue damage (Chamoto *et al.*, 2013; Kirby *et al.*, 2006).

Following NM exposure, we noted a rapid (<1 d) accumulation of CD11b⁺ cells in the lung, which persisted for at least 28 d, although at this time the intensity of CD11b expression was reduced (Fig. 3, left panels and Table 1). CD11b was also upregulated in the alveolar epithelium after NM; however by 28 d, CD11b expression was at control levels. To assess the phenotype of lung macrophages, we analyzed expression of prototypical markers of M1 and M2 macrophages. Exposure of rats to NM was associated with increases in iNOS⁺ M1 macrophages in the lung (Fig. 3, right panels and Table 1). This was most prominent 1 d post exposure; subsequently, numbers of iNOS⁺ cells declined. CD68, CD163 and CD206 are scavenger receptors expressed on M2 macrophages (Martinez and Gordon, 2014; Zaynagetdinov *et al.*, 2013). In control rats,

resident alveolar macrophages were found to express CD68 and CD206, but not CD163 (Fig. 4). NM exposure resulted in a time related increase in numbers of CD68⁺, CD163⁺ and CD206⁺ macrophages in the lung. At 1 d post exposure, positively stained cells were small and round, however, by 3 d these cells began to increase in size; this continued for at least 28 d. At this time, the cells appeared vacuolated and were mainly clustered in the airspaces adjacent to fibrotic areas. Expression of two additional markers of an M2 phenotype, ARG-II and YM-1 was also analyzed. Within 1 d of NM, a prominent increase in small ARG-II⁺ macrophages was noted in the lung (Fig. 5, left panels). Low level ARG-II staining was also observed in the alveolar epithelium. With time following NM exposure, macrophages staining positively for ARG-II became enlarged and by 28 d, these cells appeared in clusters. YM-1⁺ macrophages also increased in the lung after NM, but their appearance was delayed for 3 d. As observed with ARG-II⁺ macrophages, by 28 d, clusters of enlarged YM-1⁺ macrophages were evident in the lung (Fig. 5, right panels).

Expression of genes associated with M1 and M2 phenotypes was next analyzed in isolated lung macrophages. M1 associated genes, including iNOS, TNF α , COX-2, IL-12 α , MMP-9 and MMP-10 (Huang *et al.*, 2012; Martinez and Gordon, 2014; Zaynagetdinov *et al.*, 2013), were upregulated in macrophages within 1 d of NM exposure (Fig. 6). While increases in TNF α and MMP-10 were transient, declining to control levels by 3 d, iNOS, COX-2, IL-12 α and MMP-9 remained significantly elevated for at least 28 d, although at reduced levels. NM exposure also resulted in increased expression of genes associated with M2 macrophages; these included IL-10, PTX-2, and CTGF (Blom *et al.*, 2002; Martinez and Gordon, 2014). Expression of each of these genes increased rapidly (< 1 d) in lung macrophages after NM exposure, and persisted for at least 7 d; by 28 d, expression was similar to control (Fig. 6). We also analyzed expression of ApoE, which has been shown to dampen M1-driven gene expression and

enhance M2 macrophage activation (Baitsch *et al.*, 2011). Following NM exposure, ApoE expression increased significantly, peaking at 7 d (Fig 6).

Flow cytometry was next used to characterize macrophage subpopulations responding to NM. We found that the majority (~98%) of macrophages from control rats were CD11b⁻ CD43⁻ and CD68⁺ (Fig. 7 and Table 2), consistent with a mature resident macrophage phenotype (Davies *et al.*, 2013a; Howell *et al.*, 1994). Whereas numbers of resident macrophages decreased following NM exposure, CD11b⁺ infiltrating cells increased (Fig. 7 and Table 2). CD11b⁺ cells were found to consist of two subpopulations: immature CD43⁺ and mature CD43⁻ macrophages (Fig. 7). While maximum numbers of immature macrophages were observed in the lung after 3 d, mature macrophages peaked at 7 d. CD11b⁺CD68⁺ macrophages also increased in the lung 3 d after exposure to NM (Table 2). At 28 d, only a small number of CD11b⁺ infiltrating macrophages were present in the lung, and these cells were mainly mature macrophages (CD43⁻). To assess whether increases in CD11b⁺ macrophages were due to proliferation, we analyzed Ki67 expression (Kee *et al.*, 2002). In control rats, ~2% of resident CD11b⁻CD43⁻ macrophages were found to be proliferating. Following NM exposure, proliferation of these cells increased up to 7 d, returning to control levels by 28 d. Increased proliferation of both mature and immature CD11b⁺ lung macrophages was also observed after NM; this was evident within 3 d in the mature infiltrating macrophage subpopulation, but was delayed for 7 d in immature infiltrating macrophages (Fig. 8).

To further characterize these subpopulations, resident and infiltrating macrophage populations were sorted and examined for relative expression of M1 and M2 genes. RT-PCR analysis showed that 3 d post NM exposure, M1 (iNOS, IL-12 α) gene expression was greater in immature CD11b⁺CD43⁺ infiltrating macrophages than in resident macrophages or mature CD11b⁺CD43⁻ infiltrating macrophages (Fig. 9); there

was also a trend towards increased CCR2 expression. By comparison, mature CD11b⁺CD43⁻ macrophages expressed greater levels of IL-10, CX₃CR1 and ApoE than resident or immature CD43⁺ infiltrating macrophages. In general, these differences in gene expression between the cells persisted for 7 d, with the exception ApoE, which was significantly increased at this time in CD11b⁺CD43⁺ macrophages and IL-12 α , which was at control levels (Fig. 9).

Macrophage trafficking to sites of injury is mediated by chemokines and chemokine receptors (Mantovani *et al.*, 2010). Whereas proinflammatory M1 macrophages accumulate in tissues in response to chemokines CCL2 and CCL5, and express chemokine receptors CCR2 and CCR5, fractalkine and CX₃CR1 are involved in M2 macrophage migration (Ingersoll *et al.*, 2011). Treatment of rats with NM resulted in increased expression of the M1 chemokine receptors, CCR2 and CCR5 and their respective ligands, CCL2 and CCL5 on lung macrophages, which was maximal at 1-3 d (Fig. 10). Expression of CX₃CR1 and its ligand, fractalkine also increased rapidly after NM (< 1 d) and remained elevated for at least 7 d. Upregulation of CCR2 and CX₃CR1 mRNA in lung macrophages following NM exposure was correlated with increased protein expression in histological sections. Thus, within 1 d of NM exposure, positively staining CCR2 and CX₃CR1 macrophages were identified in the lung (Fig. 11). By 3 d, staining was also upregulated in epithelial cells, which persisted for 28 d.

DISCUSSION

NM-induced lung injury and fibrosis are associated with increased numbers of macrophages in the peribronchial and perivascular regions of the lung (Malaviya *et al.*, 2012). The present studies demonstrate that these cells consist of subpopulations of CD11b⁺ infiltrating macrophages exhibiting M1 and M2 phenotypes. While M1

macrophages release cytotoxic/proinflammatory mediators that contribute to injury, M2 macrophages are involved in the development of fibrosis (Laskin *et al.*, 2011; Martinez and Gordon, 2014; Sica and Mantovani, 2012). The fact that the sequential appearance of M1 and M2 macrophages in the lung after NM exposure correlates with early tissue injury and subsequent fibrosis suggests that these cells may play a role in the development of these pathologies.

A characteristic feature of infiltrating macrophages is expression of CD11b, a cell adhesion molecule important in phagocyte diapedesis (Chamoto *et al.*, 2013). Following NM exposure, we noted a persistent increase in CD11b⁺ macrophages in histologic sections indicating the continuous infiltration of inflammatory cells into the lung. However, the intensity of CD11b expression was reduced in these cells 28 d after NM exposure, suggesting that the inflammatory response was declining. This is supported by our flow cytometric findings of decreased numbers of CD11b⁺ cells in the lung at this time. Further immunohistochemical analysis of macrophages responding to NM, revealed time related alterations in their phenotype, which paralleled histological changes in the lung (Malaviya *et al.*, 2012). Thus, acute lung injury induced by NM was associated with increases in iNOS⁺ M1 macrophages in lung sections within 1 d of exposure. Cells, isolated from the lung 1 d post NM, also expressed increased levels of iNOS mRNA, as well as other markers of M1 activation including TNF α , COX-2, IL-12 α , MMP-9 and MMP-10 (Martinez and Gordon, 2014). The fact that M1 macrophages remained in the tissue for at least 28 d and that iNOS, COX-2, IL-12 α and MMP-9 genes were upregulated suggests the persistence of a cytotoxic/proinflammatory response. Findings that TNF α gene expression was transient are consistent with its role as an early response cytokine (Moldoveanu *et al.*, 2009). We also identified populations of CD68⁺, CD163⁺ and CD206⁺ M2 macrophages in histologic sections beginning 1-3 d after NM exposure; these cells increased in number and size with time, a response correlated with

decreases in M1 macrophages and the development of fibrosis. By 28 d, M2 macrophages were also vacuolated in appearance and found clustered in thickened alveoli surrounding areas of fibrosis, supporting their profibrotic activity (Boven *et al.*, 2006; Martinez and Gordon, 2014; van Tits *et al.*, 2011). Resident lung macrophages were also found to express CD68 and CD206, which is consistent with their M2-like phenotype (Zaynagetdinov *et al.*, 2013). Macrophages expressing YM-1 and ARG-II, two other M2 markers were also identified in the lung after NM. While YM-1⁺ macrophages appeared within 1 d, ARG-II⁺ macrophages were delayed for 3 d. These data support the notion that M2 macrophages responding to NM consist of phenotypically distinct subpopulations (Martinez and Gordon, 2014; Mosser and Edwards, 2008). Following NM exposure, we also noted early (1-7 d) upregulation of IL-10, PTX-2, ApoE, and CTGF gene expression in isolated lung macrophages. Each of these proteins has been shown to play a role in blunting inflammation and regulating tissue remodeling and extracellular matrix turnover, characteristics of M2 macrophages (Baitsch *et al.*, 2011; Castano *et al.*, 2009; Ponticos *et al.*, 2009). The observation that increased numbers of M2 macrophages were identified in the lung as early as 1 day post NM and that several M2 genes were upregulated, indicates that processes associated with tissue repair and fibrosis begin early after tissue injury. Previous studies have characterized three subsets of murine M2 macrophages (Martinez and Gordon, 2014): M2a macrophages, which express high levels of CD68, CD163, CD206 and arginase, and are involved in type-II immune responses and fibrosis; M2b macrophages which are considered immunoregulatory; and M2c macrophages which express CD68, CD163, CD206, YM-1, PTX and ApoE, and function to down regulate inflammation and initiate tissue remodeling (Martinez and Gordon, 2014; Moestrup and Moller, 2004; Zhou *et al.*, 2014). It is tempting to speculate that M2 macrophages identified in histologic sections early after NM are M2a- and M2c-like and function mainly to phagocytize cellular debris

and counterbalance M1 cell activation, while during the chronic phase (up to 28 d), these macrophages promote matrix deposition, tissue remodeling and the development of fibrosis, however this remains to be established.

Heterogeneity within the macrophage populations responding to NM was further analyzed by flow cytometry. Three distinct subpopulations of cells were identified based on expression of CD11b and CD43 or CD68. These included resident CD11b⁻CD43⁻ and CD68⁺ macrophages, and two populations of CD11b⁺ infiltrating macrophages: mature CD43⁻ and immature CD43⁺ cells. Following NM exposure, numbers of resident macrophages decreased for at least 7 d, likely due to the cytotoxic effects of NM (Barth *et al.*, 1995; Rappeneau *et al.*, 2000). Similar decreases in resident macrophages have been described in the lung, skin and peritoneum after infection or injury (Davies *et al.*, 2013b; Kirby *et al.*, 2009; Lauder *et al.*, 2011). By 28 d post NM, resident macrophage numbers were above control levels. Our findings of increased Ki67 expression in these cells suggest that this is due to proliferation of mature residual resident macrophages. This is supported by previous reports of local resident macrophage proliferation in the absence of monocyte influx (Ajami *et al.*, 2007; Cote *et al.*, 2013; Davies *et al.*, 2011; Hashimoto *et al.*, 2013; Jenkins *et al.*, 2011). In contrast to resident macrophages, immature CD43⁺ and mature CD43⁻ infiltrating (CD11b⁺) macrophages increased in the lung after NM exposure. Analysis of Ki67 expression in the CD11b⁺ macrophages showed that both of these subpopulations proliferated, confirming that macrophages accumulating to the lung after NM exposure arise from cellular infiltration, as well as self-renewal. Proliferation of immature CD11b⁺CD43⁺ and mature CD11b⁺CD43⁻ infiltrating macrophages peaked at 3 d and 7 d, respectively, which is consistent with their pattern of accumulation in the lung. These findings are in accord with earlier studies showing increased expression of the proliferation marker PCNA in lung macrophages at 3 d after NM, which remained upregulated for at least 28 d (Malaviya *et al.*, 2012).

Analysis of the sorted macrophage subpopulations confirmed their distinct phenotypes. Thus, immature CD11b⁺CD43⁺ macrophages expressed higher levels of iNOS and IL-12 α when compared to mature CD11b⁺CD43⁻ cells; these data suggest that these cells are polarized towards a proinflammatory M1 phenotype. Conversely, our findings that infiltrating mature CD11b⁺CD43⁻ macrophages expressed significantly higher levels of IL-10, ApoE, and CX₃CR1, relative to immature CD11b⁺CD43⁺ macrophages, indicate that these cells are M2-biased. The timing of accumulation of the CD11b⁺CD43⁺ and CD11b⁺CD43⁻ populations in the lung corresponded with M1 and M2 macrophages in histological sections and with acute injury and fibrosis, suggesting a potential role of these subpopulations in the pathogenic response to NM. Interestingly, by 7 d post NM, levels of ApoE in immature CD43⁺ macrophages were increased relative to those observed in mature CD43⁻ macrophages. This indicates that there may be M1 to M2 macrophage phenotypic switching during the pathogenic response to NM. Similar phenotypic switching has been described in renal and peritoneal models of inflammation (Gordon and Taylor, 2005; Lin *et al.*, 2009; Liu *et al.*, 2011b).

The accumulation of M1 and M2 macrophages in the lung correlated with increased expression of chemokines and chemokine receptors associated with trafficking of M1 (CCL2, CCL5, CCR2 and CCR5) and M2 (fractalkine and CX₃CR1) macrophages to sites of injury (Ingersoll, Platt, Potteaux and Randolph, 2011; Mantovani, Savino, Locati, Zammataro, Allavena and Bonecchi, 2010). A similar correlation in expression of chemokine receptors and M1/M2 macrophage accumulation has been described in models of bleomycin-induced lung fibrosis and lung cancer, as well as in skin fibrosis and atherosclerosis (Arai *et al.*, 2013; Okuma *et al.*, 2004; Schmall *et al.*, 2014; Tacke *et al.*, 2007). Increased expression of both M1 and M2 chemokines 1-7 d after NM exposure is consistent with the idea that the lung actively recruits both macrophage subtypes to sites of injury. This is supported by findings of

increased numbers of M1 and M2 macrophages expressing M1 and M2 chemokine receptors in the lung 1-7 d post NM. These data suggest that chemokines and chemokine receptors may be potential pharmacological targets for reducing lung inflammation, injury and fibrosis.

NM-induced injury is associated with a complex cascade of events including acute inflammation, tissue injury, remodeling and fibrosis. The present studies show that after NM exposure, M1 macrophages accumulate in the lung, followed by infiltration of M2 macrophage subsets. These cells are known to regulate pathogenic responses to toxicants. Elucidating the phenotype of macrophages accumulating in the lung after NM exposure and mechanisms mediating their recruitment is important for the development of targeted clinical therapies aimed at blunting macrophage activation and mitigating NM-induced injury.

PART II. ROLE OF SPLEEN-DERIVED MACROPHAGES IN NITROGEN MUSTARD INDUCED LUNG INFLAMMATION, INJURY AND FIBROSIS

INTRODUCTION

Nitrogen mustard (NM) is a bifunctional alkylating agent and cytotoxic vesicant known to damage the respiratory tract. Exposure to NM is characterized by acute lung injury which progresses to fibrosis (Ghanei and Harandi, 2007; Ghanei *et al.*, 2010; Malaviya *et al.*, 2012; Weinberger *et al.*, 2011). This is associated with a persistent macrophage inflammatory response. Macrophages are known to contribute to the development, progression and resolution of lung damage (Laskin *et al.*, 2011; Mosser and Edwards, 2008). These activities are mediated by distinct subpopulations, broadly classified as proinflammatory/cytotoxic M1 and antiinflammatory/wound repair M2 macrophages (Murray and Wynn, 2011). Overactivity of these macrophage subpopulations has been shown to contribute to tissue injury, fibrosis and disease pathogenesis. In previous studies we reported that M1 and M2 macrophages sequentially accumulate in the lung after exposure of rats to NM; moreover, this correlated with acute lung injury and fibrogenesis (Malaviya *et al.*, 2012; Venosa *et al.*, 2014). In the present studies we analyzed the origin of lung macrophages with a focus on the spleen as an extramedullary source of these cells.

The spleen is the largest lymphatic organ in the body, playing an important role in pathogen recognition, iron recycling and clearance of effete erythrocytes. The spleen has also been shown to act as a reservoir of inflammatory monocytes which are readily mobilized in large numbers to sites of tissue injury (Hiroyoshi *et al.*, 2012; Robbins *et al.*, 2012; Swirski *et al.*, 2009; Wystrychowski *et al.*, 2014), where they differentiate into macrophages and participate in both pro- and antiinflammatory responses (Auffray *et al.*, 2007). In contrast to leukocyte trafficking from the bone marrow, which depends on the

chemokine receptor, CCR2 and its ligand, CCL2 (Tsou *et al.*, 2007), spleen monocyte migration is mediated by angiotensin-II (AT-2) released from injured tissues (Filippatos *et al.*, 2001; Li *et al.*, 2006; Wang *et al.*, 1999) and AT-2 receptor-1 α (ATR-1 α) expressed on inflammatory leukocytes (Swirski *et al.*, 2009). To assess the contribution of spleen monocytes to NM-induced lung inflammation, we used splenectomized (SPX) rats. We found that splenectomy resulted in a decrease in a mature subset of M2 macrophages in the lung following NM exposure; this was accompanied by an increase in M1 macrophages, upregulation of proinflammatory/cytotoxic gene expression, and heightened tissue injury. These data indicate that the spleen is a source of mature infiltrating macrophages that function to limit NM-induced lung injury and fibrogenesis. Identification of the origin of the inflammatory cells that participate in the pathogenic response to vesicants may lead to the development of novel approaches for mitigating pulmonary injury.

RESULTS

Treatment of rats with NM resulted in increased numbers of BAL cells (Table 4); this was observed within 1 d and persisted for at least 7 d. Splenectomy was associated with a delayed response to NM; thus increases in BAL cells were not observed until 3 d post NM. To determine if splenectomy altered the phenotype of cells responding to NM, we analyzed M1 and M2 macrophages in histologic sections. Following NM exposure, a persistent increase in CD11b⁺ inflammatory cells in the lung was observed (Fig. 12, upper panels). Splenectomy had no significant effect on these cells. In contrast, numbers of iNOS⁺ proinflammatory/cytotoxic M1 macrophages were significantly increased in the lungs of SPX rats, relative to sham controls. This was most prominent 7 d post NM, when notable iNOS staining was also noted in the epithelium of SPX rats,

but not sham control rats (Fig. 12, lower panels and Table 6). Expression of iNOS mRNA in inflammatory cells isolated from SPX rats was also significantly upregulated 7 d post NM, when compared to sham rats (Fig. 13). At this time COX-2 mRNA expression was also greater in cells from SPX rats, while levels of MMP-9 were similar. Conversely, 3 d post NM, COX-2, MMP-9 and IL-12 β were significantly reduced in SPX macrophages relative to sham rats (Fig. 13). The effects of splenectomy on NM-induced accumulation of M2 macrophages were also analyzed. While numbers of macrophages staining positively for M2 markers including CD68, CD163, CD206 or YM-1 were generally unaltered by splenectomy (Figs. 14-15 and Table 6), macrophage expression of M2 genes including IL-10, ApoE, PTX-2 and PTX-3, which are upregulated in response to NM in sham rats, were reduced in SPX rats (Fig. 13). Similarly, NM-induced increases in 5-HT2 α and 5-HT7, genes associated with M1 to M2 macrophage phenotypic switching (de las Casas-Engel *et al.*, 2013), were reduced in SPX rats, relative to sham controls (Fig. 13).

To further characterize changes in the phenotype of lung macrophages responding to NM after splenectomy, we used techniques in flow cytometry/cell sorting. Consistent with studies described in Part I above, in sham control rats two CD11b⁺ infiltrating subpopulations were identified in the lung after NM exposure: immature CD43⁺ M1 macrophages and mature CD43⁻ M2 macrophages (Fig. 18). Whereas peak accumulation of CD11b⁺CD43⁺ macrophages was noted 1-3 d post NM, CD11b⁺CD43⁻ macrophages increased gradually for at least 7 d. Splenectomy resulted in a significant increase in CD11b⁺CD43⁻ macrophages in the lung at all times after NM-exposure, while a significant decrease in CD11b⁺CD43⁺ macrophages was observed (Fig. 18). Resident (CD11b⁻CD43⁻) macrophages were also identified in the lungs of both sham and SPX rats. NM exposure resulted in a time related decrease in these cells, most notably at 7 d.

At this time, resident macrophages from SPX rats were more sensitive to NM than cells from sham rats. To determine if splenectomy altered the activity of these cells, we analyzed expression of M1 and M2 genes in sorted subpopulations. In sham rats, immature CD11b⁺CD43⁺ macrophages infiltrating into the lung at 3 d and 7 d post NM expressed iNOS and CCR2, prototypical markers of infiltrating M1 macrophages, while CD11b⁺CD43⁻ infiltrating macrophages expressed IL-10 and ApoE, which are characteristics of M2 macrophages (Table 3). Splenectomy resulted in increases in iNOS and CCR2 expression in CD11b⁺CD43⁺ cells, 3 d after NM exposure. In contrast, CD11b⁺CD43⁻ infiltrating macrophages from SPX rats expressed reduced levels of IL-10 and ApoE; these effects were most prominent 7 d post NM (Table 3). Interestingly, following NM exposure, CCR2 expression also increased in resident alveolar macrophages from SPX rats relative to sham rats.

We also analyzed the effects of splenectomy on expression of genes involved in monocyte/macrophage trafficking to sites of tissue injury. In sham control rats, NM exposure resulted in increased mRNA expression of chemokines/chemokine receptors associated with M1 (CCR2/CCL2, CCL5/CCR5) and M2 (CX₃CR1) macrophage migration to sites of injury (Jacquelin *et al.*, 2013; Tighe *et al.*, 2011; Tsou *et al.*, 2007). NM-induced upregulation of each of these genes was reduced in lung macrophages isolated from SPX rats (Fig. 16). Similarly, NM-induced expression of ATR-1 α , a chemokine receptor important in trafficking of spleen monocytes (Leuschner *et al.*, 2010), was also significantly reduced in lung macrophages from SPX rats relative to sham rats. Decreases in CX₃CR1 and ATR-1 α mRNA levels were correlated with a reduction in protein expression of these receptors in histological sections (Fig. 17). In contrast, numbers of CCR2⁺ macrophages were increased in lungs of SPX rats at 3 d post NM; by 7 d, however, expression levels were similar in sham and SPX animals.

In further studies we determined if changes in macrophage subpopulations in lungs of SPX rats were associated with alterations in NM-induced tissue injury. Following exposure of sham control animals to NM, pronounced cellular infiltration, bronchioalveolar hyperplasia and edema were observed, along with mild mesothelial proliferation, emphysema, metaplasia and fibroplasia at 3 d and 7 d; bronchioectasis was also observed at 7 d; these changes were more rapid and pronounced in SPX rats (Fig. 19, upper panels and Table 4). We also noted extensive perivascular cuffs of leukocytes, and fibrosis beginning within 3 d in SPX rats, but not in sham rats. This was confirmed by Gomori's trichrome staining, which showed increased collagen deposition in SPX rats relative to sham control animals (Fig. 19, lower panels). Splenectomy also resulted in an increase in alveolar epithelial barrier dysfunction, as measured by BAL protein content; however this was not evident until 7 d post NM.

DISCUSSION

NM-induced lung injury and fibrosis are associated with the sequential accumulation of distinct inflammatory macrophage populations in the lung, which display a proinflammatory/ cytotoxic M1 and an antiinflammatory/wound repair M2 phenotype (Malaviya *et al.*, 2012; Sunil *et al.*, 2011b; Sunil *et al.*, 2014; Venosa *et al.*, 2014). When overactivated, these cells contribute to tissue injury and fibrosis, respectively (Murray and Wynn, 2011). The present studies demonstrate that the spleen is a source of a subset of antiinflammatory/wound repair macrophages responding to NM-induced lung injury. Thus, in the absence of the spleen, NM toxicity is exacerbated and fibrosis develops more rapidly. These data suggest that spleen-derived macrophages participate in the resolution phase of vesicant-induced injury.

Cell accumulation in BAL is a marker of an active inflammatory response in the lung (Barnes *et al.*, 2006; Bhalla, 1999; Silkoff *et al.*, 2003). Following NM exposure, a time related increase in BAL cell number was observed. Our findings that splenectomy resulted in a delayed increase in BAL cells relative to sham controls, suggest that the initial wave of inflammatory cells that localize in the lung after NM-induced injury originates in the spleen. At 3 d and 7 d post NM, numbers of BAL cells were comparable in SPX and sham rats. This is consistent with our findings of similar numbers of CD11b⁺ cells in the lung in histologic sections of sham and SPX rats at these times, and by our flow cytometric analysis of isolated lung macrophages. Conversely, after NM exposure, increased numbers of iNOS⁺ M1 macrophages were observed in lung sections from SPX rats, when compared to sham controls, and an increase in the percentage of CD11b⁺CD43⁺ proinflammatory macrophages were recovered from the lung. Macrophages isolated 7 d after exposure of SPX rats to NM also expressed greater levels of iNOS, as well as COX-2 mRNA than cells from sham rats and iNOS was upregulated in sorted CD11b⁺CD43⁺ cells. Reactive nitrogen species and proinflammatory prostaglandins generated via iNOS and COX-2, respectively, have been implicated in tissue injury induced by vesicants (Malaviya *et al.*, 2012; Mantovani *et al.*, 2004; Sunil *et al.*, 2012), and they may contribute to the heightened sensitivity of SPX rats to the toxic effects of NM; they may also play a role in reducing numbers of CD11b⁺CD43⁺ resident macrophages recovered from the lung. Of note, 3 d post NM, macrophage expression of COX-2, MMP-9 and IL-12 α was decreased in SPX rats, relative to sham controls; IL-12 α was also decreased at 7 d. These findings are in agreement with reports that the spleen is a source of mediators which regulate the sensitivity of macrophages to M1 inducers (Billiar *et al.*, 1988; Steeg P.S., 1980; Wang *et al.*, 2014).

The effects of splenectomy on NM-induced accumulation of M2 macrophages in the lung varied depending on the subset. Thus, while CD68⁺, CD163⁺, CD206⁺ and YM-1⁺ macrophages were largely unaffected by splenectomy, the accumulation of mature CD11b⁺CD43⁻ M2 macrophages in the lung in response to NM was delayed, and the cells were reduced in number. This indicates that M2 macrophage subpopulations originate from distinct hematopoietic sites, and that CD11b⁺CD43⁻ M2 macrophages are derived, at least in part, from the spleen. Loss of these cells most likely accounts for the reduced numbers of BAL cells recovered from the lung 1 d post NM. Expression of M2 genes involved in down-regulating inflammation and fibrosis (IL-10, PTX-2 and PTX-3), and inducing M1 to M2 phenotypic switching (ApoE, 5-HT2 α and 5-HT7) (Baitsch *et al.*, 2011; de las Casas-Engel *et al.*, 2013; Murray *et al.*, 2011; Murray, 2005; Pilling and Gomer, 2014) was significantly reduced in macrophages isolated from SPX rats, when compared to sham controls. A similar reduction in M2 (IL-10 and ApoE) gene expression was also observed in mature infiltrating CD11b⁺CD43⁻ cells from SPX rats. This suggests that some M2 macrophage subpopulations accumulating in the lung of SPX rats in response to NM may be functionally impaired. In this regard, previous studies have shown that the splenic stroma releases mediators such as IL-10, which support maturation of antiinflammatory macrophages and dendritic cells (Gotoh *et al.*, 2012; Svensson *et al.*, 2004; Tang *et al.*, 2006). Increases in M1 macrophages in lungs of SPX rats may be due, in part, to a loss of spleen-derived suppressive M2 macrophages which counteract their activity, a deficit which may also contribute to exacerbated NM toxicity. This is supported by findings that splenectomy results in blunted antiinflammatory signaling after acute endotoxemia and increased lethality (Huston *et al.*, 2006; Rosas-Ballina *et al.*, 2008).

During the inflammatory response, monocytes and macrophages are recruited to sites of injury through a complex network of chemokines and chemokine receptors.

Whereas proinflammatory cells are recruited in large part via CCL2/CCR2 and CCL5/CCR5, fractalkine/CX₃CR1 regulates antiinflammatory/wound repair macrophage trafficking (Auffray *et al.*, 2007; Mack *et al.*, 2001; Tighe *et al.*, 2011; Tsou *et al.*, 2007). Macrophages isolated from NM exposed rats expressed increased levels of chemokines and chemokine receptors associated with M1 (CCR2, CCR5, CCL2 and CCL5) monocyte/macrophage trafficking, confirming that some subpopulations of proinflammatory macrophages accumulating to the lung after NM originate in the bone marrow. Following splenectomy, expression of chemokines/chemokine receptors was attenuated, most prominently 3 d after NM exposure. These results were surprising, since M1 macrophages were increased in lungs of SPX rats. It may be that peak expression of these chemokines/chemokine receptors occurred earlier than 3 d. Numbers of CCR2⁺ macrophages were significantly greater in SPX rats compared to sham, consistent with the notion of increased recruitment of proinflammatory M1 macrophages from the bone marrow in the absence of the spleen, likely due to a loss of splenic suppressive/regulatory factors (Gotoh *et al.*, 2012). CX₃CR1 mRNA and protein expression were also increased at 3 d and 7 d post NM in sham rats. This was significantly reduced in SPX rats, consistent with reduced antiinflammatory CD11b⁺CD43⁻ M2 macrophage recruitment after splenectomy.

Recent studies have identified ATR-1 α as important in splenic leukocyte trafficking (Arndt *et al.*, 2006; Leuschner *et al.*, 2010; Swirski *et al.*, 2009). Our findings of increased ATR-1 α mRNA and protein expression by macrophages after NM are in accord with a splenic origin of some of these cells. A significant reduction in ATR-1 α expression was observed in macrophages from SPX rats, suggesting that spleen-derived factors may regulate ATR receptor expression in inflammatory cells. AT-2 has been shown to promote bone marrow myeloid stem cell proliferation and CCR2-dependent macrophage migration (Strawn *et al.*, 2004; Tsubakimoto *et al.*, 2009) in

models of hypertension, atherosclerosis and fibrosis (Ishibashi *et al.*, 2004; Xu *et al.*, 2011). It is possible that following splenectomy, AT-2 released from NM-injured lung contributes to the recruitment of CCR2⁺ M1 bone marrow-derived macrophages to the lung resulting in exacerbated tissue injury. Further experiments are required to explore this possibility.

Changes in M1 and M2 macrophage subpopulations in SPX rats were associated with more rapid and pronounced tissue damage in response to NM. This was characterized by bronchioalveolar hyperplasia and edema, mesothelial proliferation, emphysema, metaplasia and fibroplasia. Interestingly, perivascular cuffs of leukocytes, and fibrosis were evident, a response not previously observed 7 d post NM exposure (Malaviya, Sunil, Cervelli, Anderson, Holmes, Conti, Gordon, Laskin and Laskin, 2010). Prolonged increases in NM-induced BAL protein levels, a marker of increased alveolar epithelial permeability, were also observed in SPX rats. The role of spleen-derived leukocytes and mediators they release in the acute and chronic inflammatory responses to NM has not been established. Previous studies have shown that the spleen functions as a reservoir of proinflammatory monocytes in models of myocardial infarction (Swirski *et al.*, 2009) and fibrosis (Tanabe *et al.*, 2015). In contrast, our studies suggest that spleen-derived macrophages are involved in limiting tissue injury and fibrosis after NM. Moreover, in their absence, processes related to tissue repair are delayed. We speculate that after NM exposure, spleen-derived macrophages function to counterbalance cytotoxic/proinflammatory M1 macrophages and that in their absence, tissue injury predominates. Our findings that M1 gene expression was unaffected by splenectomy, while M2 gene expression was reduced, provides support for the idea of an imbalance between proinflammatory and anti-inflammatory macrophages contributes to NM toxicity.

Taken together these studies demonstrate that there are distinct subsets of M2 macrophages participating to the pathogenic response to NM, and that they originate

from different tissue precursors. They also provide evidence for a role of spleen monocytes as important in dampening the inflammatory response and promoting wound repair. Characterization of lung macrophage subpopulations and their origin represents an important step in understanding mechanisms of macrophage recruitment after NM-injury and may provide novel insights into specific targets for therapeutic interventions.

PART III. ELUCIDATE EPIGENETIC MECHANISMS REGULATING LUNG MACROPHAGE ACTIVATION IN RESPONSE TO NM-INDUCED TISSUE INJURY INTRODUCTION

NM-induced pulmonary injury and fibrosis is associated with oxidative stress and a persistent macrophage dominant inflammatory response (Malaviya *et al.*, 2012; Weinberger *et al.*, 2011). Macrophages are key cellular mediators of innate immune responses to tissue injury (Laskin *et al.*, 2011; Mantovani *et al.*, 2004; Martinez and Gordon, 2014). In response to inflammatory mediators they encounter in the tissue microenvironment, macrophages become activated, developing into proinflammatory/cytotoxic M1 or antiinflammatory/wound repair M2 subpopulations (Mantovani *et al.*, 2010). Excessive release of mediators by M1 and M2 macrophages has been implicated in cytotoxicity and fibrosis, respectively (Murray and Wynn, 2011).

Accumulating evidence suggests that macrophage activation is controlled, in part, by epigenetic regulatory mechanisms that modify chromatin activity and gene expression, including alterations in histone structure and function and microRNAs (miRNA) expression (Berger, 2007; He and Hannon, 2004; Jaenisch and Bird, 2003; Shanmugam and Sethi, 2013). miRNAs are small (18-22 base pairs) RNAs synthesized from non-coding regions of genes and processed within the nucleus. These ncRNAs act by inhibiting the translation of cytoplasmic target mRNAs (Orom *et al.*, 2008). miRNAs are differentially regulated by inflammatory mediators resulting in initiation, propagation and resolution of the inflammatory response; this is thought to be due to differential activation of macrophages and inflammatory gene expression (Roy and Sen, 2012; Sonkoly and Pivarcsi, 2009; Vettori *et al.*, 2012; Zhang *et al.*, 2013).

Histones are proteins involved in packaging DNA into nucleosomes. Posttranslational modifications at specific sites on histone proteins alter their interaction with nuclear proteins and DNA, leading to changes in gene expression. It appears that

the balance between the acetylated and deacetylated state of histones plays a role in regulating macrophage gene expression during acute and chronic inflammatory responses (Bayarsaihan, 2011; Ishii *et al.*, 2009; Ivashkiv, 2013; Kittan *et al.*, 2013; Wen *et al.*, 2008). Two families of enzymes regulate histone acetylation: histone acetyltransferases (HAT), which catalyze the addition of acetyl moieties to histones, and histone deacetylases (HDAC), which removes them from histones (Peserico and Simone, 2011). Valproic acid (VPA) is a short aliphatic acid originally developed as a mood stabilizer and antidepressant (Ueda and Willmore, 2000). Studies have shown that VPA exerts antiinflammatory activity, a response due to its ability to inhibit histone deacetylases (Ximenes *et al.*, 2013). In our next series of studies we characterized the effects of NM on histone structure and miRNA expression in lung macrophages. We also assessed the role of histone deacetylases in macrophage activation following NM-induced lung injury using VPA.

A. EFFECTS OF NM ON MACROPHAGE miRNA EXPRESSION AND HISTONE STRUCTURE

RESULTS

In our first series of studies we analyzed the effects of NM on expression of a panel of 84 miRNAs which are known to play important roles in inflammation (Sonkoly and Pivarcsi, 2009) and fibrosis (Jiang *et al.*, 2010; Vettori *et al.*, 2012) using RT-PCR. Within 1 d of NM exposure, a number of miRNAs were upregulated, most significantly those associated with the inflammatory response (miR125a and -b, -141, -144, -200, -221, -34c, -497 and -9) (Fig. 26). Increases in miR125, -141, -144, -221, -322, -34c, -497 and -9 persisted up to 3 d, while only miRNA141, -144, -497 and -9 remained upregulated up to 28 d. miRNAs associated with chronic inflammation and fibrosis (miR29, -23, let7a-d) were unchanged 1 d post NM, while, by 3 d and 7 d, expression of

these miRNAs was upregulated (let7a, -d, -e, -23) or downregulated (let7f, -26a, -b, -448); although the majority of miRNAs returned to baseline levels by 28 d, the ones associated with fibrosis remained altered up to 28 d (miR9, -29b, -29c, -497). Changes in miRNA expression detected by microarray were next validated using RT-PCR. We found that expression of miR146 and let7a was decreased in a time dependent manner following NM exposure, while expression of miR9 and -125b were upregulated acutely (1 day) and persisted up to 7 days. In addition, whereas miR127 was increased in the early inflammatory phase and returned to control levels during tissue fibrosis, miR21 was increased in a time related manner peaking at 28 d.

NM exposure resulted in increased phosphorylation of the histone variant H2A.X, a marker of DNA double strand breaks in macrophages, peaking within 1 d. By 3 d both macrophages and epithelial cells expressed γ -H2A.X, although at reduced levels (Fig. 20). In further studies we analyzed alterations in lung macrophage, focusing on modifications that promote (H3K4TM, H3K9Ac, H3K36DM) or repress (H3K4MM, H3K9TM, H3K27TM) gene expression. Western blot analysis showed that NM exposure was associated with a significant increase in expression of H3K4TM and H3K9Ac, with no effects on H3K4MM, H3K9TM or H3K27TM (Fig. 21). To confirm these observations we analyzed their expression in histologic sections. We found increased H3K9Ac expression at 1 d, which persisted up to 7 d in macrophages, while epithelial cells were positive only at 28 d. H3K9TM was marginally increased, but only at 3 d (Fig. 22). Analysis of the histone dimethylation status on lysine-36 (H3K36) showed elevated expression in controls which were unaffected by NM exposure (Fig. 23). A similar trend was also observed for H3K4MM, while H3K4TM steadily increased in macrophages at 1 d and 3 d, but returned to baseline by 7 d (Fig. 23).

In further studies we analyzed expression of histone acetyltransferases (HAT) and deacetylases (HDAC). A time related increase in expression of histone

acetyltransferase, p300, was evident at 1 d which peaked at 7 d, returning to control levels by 28 d (Fig. 24, left panels). Expression of the NAD-dependent histone deacetylase, SIRT-1, was only minimally upregulated after NM exposure, while the type I deacetylase, HDAC2, was highly expressed in the lung after NM. Expression of HDAC2 was biphasic after NM, peaking at 3 d and at 28 d. At 3 d expression was evident in macrophages and epithelium, while at 28 d positive staining was predominantly epithelial (Fig. 24, right panels). We also observed a biphasic increase in HDAC activity at 1 d and 28 d after NM exposure (Fig. 25).

DISCUSSION

The present studies represent the first to characterize changes in miRNA expression in lung macrophages following NM exposure. We hypothesized that these alterations may be important in controlling macrophage activation towards a proinflammatory or profibrotic phenotype. Previous studies have shown that immature macrophages and monocytic precursors express lower levels of miRNA, in part due to lack of Dicer protein, the master regulator for their synthesis (Coley *et al.*, 2010). As these cells mature, Dicer expression increases, resulting in increased global miRNA abundance (Coley *et al.*, 2010). In accord with notion, our array analysis showed that within 1 d NM exposure, there was an overall trend towards increased miRNA expression, which persisted at 3 d and 7 d. In addition their expression was significantly more variable. This suggests that a multitude of events are occurring at these times, including suppression of the acute inflammatory response. This is supported by findings that proinflammatory (miR125 and -127) and immunosuppressive miRNAs (miR181), proresolution (miR26), profibrosis (miR21, miR29c) were all upregulated at 3 d (Xie *et al.*, 2013; Ying *et al.*, 2015). Our findings that miR9, miR125b and miR351, thought to promote inflammation by stimulating TNF α and its downstream targets (Chaudhuri *et al.*, 2011), were also

upregulated in macrophages suggest that these miRNAs may contribute M1 macrophage activation. Conversely, a time related decrease in miR146 expression was observed; although miR146 is induced by similar stimuli (i.e. NFkB and TNF α), it functions by tempering inflammatory signaling (Taganov *et al.*, 2006), and reduce cytokine production (Iyer *et al.*, 2012). These findings are interesting, as downregulation of miR146 may favor early activation of inflammatory macrophages during the acute injury after NM, whereas it suggests that it may not participate to inflammation termination.

miR34 has been identified as a tumor suppressor and has recently been associated with suppression of the inflammatory response in macrophages and T cell activation (Jiang *et al.*, 2012; Shin *et al.*, 2013). Consistent with these findings, we found increased levels of miR34c in lung macrophages after NM, which persisted up to 28 d. This suggests that miR34c may contribute to the resolution of the inflammatory response, and that this begins early after vesicant exposure. The inflammatory miR200 cluster (miR200a/c, miR429 and miR141) was also upregulated following exposure to NM, peaking at 1 d, and persisting up to 28 d. miR141 and -200 have been shown to be increased during oxidative stress and to participate in a negative feedback loop by inhibiting IL-6 and TNF α expression in macrophages (Wendlandt, 2012). It is possible that following early NM-induced oxidative, these miRNAs participate in re-establishing homeostasis, potentially by reducing proinflammatory cytokine release. One of the targets of miR200 is the E-cadherin suppressor, ZEB1. Overexpression of miR-200 caused up-regulation of E-cadherin and reduced epithelial-mesenchymal transition (EMT) by reducing cell motility (Park *et al.*, 2008). Conversely, suppression of miR-448 was shown to favor EMT in breast cancer both *in vitro* and *in vivo* (Li *et al.*, 2011). Our findings of persistent downregulation of miR448, but increased miR200 suggest that there is redundancy in the regulation of the macrophage motility in response to NM.

miR-17 and miR-106a were also upregulated after NM. These miRNAs blunt expression of macrophage differentiation marker, signal-regulatory protein α (SIRP α), which promotes peripheral monocyte recruitment and cellular activation (Janssen *et al.*, 2008; Zhu *et al.*, 2013). Increases in these miRNAs may contribute to macrophage proinflammatory activation during the acute inflammatory response to NM. Ly6C^{hi} inflammatory macrophages isolated from the spleen in a model of lateral sclerosis, have previously been used to identify a miRNAs signature for macrophage activation; (Butovsky *et al.*, 2012). Although the signature suggested by Butovsky *et al.* consisted of 9 miRNAs, only two (let7b and miR142) showed analogous increases after NM, confirming that these miRNAs indeed participate in the inflammatory response. Using cultured bone marrow-derived macrophages (BMDMs) programmed to towards an M1 (LPS+IFN γ) or M2 (IL-4) phenotype, Zhang *et al.* (2013) characterized miRNAs changes in these cells. They found that miR181 was upregulated, while miR146a-3p, miR143-3p and miR145-5p were downregulated in M1, when compared to M2 macrophages (Zhang *et al.*, 2013). Our findings of reduced miR146 and miR145, but elevated miR181, are consistent with these results. Thus, whereas miR145 was significantly upregulated 1-7 d after NM exposure, its expression was reduced at 28 d, suggesting that there may be a transition in macrophage phenotype at this time. In support of this notion, miR125a, which has been associated with macrophage phenotype switching, was upregulated after NM exposure (Banerjee *et al.*, 2013). Notably, our array analysis showed no changes in miR98, while miR21 was significantly upregulated. miR98 and miR21 have been reported to inhibit the expression of inflammatory genes in macrophages through IL-10 regulation (Sheedy *et al.*, 2010). miR21 is one of the most well studied miRNAs and it has been shown to be important in the generation of ROS, and the development of lung fibrosis production by altering superoxide dismutase and TGF β expression, respectively (Liu *et al.*, 2010; Wang *et al.*, 2012b; Zhang *et al.*, 2012). Another miRNA

associated with lung, kidney and liver fibrosis is miR29 (Qin *et al.*, 2011; Roderburg *et al.*, 2011; Xiao *et al.*, 2012). We found a persistent reduction in miR29 expression compared to control, suggesting a potential role in NM-induced fibrosis; however, this remains to be established, as our RT-PCR validation studies did not show significant decrease in its expression.

NN is known to cause DNA alkylation leading to single and double strand breaks (Boldogh *et al.*, 2003). One of the early mechanisms signaling DNA damage is phosphorylation of the histone variant H2A.X (Clingen *et al.*, 2008; Kuo and Yang, 2008; Rossetto, Avvakumov and Côté, 2012; Sharma *et al.*, 2012). Our findings of increased γ -H2A.X expression 1 d and 3 d post NM are consistent with the acute DNA damaging effects of NM. Of note, macrophages were the predominant cell type expressing H2A.X suggesting that these cells may be preferentially targeted by NM or that macrophages phagocytize dying cells which have been modified by NM. As a result of H2A.X phosphorylation, cells rapidly cease proliferating and increased gene expression to initiate DNA repair.

Histone modifications associated with euchromatin and heterochromatin formation were also assessed in macrophages after NM, as these are important in regulating gene expression (Ivashkiv, 2013). While there were no changes in histone modifications associated with silencing the chromatin (H3K27TM and H3K9TM), increases in heterochromatin (H3K9Ac, H3K4TM and H3K36DM) were observed indicating that 1-3 d after exposure to NM, macrophage initiate chromatin rearrangement directed towards increased gene expression. This is in accord with previous studies from our laboratory demonstrating that shortly after NM exposure there is increase expression of several inflammatory genes (Malaviya *et al.*, 2012; Sunil *et al.*, 2012; Venosa *et al.*, 2014). Furthermore, in support of our findings the triad of histone modifications H3K4TM, H3K9Ac and H3K36TM has been identified as a specific signature of transcriptionally

active genes (Guenther *et al.*, 2007). In addition to its role in promoting gene expression, histone acetylation has been associated with DNA repair, macrophage activation and phenotypic switching (Ishii *et al.*, 2009; Ogiwara *et al.*, 2011; Qin and Parthun, 2002; Sica and Mantovani, 2012). Histone acetyltransferases and deacetylases are the two families of enzymes pivotal in regulating histone acetylation during homeostatic conditions. Dysfunction of these enzymes has been shown to impair cellular differentiation, proliferation and activation (Peserico and Simone, 2011). Our observation that both of these enzymes are upregulated 3 d after NM exposure supports the notion that a key factor in controlling macrophage activation is a balance between acetylation and deacetylation. Whereas HAT (p300) expression was maximum 7 d post NM, peak HDAC2 expression was observed at 3 d and 28 d. Increased expression of HDACs correlated with the total activity of these enzymes at 1 d and 28 d. These findings suggest distinct roles for HDACs in the acute inflammatory phase and fibrogenesis. Thus, whereas early HDAC upregulation may be directed to counter NM-induced increases in histone acetylation (Barnes *et al.*, 2005; Correa *et al.*, 2011; Li and Alam, 2012; Rahman *et al.*, 2004), its upregulation at 28 d, when the acute inflammatory response is terminated, appears to be linked to fibrogenesis (Pang and Zhuang, 2010; Yoshikawa *et al.*, 2007).

In summary, these studies suggest that NM exposure is associated with altered histone remodeling consistent with an increase in gene expression, while miRNA expression appears more elaborate and redundant. Our findings of late miRNA expression associated with phenotype switching and fibrogenesis, suggest that epigenetic mechanisms may regulate several processes progressing to fibrosis. These studies may lead to the identification of an epigenetic signature to characterize activated macrophages after NM exposure.

B. THE ROLE OF HISTONE DEACETYLASES IN REGULATING NM-INDUCED LUNG MACROPHAGE ACTIVATION

RESULTS

In our next series of studies, we used the histone deacetylase inhibitor, valproic acid, to analyze the role of these enzymes in macrophage activation following NM exposure. As described above, NM exposure resulted in upregulation of the histone deacetylase, HDAC2 and the histone acetyltransferase, p300. This was observed at 3 d and 7 d post NM in both macrophages and epithelial cells and was associated with an increase in acetylation of histone H3K9 (Fig. 27). Treatment of rats with VPA blunted the effects of NM on expression of HDAC2, p300; reduced H3K9 acetylation was also noted, a response most prominent 3 d following NM exposure.

We next assessed the effects of VPA on the phenotype of macrophages responding to NM. VPA administration was found to reduce the number of iNOS⁺ proinflammatory M1 macrophages in the lung at 3 d and 7 d post NM (Fig. 28 and Table 8). mRNA expression of iNOS, as well as other M1 markers including COX-2, IL-12 β and MMP-9 (Mantovani *et al.*, 2004) was also reduced in macrophages isolated from lungs of VPA treated rats (Fig. 29). In contrast, VPA administration augmented the stimulatory effects of NM on the accumulation of CD68⁺ and CD163⁺ antiinflammatory M2 macrophages in the lung, and on macrophage mRNA expression of the M2 markers, IL-10 and ApoE (Fig. 28, center and lower panels and Fig. 29); this was most prominent 3 d post NM.

In our next series of studies, we used techniques in flow cytometry to further characterize the effects of VPA on macrophages responding to NM. Three macrophage subpopulations were identified in the lung after NM: resident CD11b⁻CD43⁻, immature infiltrating CD11b⁺CD43⁺ and mature infiltrating CD11b⁺CD43⁻ macrophages (Venosa *et*

al., 2014). While maximal accumulation of immature infiltrating macrophages was evident 3 d post NM, mature macrophages gradually increased in numbers for 7 d (Fig. 31). VPA administration resulted in a rapid (3 d) and persistent (7 d) increase in immature CD11b⁺CD43⁺ macrophages in the lung; in contrast, NM-induced increases in mature CD11b⁺CD43⁻ macrophages was delayed for 7 d post NM. Following NM exposure, numbers of resident CD11b⁻CD43⁻ macrophages decreased; VPA treatment had no effect on these cells (Fig. 31).

The chemokine receptors CCR2 and CX₃CR1, which are known to regulate trafficking of M1 and M2 macrophages, respectively (Nahrendorf *et al.*, 2007; Tighe *et al.*, 2011; Tsou *et al.*, 2007), were upregulated in the lung after NM exposure. CCL2, the ligand for CCR2 was also upregulated after NM exposure. Administration of VPA caused a significant reduction in NM-induced CCR2 and CCL2 gene expression in lung macrophages at 3 d and 7 d post exposure (Fig. 29). This was also observed at the protein level in histologic sections (Fig. 30, upper panels). CX₃CR1 mRNA expression was also reduced by VPA, but only at 7 d post NM (Fig. 29), while its protein expression was unaltered (Fig. 30, center panels). Conversely, after VPA administration, we noted a significant increase in NM-induced mRNA and protein expression for ATR-1 α , a receptor important in spleen monocyte migration (Nahrendorf *et al.*, 2007), when compared to vehicle treated animals (Figs. 29 and 30, lower panels).

We next assessed the effects of VPA on NM-induced oxidative stress and toxicity. NM exposure resulted in increased CYPb5 expression, a marker of oxidative stress (Menoret *et al.*, 2012; Roman, 2002), in lung macrophages and epithelial cells; this was reduced by VPA at both 3 d and 7 d post NM (Fig. 32, upper panels). VPA treatment also reduced NM-induced epithelial and type-II cell proliferation, as measured by PCNA staining (Fig. 32, center panels). Conversely, VPA augmented NM-induced increases in expression of the histone variant H2A.X, which is associated with DNA

damage and cell cycle arrest (Fragkos *et al.*, 2009; Podhorecka *et al.*, 2010) (Fig. xx, lower panels). VPA administration also resulted in significantly reduced numbers of cells recovered in BAL after NM (Fig. 33), with no effect on BAL protein levels or histopathological changes in the lung (Figs. 33 and 34 and Table 7).

DISCUSSION

Evidence suggest that chromatin rearrangements, in large part as a consequence of histone modifications, play a role in regulating macrophage activation state and function during the initiation, progression and resolution of the inflammatory response (Ishii *et al.*, 2009; Kittan *et al.*, 2013; Mantovani *et al.*, 2010; Zhu and Wani, 2010). Three major chromatin states have been characterized in macrophages: a repressed/stimulus-refractory state, which is associated with negative histone markers [H3K9TM and H3K27TM], an active/open state, characterized by positive histone markers [H3K4TM and H3K9Ac]; and a poised/intermediate state, typical of resting macrophages, characterized by both positive and negative histone marks. These poised cells exhibit a partially open chromatin conformation, easily susceptible to stimuli (Bayarsaihan, 2011; Ivashkiv, 2013; Natoli *et al.*, 2011). The present studies are important in understanding the dynamics of epigenetic mechanisms mediating macrophage activation, and suggest that histone deacetylases play a role in macrophage polarization following NM exposure.

HDACs play an important role in limiting inflammatory gene expression. Pulmonary degenerative diseases such as asthma and chronic obstructive pulmonary disease, have demonstrated that chronic inflammation results in reduced HDAC2 expression, thus contributing to disease pathogenesis and progression (Barnes *et al.*, 2005; Cosio *et al.*, 2004). Conversely, acute injury induced by NM was associated with

upregulation in HDAC2 expression 1 d and 3 d post NM exposure, confirming that these enzymes participate in the inflammatory response. Notably, VPA suppressed NM-induced HDAC2 upregulation, a response that may be responsible for the altered gene expression observed in isolated lung cells. Similar reduction of HDAC2 was observed in previous studies using VPA (Kramer *et al.*, 2003; Pufahl *et al.*, 2012). As predicted, decreased HDAC2 expression in lung histologic section was associated with increased histone H3K9 acetylation, confirming that VPA was an effective HDAC inhibitor in our model. We also found that NM-induced histone acetyltransferase expression was decreased after VPA treatment. These results were surprising as previous reports have shown that HDAC inhibition is associated with p300 transactivation (Liu *et al.*, 2006; Stiehl *et al.*, 2007). This may be due to VPA-dependent activation of protein phosphatase 2A, an enzyme known to increase p300 ubiquitin degradation (Chen *et al.*, 2005).

Inhibition of HDACs with VPA was correlated with reduced numbers of iNOS⁺ M1 macrophages in the lung after NM, and with dampening of proinflammatory gene expression (iNOS, COX-2, IL-12 β and MMP-9). Similar antiinflammatory effects of VPA and other histone deacetylase inhibitors have been reported in macrophages in models of neuritis and rheumatoid arthritis (Grabiec *et al.*, 2010; Zhang *et al.*, 2008b; Zhang *et al.*, 2010; Zheng *et al.*, 2014), suggesting that HDACs are important in modulating proinflammatory macrophage activation. This is supported by findings that HDAC7 is upregulated in M1-elicited peritoneal macrophages, while M2 macrophage activation is suppressed by HDAC3 (Mullican *et al.*, 2011; Shakespear *et al.*, 2013). In contrast to its suppressive effects on M1 macrophages, VPA increased numbers of CD68⁺ and CD163⁺ M2 macrophages in the lung at 3 d and 7 d post NM exposure, and upregulated mRNA levels of M2 markers associated with suppressing inflammation (IL-10) (Murray,

2005), and M1 to M2 macrophage phenotype switching (ApoE) (Baitsch *et al.*, 2011), after VPA treatment. These results are in agreement with recent reports showing that HDAC inhibition is associated with M1 to M2 phenotype switching in cultured macrophages and in a model of traumatic brain injury (Wang *et al.*, 2015; Wu *et al.*, 2012), and with increased macrophage IL-10 production (Park *et al.*, 2007).

VPA was also found to augment early NM-induced accumulation of immature CD11b⁺CD43⁺ macrophages in the lung as well as subsequent mature CD11b⁺CD43⁻ infiltrating macrophages. Thus, at 3 d post NM, significantly greater numbers of CD11b⁺CD43⁺ cells were observed, with only minimal infiltration of CD43⁻ macrophages. By 7 d these infiltrating populations were comparable in numbers. These findings suggest that VPA may recruit a distinct subset of macrophages to the lung which exhibits a more immature phenotype, which is in accord with earlier findings showing reduced cell maturation (Rosborough *et al.*, 2012). Although our mRNA and protein analysis showed imbalanced macrophage activation towards an M2 polarized state, it remains unclear whether the activation of CD43⁻ and CD43⁺ subsets is also altered after VPA administration (Venosa, 2014).

Expression of chemokines and chemokine receptors involved in leukocyte trafficking to sites of injury were also altered by VPA in our NM-induced lung injury model. Thus, HDAC inhibition resulted in reduced mRNA expression for CCR2 and CCL2, as well as numbers of CCR2⁺ M1 macrophages in the lung, which is consistent with our observation of reduced numbers of iNOS⁺ M1 macrophage in the lung. In contrast, CX₃CR1 expression, which is associated with M2 trafficking was unaffected by VPA. These findings are in accord with reports that broad spectrum HDAC inhibitors modulate leukocyte migration in models of rheumatoid arthritis and orthotopic glioblastoma suggested (Brogdon *et al.*, 2007) by blunting synthesis and release of

macrophage chemokines, including CCL2 and CX₃CR1 (Alvarez-Breckenridge *et al.*, 2012; Grabiec *et al.*, 2010; Kim *et al.*, 2012; Roger *et al.*, 2011; Vinolo *et al.*, 2011; Zain, 2012). However, it appears that in our model, the effects of VPA may be limited to proinflammatory macrophage chemokines/chemokine receptors. Interestingly, VPA was associated with a significant increase in mRNA and protein expression of ATR-1 α , a receptor involved in monocyte migration from the spleen (Swirski *et al.*, 2009). These data suggest that HDAC inhibition alters cellular trafficking in favor of splenic recruitment. This is supported by previous studies demonstrating that administration of the HDAC inhibitor trichostatin-A enhances splenic macrophage mobilization (Rosborough *et al.*, 2012).

HDAC inhibitors have been shown to enhance DNA-instability resulting in decreased proliferation (Lee *et al.*, 2010). Consistent with these reports, we found that VPA suppressed NM-induced PCNA expression, a marker of cell proliferation, prominently at 7 d. This was correlated with increased activation of the histone variant H2A.X, a signal for cell cycle arrest and repair following DNA double strand breaks (Kuo and Yang, 2008; Sharma *et al.*, 2012). Together these data indicate that HDAC inhibition protects from NM-induced DNA stress through stimulation of histone variant and reduced cell proliferation.

VPA was also found to blunt NM-induced oxidative stress, as measured by CYPb5 expression (Finn *et al.*, 2011; Roman, 2002). This may be a consequence of reduced numbers of M1 proinflammatory/cytotoxic macrophages in the lung, or to VPA-dependent activation of redox-sensitive transcription factors. This is supported by findings that HDAC inhibitors reduce the oxidative burden via induction of redox-sensitive transcription factors in models of spinal cord injury and ischemia indicated that (Kawai and Arinze, 2006; Lee *et al.*, 2014; Wang *et al.*, 2012a). Earlier studies have

shown that following VPA administration, serum levels of ROS increase (Tong *et al.*, 2005). This prooxidant activity may account for the increased BAL cell numbers in control rats after VPA administration. Conversely, our findings that HDAC inhibition effectively reduced NM-induced increases in BAL cell content, an early marker of lung inflammation (Bhalla, 1999), suggest that VPA possess antiinflammatory activity. In contrast, NM-induced tissue injury, measured by BAL protein levels and histopathologic analysis were unaffected by VPA. It may be that changes in lung macrophage subpopulations after VPA administration are not sufficient to induce significant alterations in NM-induced toxicity; however, this remains to be determined.

Our mRNA and protein analysis of macrophages indicated that HDAC inhibition with VPA promotes a dominant M2-biased macrophage phenotype. This is supported by our findings of reduced expression of chemokines associated with M1 macrophages recruitment, as well as reduced numbers of M1 macrophages in the lung. Conversely, a persistent accumulation of immature CD11b⁺CD43⁺ macrophages, previously shown to be M1-biased (Venosa *et al.*, 2014), was noted in the lung after VPA. These data suggest that VPA may alter the maturation state and phenotype of the cells infiltrating into the lung after NM exposure.

Taken together our studies show that HDACs play pivotal role in macrophage activation after NM exposure. In addition, they suggest that HDACs may play a role in recruitment and maturation of these subsets. Characterization of the mechanisms mediating leukocyte activation represents an important step in understanding the role of these cells in NM-induced lung injury and may provide novel targets for therapeutic interventions.

OVERALL SUMMARY

The overall objective of these studies was to characterize macrophage subpopulations responding to NM-induced pulmonary inflammation and fibrosis, and investigate mechanisms of recruitment and activation of these cells. We hypothesized that the development and resolution of inflammation following NM exposure was associated with distinct subsets of activated macrophages, and that macrophage activation is mediated by epigenetic alterations. The results of these studies demonstrate that after vesicant exposure, there is an early (1-3 d) accumulation of iNOS⁺ CCR2⁺, and immature CD11b⁺CD43⁺ proinflammatory/cytotoxic M1 macrophages in the lung, while CD68⁺, CD163⁺, CD206⁺, and YM-1⁺ antiinflammatory/wound repair M2 macrophages, as well as CD11b⁺CD43⁻ mature macrophages, accumulate more gradually, beginning at 3 d and increasing for at least 28 d. The fact that the M2 macrophages were enlarged, vacuolated and clustered in areas of fibrosis is consistent with a role of these cells in the fibrogenic process. The timing of increases in M1 and M2 macrophage genes in the lung after NM exposure followed a similar trend, with increased M1 proinflammatory (iNOS, COX-2, MMP-9, IL-12 α) occurring early after exposure (1-3 d), while M2 (IL-10, ApoE, PTX-2 and CTGF) genes were increased later after NM (3-7 d). Changes in macrophages subpopulations and gene expression were correlated with NM-induced acute lung injury and the development of fibrosis, suggesting a potential role of these macrophage subsets in the pathological response to NM.

Increased expression of chemokines and chemokine receptors involved in macrophage trafficking from both bone marrow (CCR2, CCL2, CCR5, CCL5, CX₃CR1) and spleen (ATR-1 α), were also upregulated after NM exposure, indicating that lung infiltrating cell populations originate for both of those organs. This was supported by our findings of increased proinflammatory macrophages (iNOS, and COX-2) in the lung of

SPX rats, while a subset of antiinflammatory macrophages was significantly reduced (CD11b⁺CD43⁻), a response associated with exacerbated toxicity and premature fibrosis.

Another goal of these studies was to characterize epigenetic mechanisms potentially involved in regulating macrophage activation after NM exposure. For these studies we focused on miRNAs and histone modifications. Our observation of predominant expression of γ -H2A.X, a DNA-damage induced histone variant associated with chromatin remodeling, in macrophages suggests that histone modifications may play a role in their response to NM. Both western blotting and immunohistochemical analysis showed that within 1 d of NM exposure there was a significant increase in histone modifications associated with increased gene expression, including H3K9Ac and H3K4TM, whereas repressive markers such as H3K9TM and H3K27TM were unaltered. To assess the role of acetylation/deacetylation of histones in macrophage activation, we used the HDAC inhibitor, valproic acid (VPA). Administration of VPA resulted in reduced HDAC2 expression in the lung after NM, which correlated with an increase in H3K9 acetylation. This was associated with macrophage switching from an M1 to an M2 phenotype. Interestingly, at 3 d post exposure, significant numbers of CD11b⁺CD43⁺ macrophages were observed in the lung after VPA, while CD43⁻ macrophages infiltration was delayed. These findings suggest that VPA suppresses macrophage maturation and that HDAC inhibition may alter the phenotype of these cells.

Whereas histone modifications control macrophage gene expression, miRNAs regulate the mRNA-to-protein translation. Following NM exposure, several miRNAs associated with the inflammatory response (miR-125, miR-9, miR-127, miR-221) were upregulated within 1 d. Conversely, at 3-28 d after NM exposure, miRNA changes were more complex, as reflected by increased expression of antiinflammatory (miR-221, and miR-222) and profibrotic miRNAs (miR-21, miR-497, miR-34), and reduced expression of antiproliferative/antifibrotic miRNAs (let7, miR-448, miR29, miR-23, miR-26, miR-30).

These changes likely reflect a complex and refined network of epigenetic regulation of macrophage activation in response to NM exposure.

Taken together these results suggest that after NM exposure, both bone marrow and spleen-derived monocytes are recruited to the lung; once localized at injured sites, these cells develop into mature activated macrophages, which have the capacity to contribute to disease pathogenesis. Additional studies are required to determine their precise role in toxicity and if epigenetic alterations contribute to their activation state.

CONCLUSIONS

The current literature regarding mechanisms of macrophage subpopulation recruitment to injured sites following exposure to toxicants is still discordant. Additionally, mechanisms mediating macrophage activation have not been established. Our studies were aimed at filling this knowledge gap using a model of lung injury induced by nitrogen mustard; three major research questions were addressed:

1. What is the phenotype of macrophages accumulating in the lung after NM-induced injury?

There is a strong correlation between tissue destruction and the early appearance of proinflammatory M1 macrophages, and subsequent accumulation of M2 macrophages during the fibrotic phase, suggesting a role of M1 and M2 macrophages in these pathologic processes. Additional studies using fluorescently tagged cells adoptively transfer into recipient animals are needed to better characterize mechanisms of recruitment of these subpopulations, as well as elucidate whether macrophage phenotype switching occurs in vivo with time following exposure.

2. Where are these macrophage subsets originating from? Are these subsets distinct in phenotype?

We found that the spleen functions as a reservoir for a mature anti-inflammatory macrophage subset that plays a key role in dampening the activity of M1 macrophages and limiting tissue injury. Although still ongoing, our findings that inhibition of the recruitment of bone marrow macrophages is supportive for a role of bone marrow-derived macrophages in the early inflammatory response. This interplay between bone marrow and spleen-derived cells is novel in a model of chronic inflammation and has the potential to advance the development of more effective and targeted therapies. In this context, it remains to be investigated what the role of resident alveolar macrophages is

in the pathogenesis and resolution of the inflammatory response, as well as fibrogenesis.

3. Is macrophage activation driven by epigenetic alteration in the chromatin?

As the first two aims of this dissertation clearly show that phenotypically distinct populations accumulate in the lung after exposure to NM, we next aimed to characterize potential mechanisms of activation of these cells. Our findings that histone modifications, in particular acetylation, are upregulated in macrophages during the early phase of NM-induced cell activation, is consistent with a rapid response of these cells after insult. The biological significance of these changes was evaluated using the histone deacetylase inhibitor, valproic acid. Our studies showing that HDAC inhibition caused a marked shift in macrophage activation towards an antiinflammatory phenotype, supports the notion that HDACs are involved in macrophage activation. Due to the elevated off-target effects of valproic acid, future studies will address whether specific enzyme inhibition is more effective in reducing the extent of injury. Additionally, our observation of significant alterations in miRNA expression with time after nitrogen mustard exposure is highly novel. Together, these data support the existence of regulation of inflammatory gene expression at the transcriptional and translational level. These findings also indicate that macrophages actively participate in all phases of the injury process from the acute proinflammatory phase, to resolution and fibrogenesis.

In sum, these studies characterized in depth mechanisms of macrophage migration to the lung after insult, as well as elucidate the chromatin landscape regulating macrophage activation. These studies are fundamental to understanding immune cell behavior after injury, which may be useful in the development of targeted and effective therapies aimed improving/reversing injury outcome after vesicant exposure.

FUTURE STUDIES

Our studies characterizing phenotypically distinct subpopulations of macrophages in the lung following NM exposure, provides the basis for identification of candidate markers uniquely expressed on these two subsets that can be targeted for therapeutic suppression or activation and/or reprogramming in vivo. For example, in future studies, one could envision using a drug delivery system (i.e., particle), loaded with a drug cargo that induces phenotype switching, and coated with ligands specific for receptors on M1 or M2 macrophages to modify disease pathology. As an alternative, ex vivo programmed macrophages injected into rats at different times after exposure, could improve our understanding of the dynamics of pulmonary acute and chronic inflammation (Wang *et al.*, 2007). Future studies could also focus on the role of resident macrophages in the pathogenic response to NM. This could be accomplished using clodronate liposomes. Depending on the route of administration of the liposomes (intratracheal vs. intravenous), we could ablate different macrophage populations. These experiments could be used to characterize the role of alveolar macrophages in the absence of infiltrating cells, and vice versa. In pilot studies, we found that clodronate liposomes administered intratracheally caused a significantly reduction in resident macrophages. In these rats, NM exposure resulted in far more extensive tissue injury, compared to NM exposed sham rats, suggesting that resident cells are pivotal for balanced inflammatory response. In future studies, clodronate should be delivered systemically, so that only peripheral cells would be affected, thus addressing the role resident macrophages in early response and fibrogenesis.

As part of our studies characterizing macrophage subsets, we identified a spleen-derived macrophage subset responding to NM. Our findings of significantly reduced antiinflammatory M2 gene expression, and reduced numbers of the CD11b⁺CD43⁻ macrophage subset in SPX rats, suggest that spleen-derived mature

infiltrating macrophages are critical for controlling the inflammatory response and consequent fibrosis. A role for spleen stroma in the maturation of antiinflammatory macrophages is also suggested by these findings. To test this notion, macrophages can be collected from the spleen of a naïve animal and injected into NM exposed sham and splenectomized rats. A similar approach was found to be effective in a model of chronic kidney disease (Wang *et al.*, 2007). To address whether protective effects of the spleen result from spleen derived-cells or the splenic stroma, we could use pharmacological inhibitors of angiotensin-2 or angiotensin converting enzyme, as splenic macrophages have been shown to be recruited in a ATR-1 α dependent manner (Swirski *et al.*, 2009). Similar experiments have been successfully tested in other models of inflammation and fibrosis (He *et al.*, 2007; Medhora *et al.*, 2012; Yamamoto *et al.*, 2005).

Further studies could also focus on characterizing an epigenetic signature that mediates macrophage activation during the early and late phases of the inflammatory response. The present studies showed that a large number of miRNAs were differentially altered during the acute injury and fibrotic phase of NM toxicity. Although the identification and therapeutic use of a single miRNA to controls the acute injury and fibrosis would be ideal, this is unlikely to be successful due to target redundancy of miRNAs. However, as a therapeutic intervention we could attempt to identify miRNA candidates involved in the regulation of a specific activity and deliver a mixture of siRNA and miRNA agonists. In this regard, earlier studies have shown that inhibition of miR-21 was beneficial in sensitizing cancer cells to radiation (Ma *et al.*, 2014), reducing bleomycin-induced lung fibrosis (Liu *et al.*, 2010), and ameliorating lupus mediated splenomegaly (Garchow *et al.*, 2011). Delivery of multiple miRNAs has also revealed their potential in the treatment of cancer (Amendola *et al.*, 2009; Pencheva *et al.*, 2012). For our studies it is likely that a mixture of miRNAs will need to be administered at different times after exposure to better counter each phase of NM-induced injury. For

example, antiinflammatory miRNAs could be administered early after exposure during the acute phase of the injury, while antiinflammatory and antifibrotic miRNAs during the later stages of the inflammatory response may reduce tissue fibrosis.

Our studies also showed alterations of histone modifications and involvement of HATs and HDACs in NM-induced macrophage activation. The fact that VPA effectively skewed macrophage activation towards an M2 phenotype suggests that histone modifying therapy has the potential to be successful. However, broad spectrum (non-specific) HDAC inhibitors, such as VPA, are sometimes associated with off-target actions and fail to ameliorate inflammatory responses (Halili *et al.*, 2010). A more specific HDAC inhibitor could be used to target a specific histone deacetylase resulting in better results. Among the many HDAC inhibitors currently available (Dokmanovic *et al.*, 2007), the most promising ones to be used for our studies include MS-275 developed by Schering AG, which is more specific (inhibits only HDAC1, 2, 3) and is already in phase II trials (Lane and Chabner, 2009); SAHA (Vorinostat), although not as specific, is already approved by the FDA for cutaneous T-cell lymphoma (Marks and Breslow, 2007) may also prove useful.

PART IV. ADDITIONAL STUDIES IN PROGRESS

A. IN VITRO IMAGING OF NM-INDUCED LUNG INJURY

Our current method of analysis of NM-induced lung toxicity involves collection of cells, tissue and BAL to evaluate and quantify lung injury. The limitation of this approach is that they are terminal procedures. Thus, NM-induced injury and fibrosis cannot be serially assessed in the same animal. To overcome this, in vivo imaging studies were initiated. These analyses increase the robustness of studies by providing repeated measurements of lung injury on the same animal. Both magnetic resonance imaging (MRI) and computed tomography (CT) were used. We found that MRI scans can readily be used to detect acute lung injury, and edema after NM exposure (Fig. 1S). The total volume and intensity of areas of injury in the lung were quantified using VivoQuant software (Fig. 2S). These preliminary studies confirmed maximal fluid accumulation within 1 d of NM exposure which persisted up to 28 d; by comparison, the intensity of injury was increased in NM treated lungs only up to 7 d. These preliminary studies have allowed us to reach high quality image acquisition for both Gradient echo and Fast Spin echo. Furthermore, based on these initial experiments, it appears that CT-scans can capture similar alterations as observed with MRI, but with improved quality of the images. The possibility of generating 3D images of the lung (Fig. 3S) could lead to the characterization of a more specific signature characteristic for the visualization of fibrosis.

B. EFFECTS OF CCR2 INHIBITION ON NM-INDUCED LUNG INFLAMMATION AND INJURY

As part of the second aim of this dissertation, the role of splenic macrophages in NM-induced injury was analyzed. In preliminary studies, we assessed the contribution of bone marrow monocytes in NM-induced injury, by using a CCR2 inhibitor, BMS-741672,

provided to us by Bristol Meyers-Squibb. Pilot studies using flow cytometry determined that 150 mg/kg/day was effective in reducing numbers of CD11b⁺CD43⁺ immature infiltrating macrophages in the lung after NM (not shown). In these studies, BMS-741672 was administered to rats by oral gavage beginning 30 min before NM. These studies also showed that CCR2 inhibition resulted in blunted CCR2 expression in the lung after NM exposure (Fig. 4S). In addition, reduced cell accumulation in the BAL was noted, with no effects on tissue injury, as measured by BAL protein content (Fig. 5S). Differential analysis of BAL cells showed that the monocyte infiltration was significantly reduced, however, neutrophil counts were markedly increased (Fig. 6S). Due to the proinflammatory character of these cells, it is likely that proinflammatory neutrophil accumulation accounted for comparable tissue damage after NM exposure (Fig. 7S). On-going studies are focused on assessing whether altering the timing and duration of treatment with BMS-741672, will result in blunted toxicity.

C. RNA SEQUENCING ANALYSIS

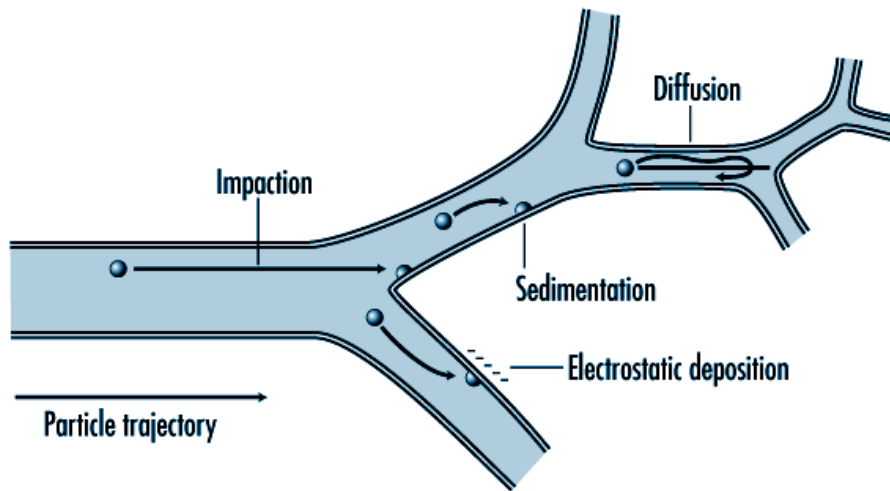
While assessing the phenotype of the macrophages infiltrating into the lung after NM exposure, we noted that both proinflammatory M1 and antiinflammatory M2 genes were upregulated within 1 d of exposure. This prompted us to perform RNA-sequencing analysis on lung cells isolated from control rats, as well as 1 d and 28 d after NM exposure. Although these studies are still in the early stages of analysis, we found more than 23,000 genes differentially expressed in these cells after NM exposure (not shown). Currently, we are screening for clusters of genes, which may be differentially regulated after NM exposure, thus highlighting the dominant pathways activated in macrophages during the acute injury phase, as well as fibrosis. These results could, in turn, have translational impact if compared with human data collected from patients exposed to vesicating agents.

D. STUDIES ON FOAM CELL FORMATION IN THE LUNG AFTER NM EXPOSURE.

Following NM exposure we observed that macrophages accumulating in the lung progressively increase in size, and that this correlated with increased expression of scavenger receptors and binding to oxidized low density lipoprotein (Fig. 4 and 8S). Earlier studies suggested that this is characteristic of foam cell formation in models of high fat diet and atherosclerosis (Shashkin *et al.*, 2005). We found that macrophages accumulate lipids after NM exposure, and that lipid laden macrophages cluster in areas of fibrosis (Fig. 9S). To begin to assess the mechanisms underlying the development of foamy macrophages, we analyzed mRNA expression of liver-X receptor (LXR), a transcription factor associated with lipid homeostasis, as well as some of its target genes (Fig. 10S). We noted significant downregulation of LXR in macrophages 3 d after NM exposure; this was associated with reduced expression of cholesterol efflux proteins, ABCA1 and ABCG1 (Fig. 10S). These data corroborates the notion that these cells accumulate lipids after NM exposure. Conversely, time related increases in CD36, ApoA and ApoE, proteins involved in both inflammation and cholesterol binding were also observed. This suggests that, in addition to its canonical role in cholesterol regulation, LXR participates to macrophages activation, however further studies are required to confirm this idea.

FIGURES

Fig. 1. Mechanisms of particle deposition



(Adapted from International Labour Office encyclopaedia of occupational health and safety)

Fig. 2.

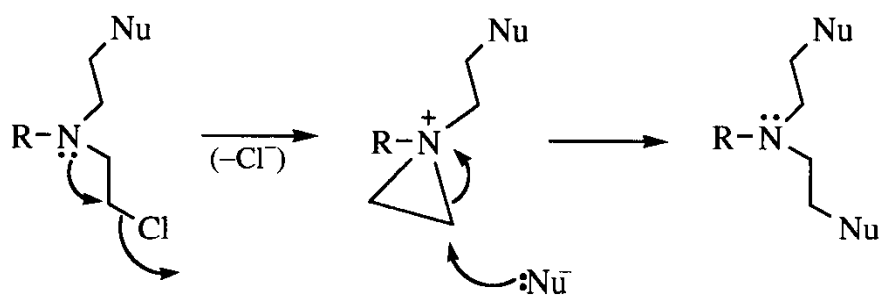
Nitrogen mustard structure and mechanism of nucleophilic attack of reactive mustards

$(\text{Cl}-\text{CH}_2-\text{CH}_2)_2-\text{N}-\text{R}$

$\text{R} = -\text{CH}_3$, Bis(2-chloroethyl)ethylamine

$-\text{CH}_2\text{CH}_2\text{Cl}$, Tris(2-chloroethyl)amine

$-\text{C}_9\text{H}_{10}\text{N}_1\text{O}_2$, 4-[bis(chloroethyl)amino]phenylalanine



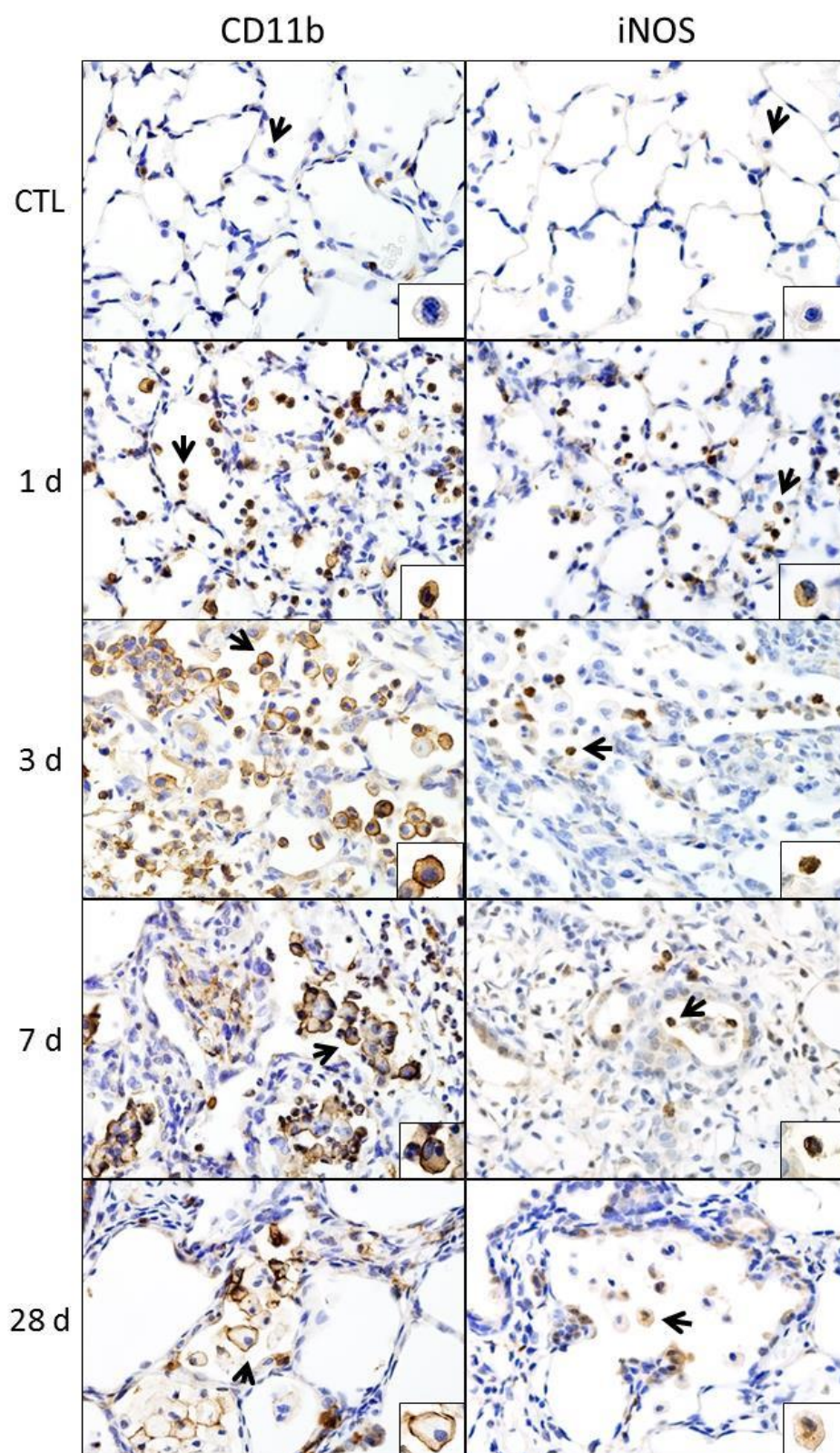


Fig. 3. Effects of NM on CD11b and iNOS expression. Lung sections, prepared 1 d, 3 d, 7 d and 28 d after exposure of rats to PBS control (CTL) or NM, were immunostained with antibodies to CD11b or iNOS. Binding was visualized using a Vectastain kit. Arrows indicate macrophage in insets. Original magnification, 60x; Insets magnification, 200x. Representative sections from 3 rats/treatment group are shown.

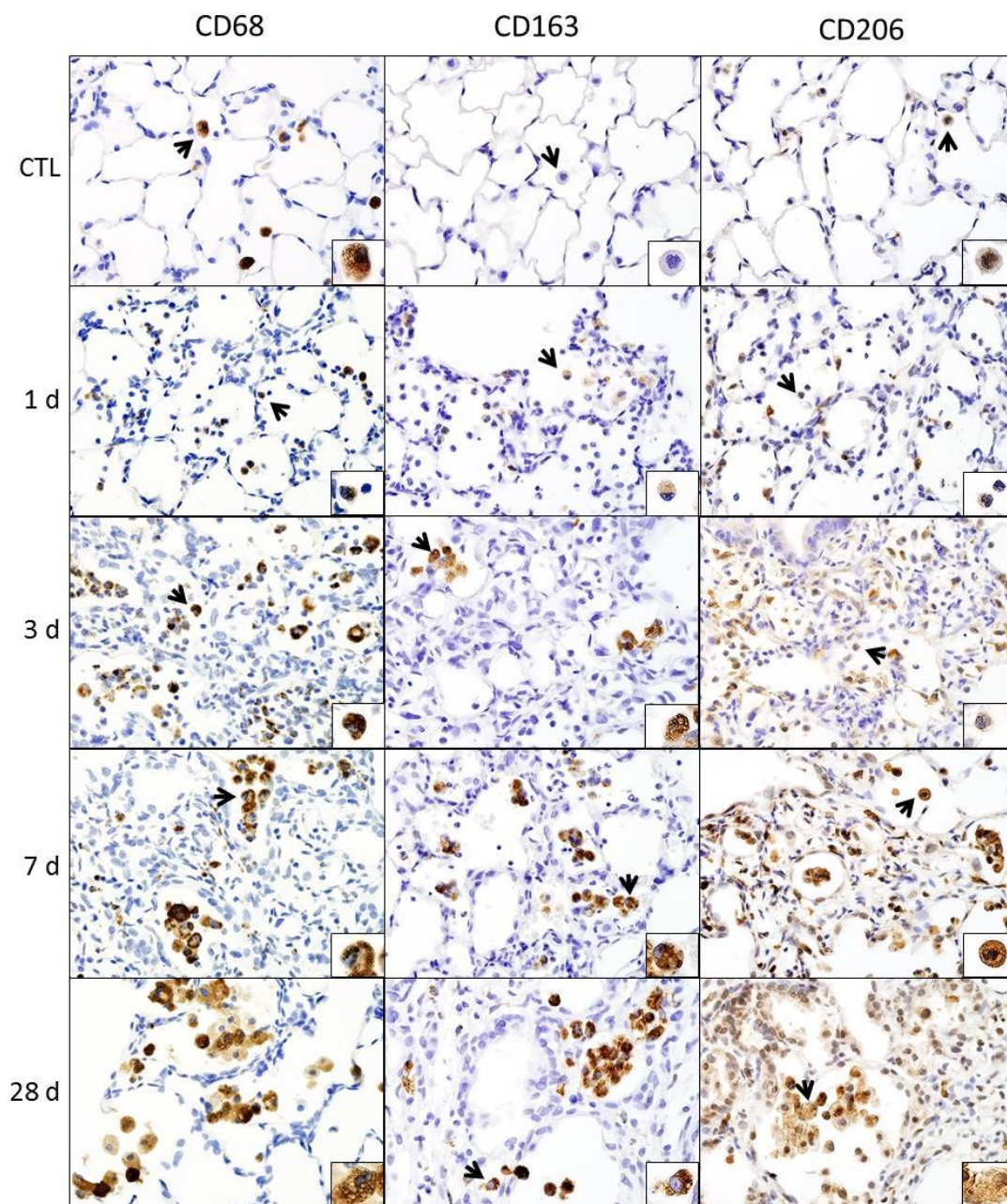


Fig 4. Effects of NM on CD68, CD163 and CD206 expression. Lung sections, prepared 1 d, 3 d, 7 d and 28 d after exposure of rats to PBS control (CTL) or NM, were immunostained with antibodies to CD68, CD206 or CD163. Binding was visualized using a Vectastain kit. Arrows indicate macrophage in insets. Original magnification, 60x; Insets magnification, 200x. Representative sections from 3 rats/treatment group are shown.

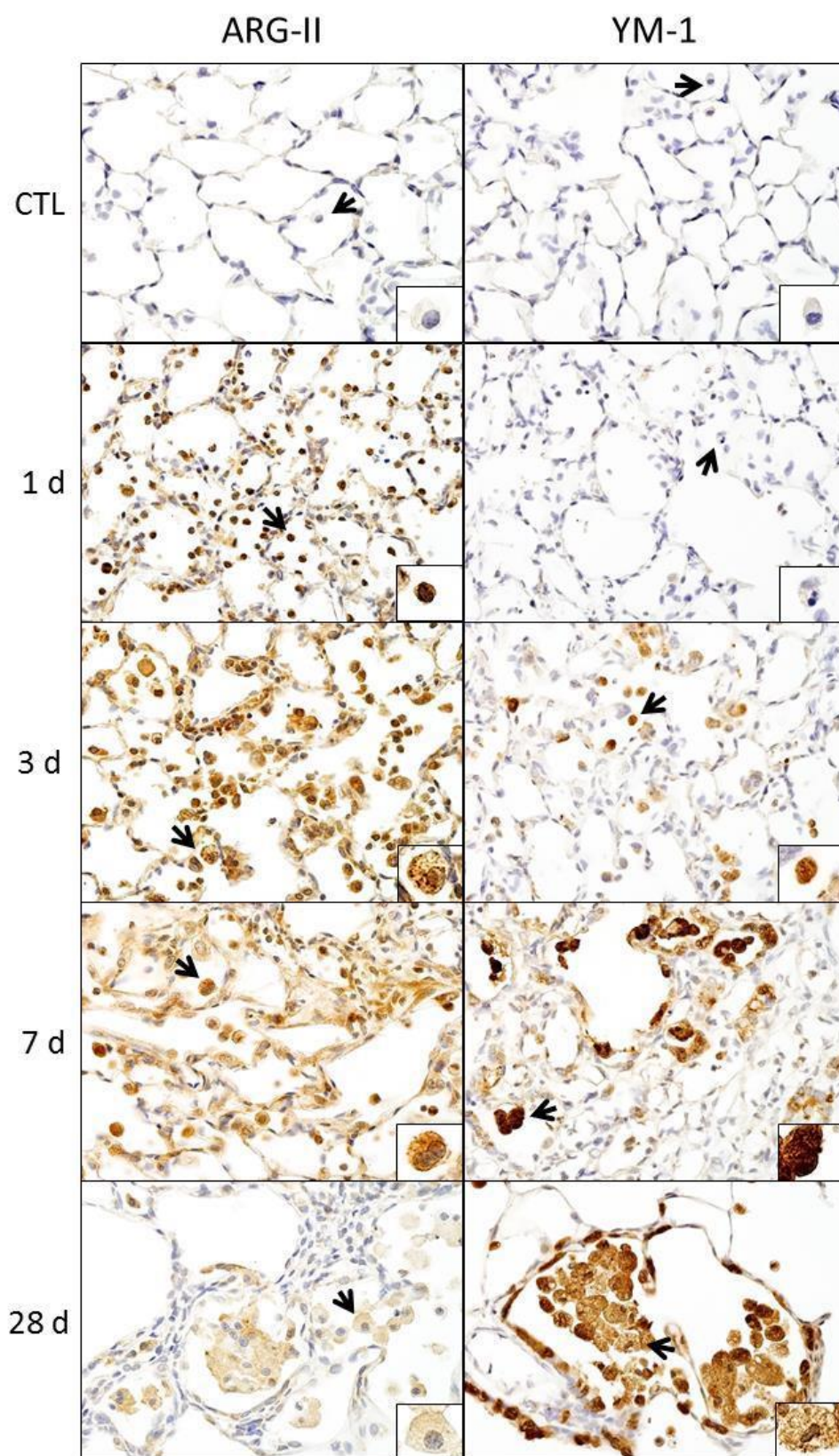


Fig 5. Effects of NM on ARG-II and YM-1 expression. Lung sections, prepared 1 d, 3 d, 7 d and 28 d after exposure of rats to PBS control (CTL) or NM, were immunostained with antibodies to ARG-II or YM-1. Binding was visualized using a Vectastain kit. Arrows indicate macrophage in insets. Original magnification, 60x; Insets magnification, 200x. Representative sections from 3 rats/treatment group are shown.

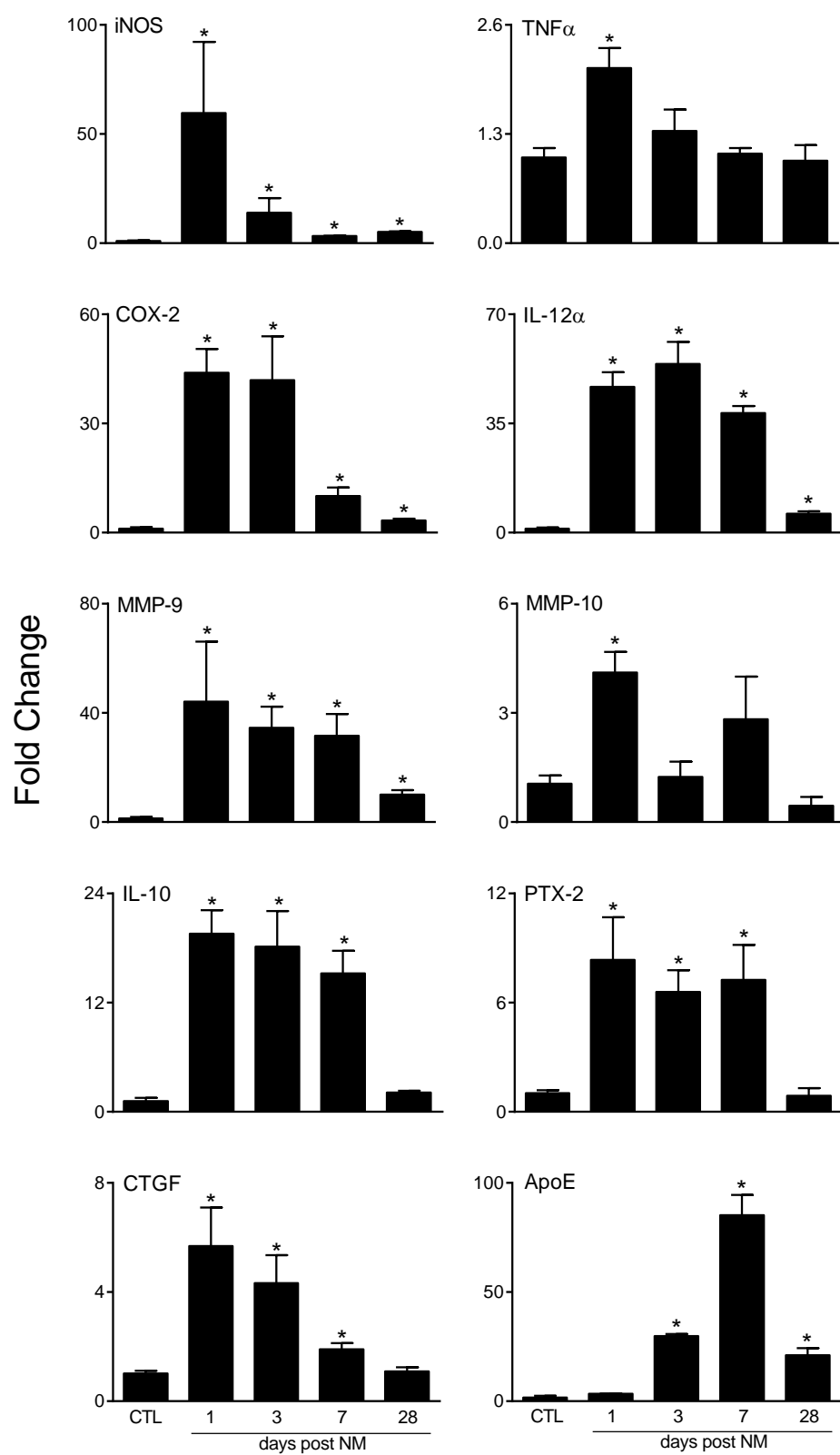


Fig. 6. Effects of NM on lung macrophage expression of M1 and M2 genes. Lung macrophages, isolated 1 d, 3 d, 7 d, and 28 d after exposure of rats to PBS control (CTL) or NM, were analyzed for gene expression by RT-PCR. Data were normalized relative to GAPDH. Bars, mean \pm SE (n = 3–5 rats). *Significantly different ($p \leq 0.05$) from CTL.

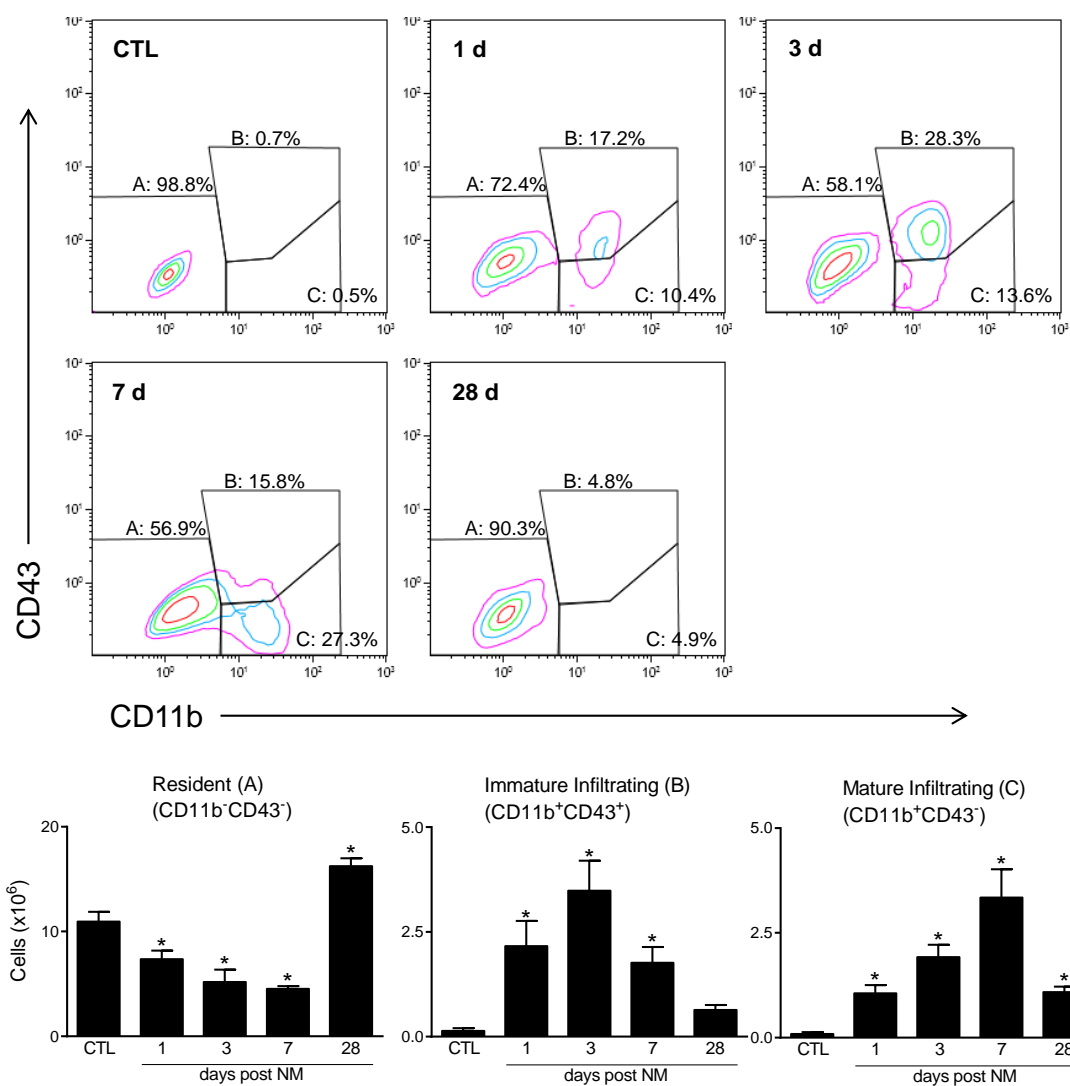


Fig. 7. Flow cytometric analysis of lung macrophages. Upper panel: macrophages, isolated 1 d, 3 d, 7 d, and 28 d after exposure of rats to PBS control (CTL) or NM, were incubated with anti-rat-FcRII/III antibody ($1 \mu\text{l}/10^6$ cells) for 10 min at 4°C , followed by incubation (30 min) with AlexaFluor 488 (AF488) anti-CD11b and AF647 anti-CD43 antibodies or appropriate isotype controls, and then with eFluor780 viability dye (30 min). Cells were then fixed in 2% paraformaldehyde and analyzed by flow cytometry. Lower panel: Resident alveolar macrophages ($\text{CD11b}^-\text{CD43}^-$), infiltrating immature macrophages ($\text{CD11b}^+\text{CD43}^+$), and infiltrating mature macrophages ($\text{CD11b}^+\text{CD43}^-$) were identified based on forward and side scatter followed by doublet discrimination of live cells. Numbers of $\text{CD11b}^-\text{CD43}^-$, $\text{CD11b}^+\text{CD43}^+$, and $\text{CD11b}^+\text{CD43}^-$ cells were calculated from the percentage positive cells relative to the total number of lung cells recovered. Bars, mean \pm SE ($n = 3-5$ rats). *Significantly different ($p \leq 0.05$) from CTL.

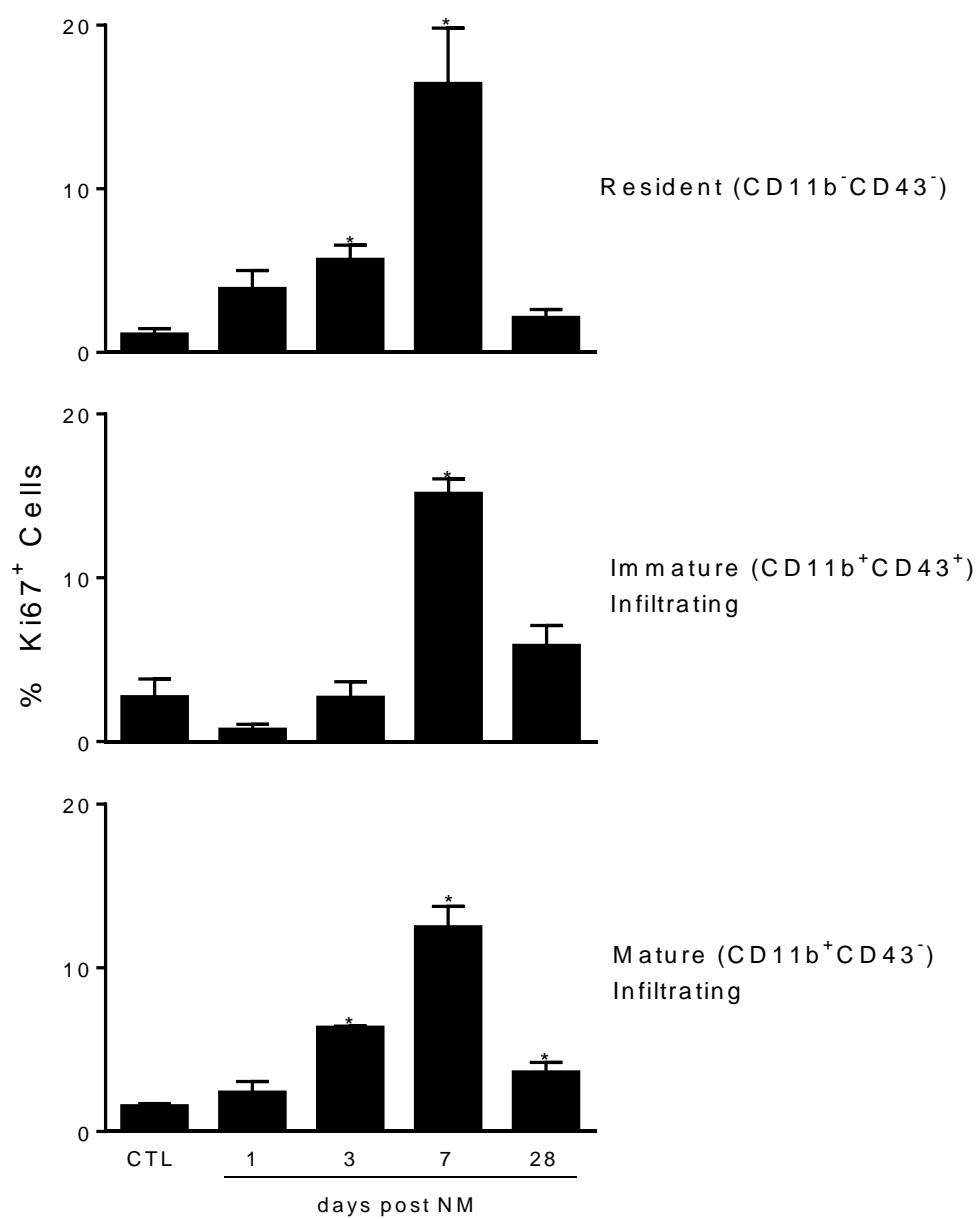


Fig. 8. Effects of NM on proliferation of macrophage subpopulations. Macrophages, isolated 1 d, 3 d, 7 d, and 28 d after exposure of rats to PBS control (CTL) or NM, were stained with antibodies to CD43, CD11b, or the appropriate isotype controls as described in the Fig. 5 legend. The cells were then incubated for 30 min in Fixation/Permeabilization buffer (eBioscience), followed by 30 min with eFluor450 Ki67 antibody. Cells were then fixed in 2% paraformaldehyde and analyzed by flow cytometry. Bars, mean \pm SE (n = 3–5 rats). *Significantly different ($p \leq 0.05$) from CTL.

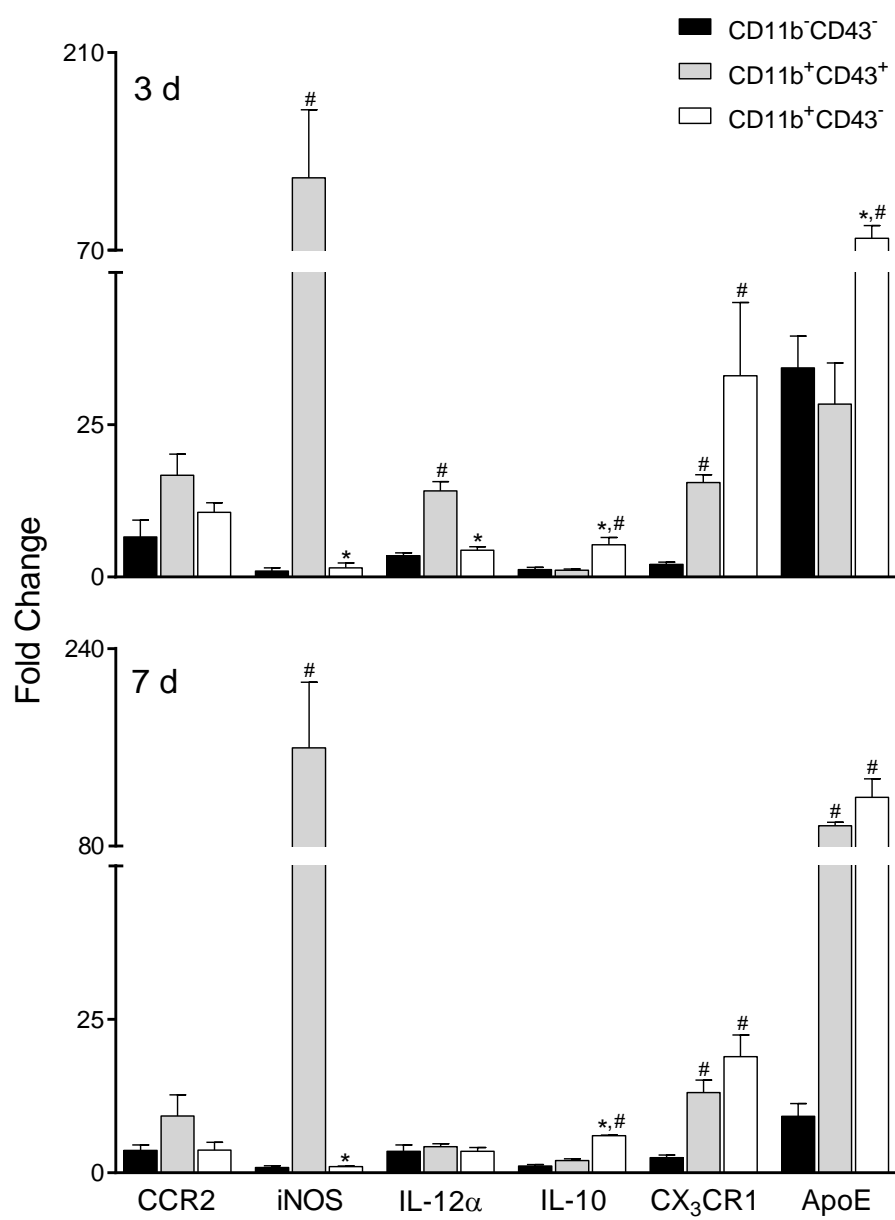


Fig. 9. Effects of NM on gene expression in macrophage subpopulations. Macrophages, isolated 3 d and 7 d after exposure of rats to PBS control (CTL) or NM, were incubated with anti-rat-FcRII/III antibody, and then stained with antibodies to CD11b and CD43 antibodies as described in the Fig. 5 legend. Viable cells (DAPI⁻) were sorted into resident (CD11b⁻CD43⁻), immature infiltrating (CD11b⁺CD43⁺), and mature infiltrating (CD11b⁺CD43⁻) subpopulations and processed immediately for RT-PCR analysis of expression of pro- (CCR2, iNOS, IL-12 α) and anti-inflammatory (IL-10, CX₃CR1, and ApoE) genes. Data were normalized to GAPDH and presented as fold change relative to resident CD11b⁻CD43⁻ macrophages from CTL rats. Bars, mean \pm SE (n = 3–4 rats).

*Significantly different ($p \leq 0.05$) from immature (CD11b⁺CD43⁺) macrophages.

#Significantly different ($p \leq 0.05$) from resident (CD11b⁻CD43⁻) macrophages.

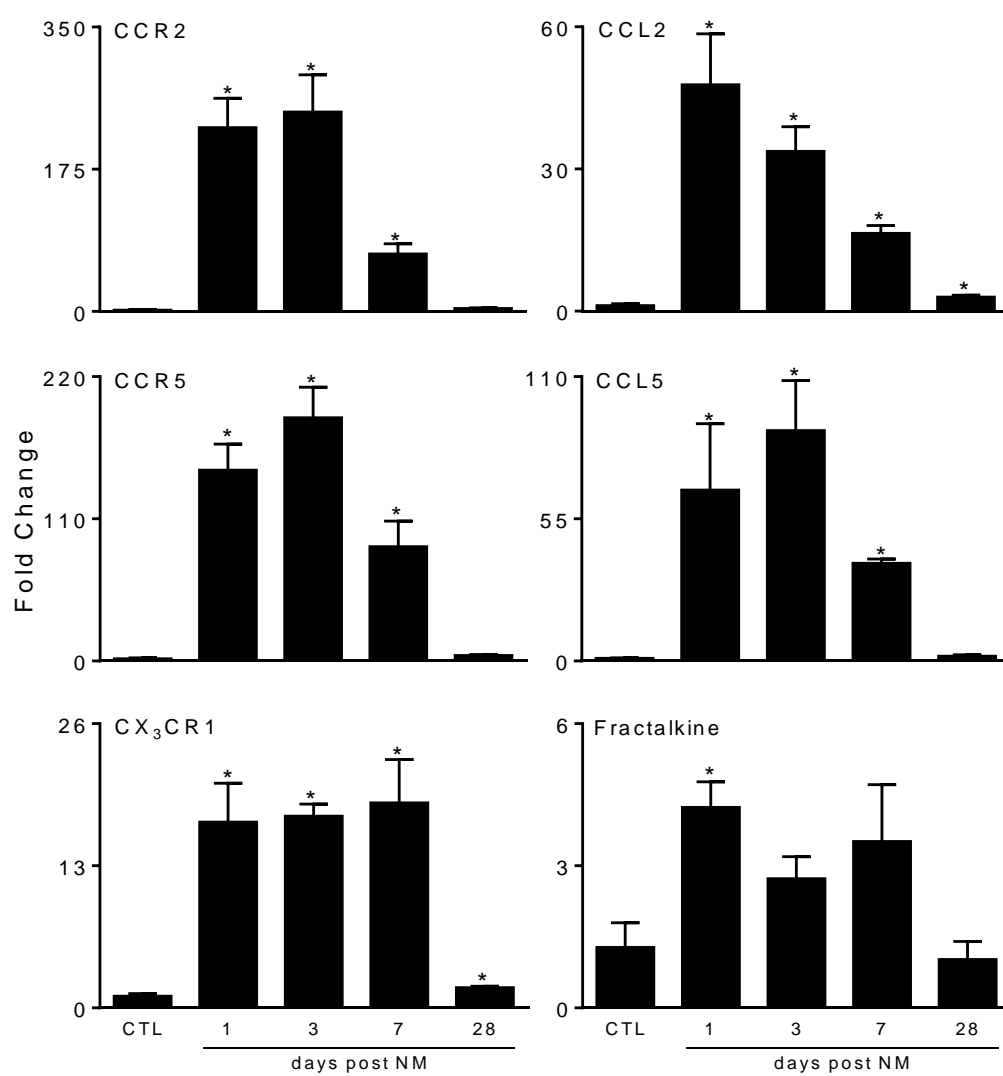


Fig. 10. Effects of NM on macrophage chemokine/chemokine receptor expression. Macrophages, isolated 1 d, 3 d, 7 d, and 28 d after exposure of rats to PBS control (CTL) or NM, were analyzed for gene expression by RT-PCR. Data were normalized relative to GAPDH. Bars, mean \pm SE (n = 3–5 rats). *Significantly different ($p \leq 0.05$) from CTL.

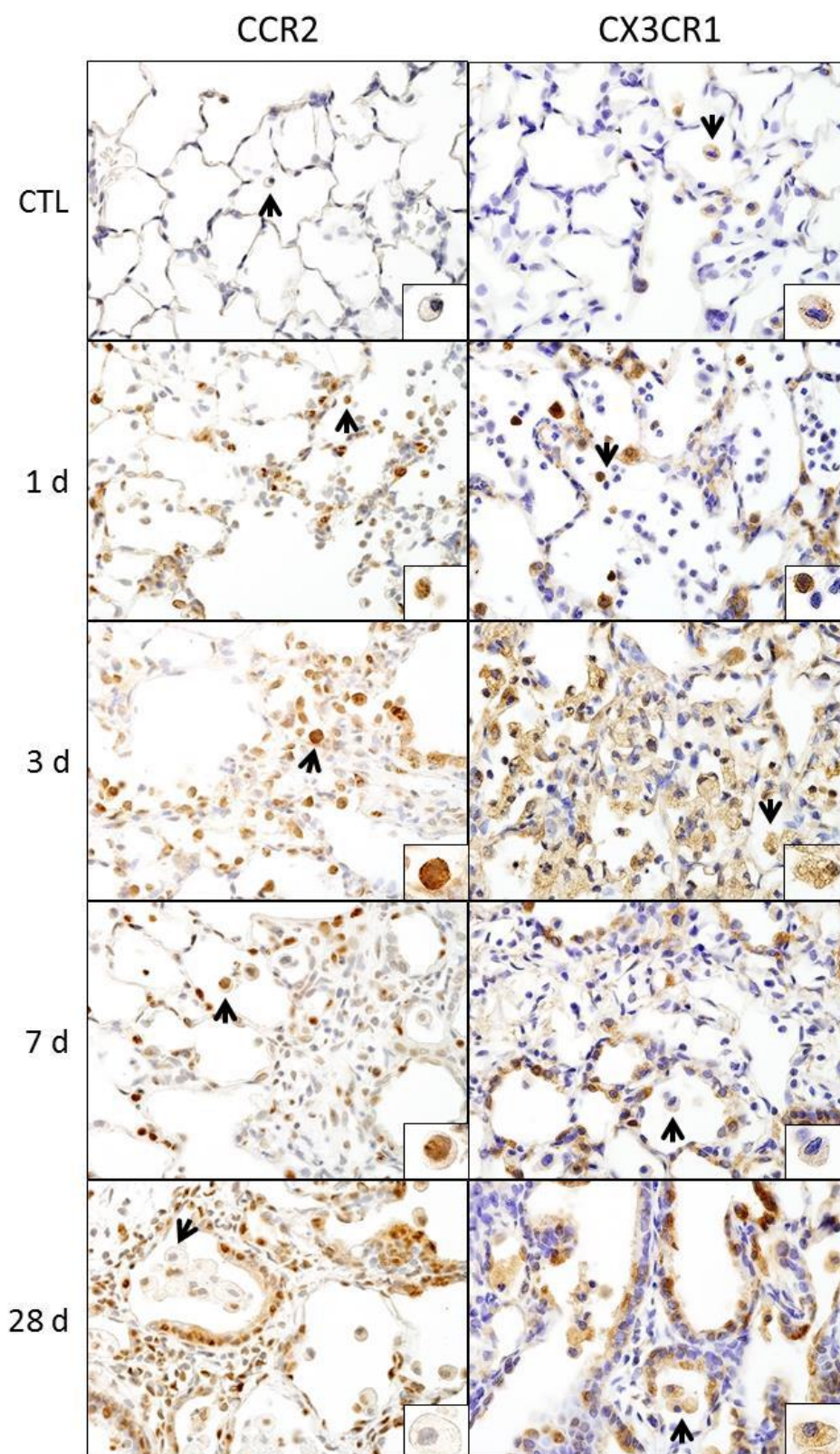


Fig. 11. Effects of NM on CCR2 and CX₃CR1 expression. Lung sections, prepared 1 d, 3 d, 7 d and 28 d after exposure of rats to PBS control (CTL) or NM, were immunostained with antibodies to CCR2 or CX₃CR1. Binding was visualized using a Vectastain kit. Arrows indicate macrophage in insets. Original magnification, 60x; Insets magnification, 200x. Representative sections from 3 rats/treatment group are shown.

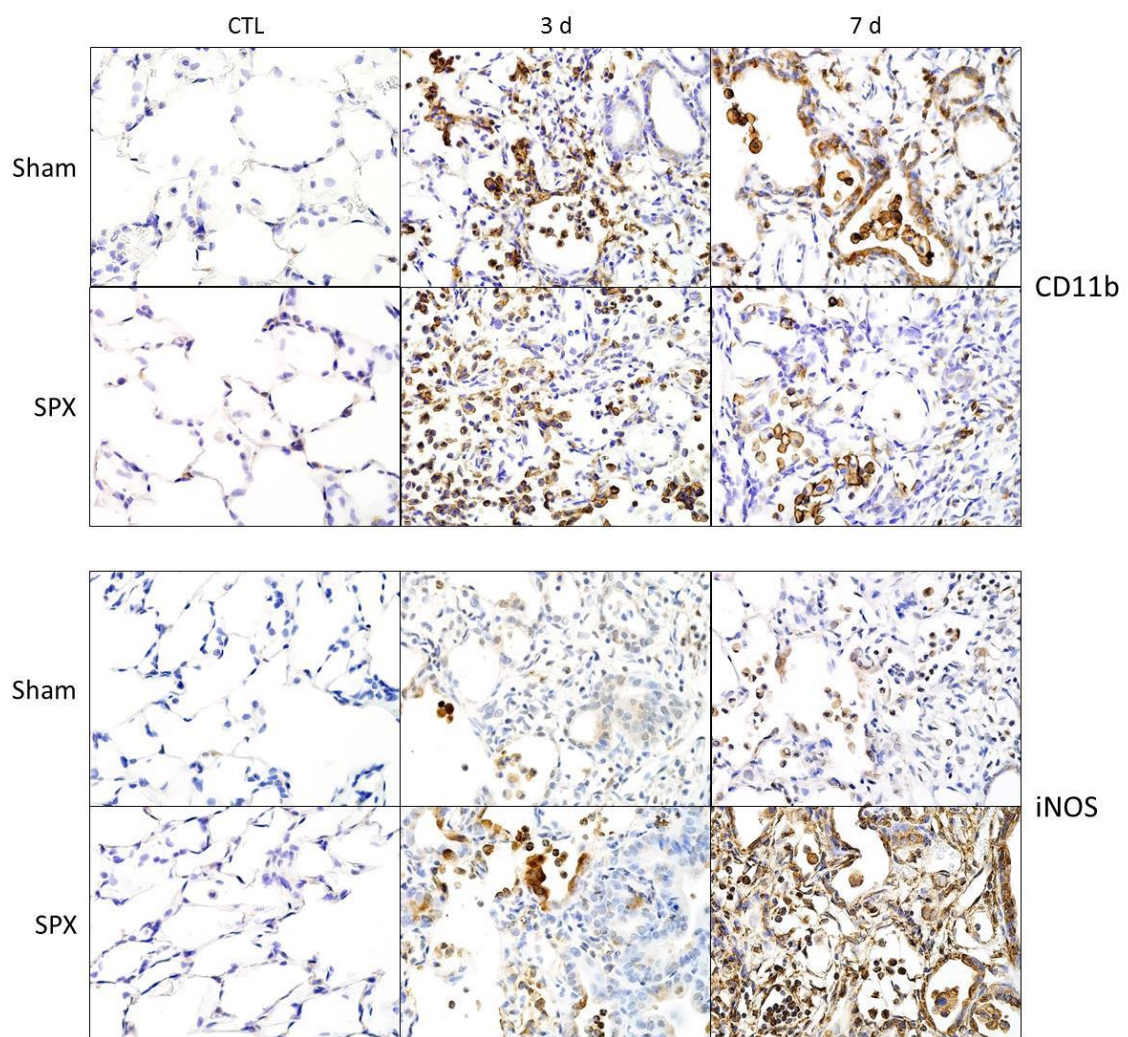


Fig. 12. Effects of splenectomy on NM-induced CD11b and iNOS expression. Lung sections, prepared 3 d and 7 d after exposure of sham and SPX rats to PBS control (CTL) or NM, were stained with antibody to CD11b (upper panels) or iNOS (lower panels). Binding was visualized using a Vectastain kit. Original magnification, 600x. Representative sections from 3 rats/treatment group are shown.

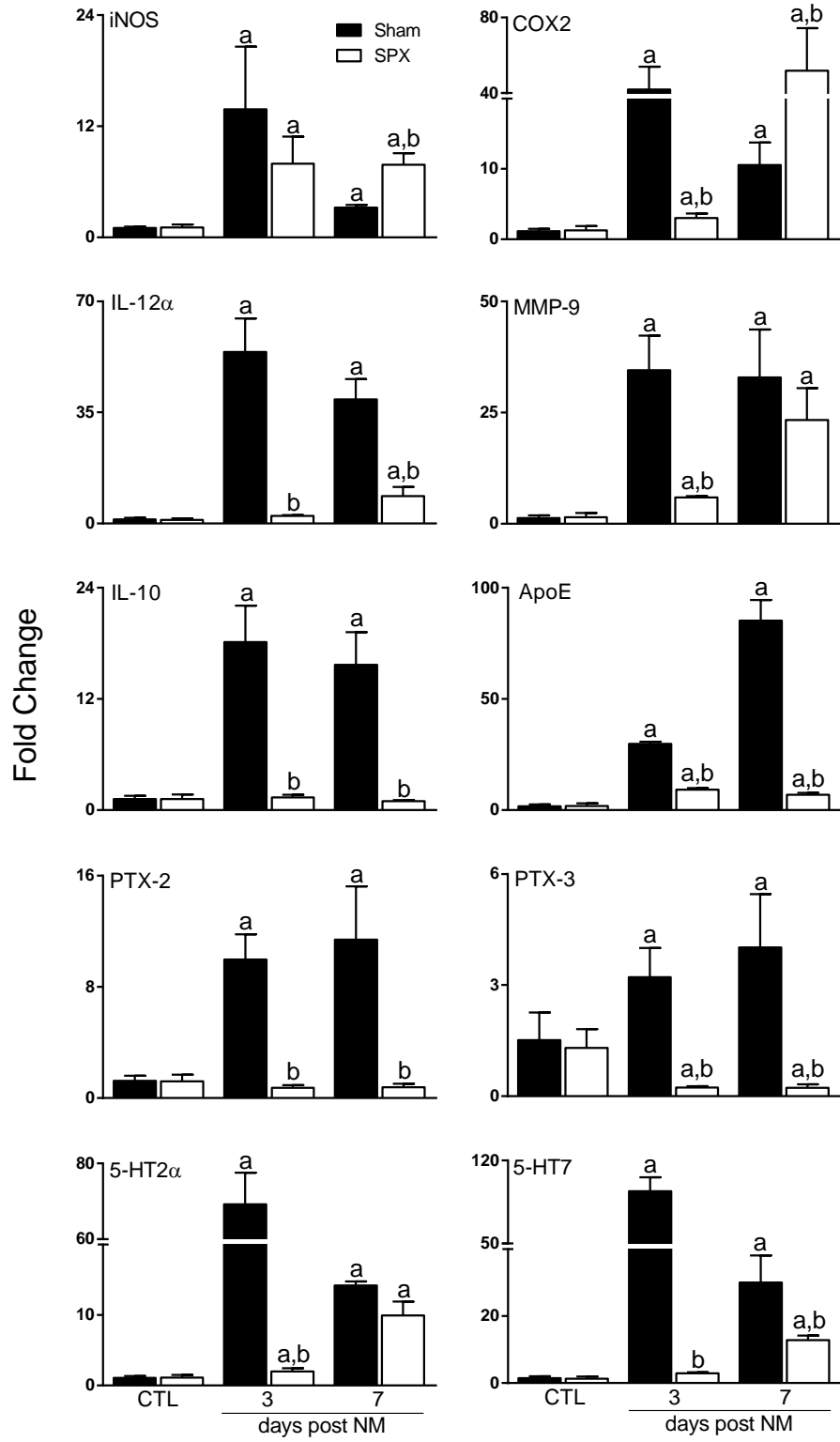


Fig. 13. Effects of splenectomy on NM-induced expression of pro- and antiinflammatory genes. Macrophages, isolated 3 d and 7 d after exposure of sham and SPX rats to PBS control (CTL) or NM, were analyzed by RT-PCR. Data were normalized relative to GAPDH. Bars, mean + SE (n = 3–5 rats). ^aSignificantly different (p < 0.05) from CTL. ^bSignificantly different (p < 0.05) from sham.

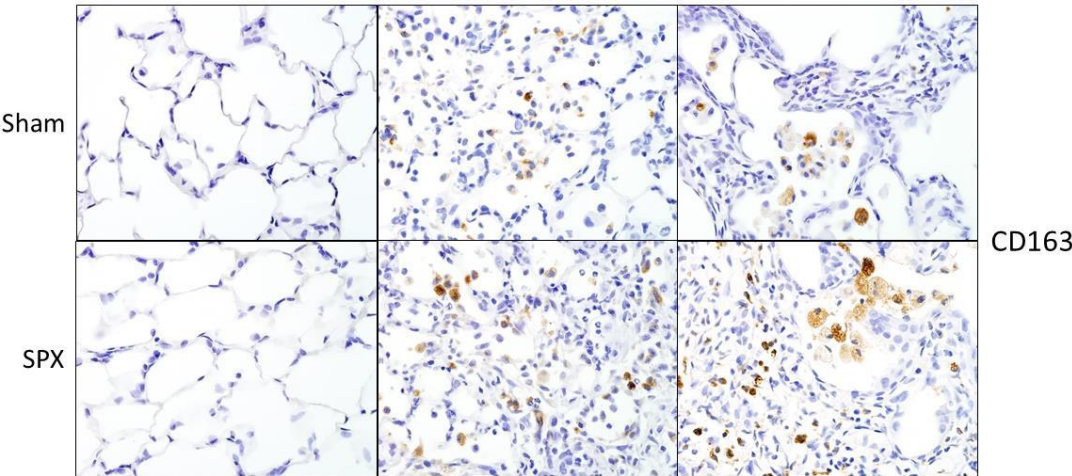
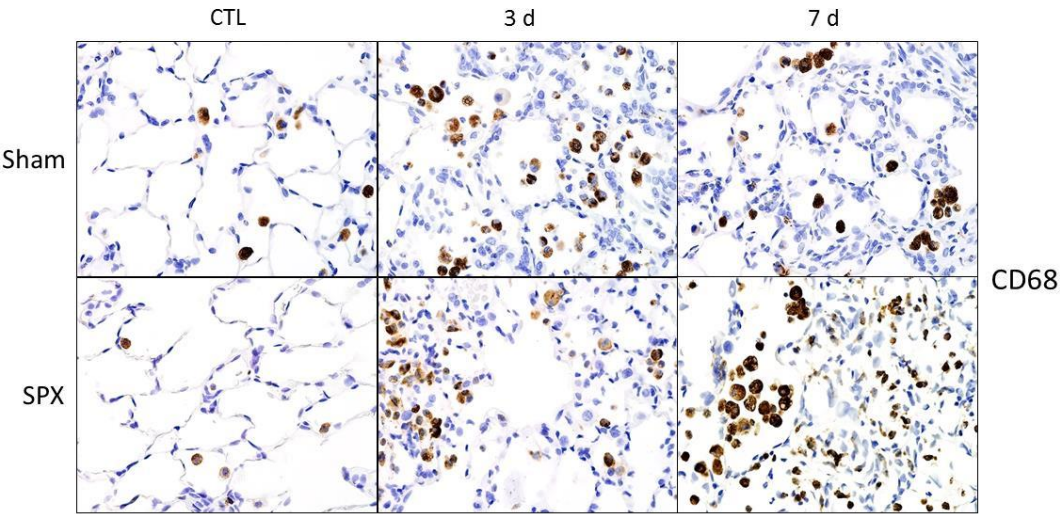


Fig. 14. Effects of splenectomy on NM-induced accumulation of CD68⁺ and CD163⁺ macrophages in the lung. Sections, prepared 3 d and 7 d after exposure of sham and SPX rats to PBS control (CTL) or NM, were stained with antibody to CD68 (upper panels) or CD163 (lower panels). Binding was visualized using a Vectastain kit. Original magnification, 600x. Representative sections from 3 rats/treatment group are shown.

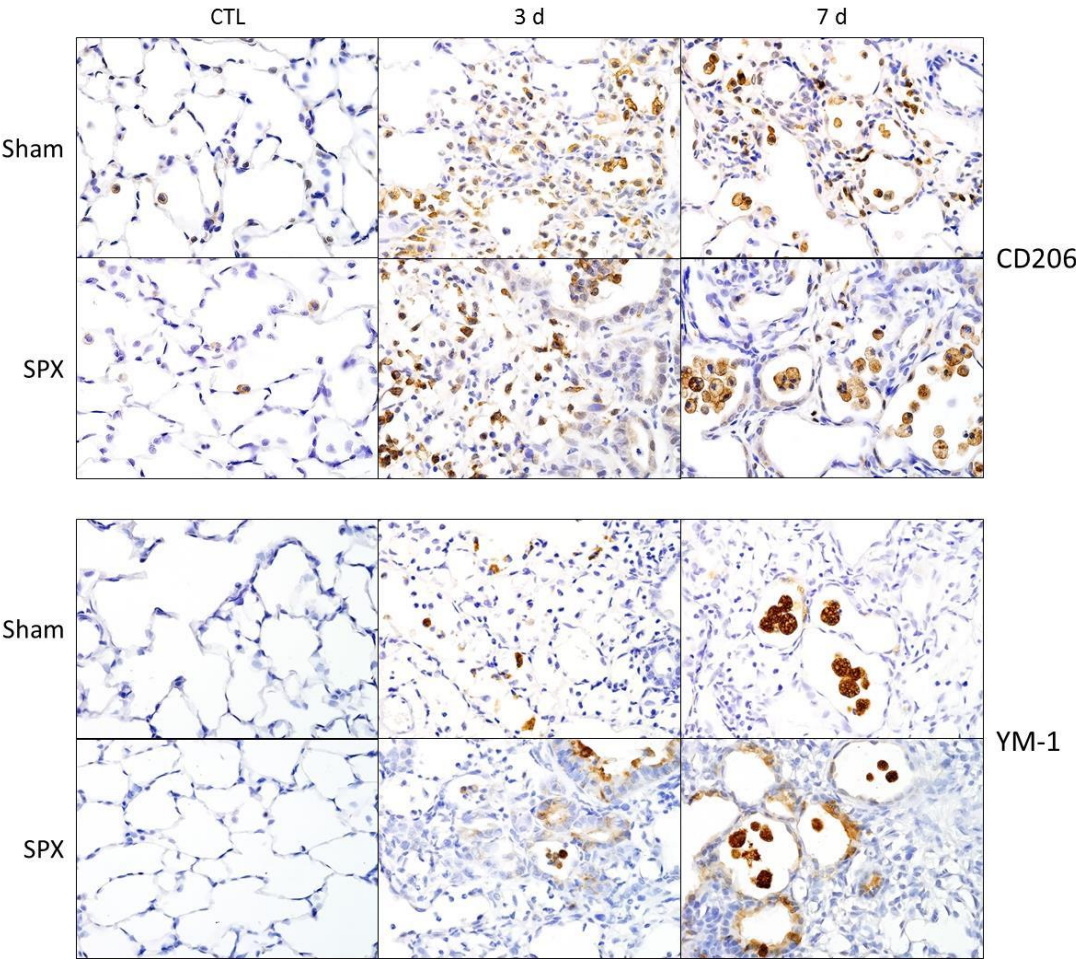


Fig. 15. Effects of splenectomy on NM-induced accumulation of CD206⁺ and YM-1⁺ macrophages in the lung. Sections, prepared 3 d and 7 d after exposure of sham and SPX rats to PBS control (CTL) or NM, were stained with antibody to CD206 (upper panels) or YM-1 (lower panels). Binding was visualized using a Vectastain kit. Original magnification, 600x. Representative sections from 3 rats/treatment group are shown.

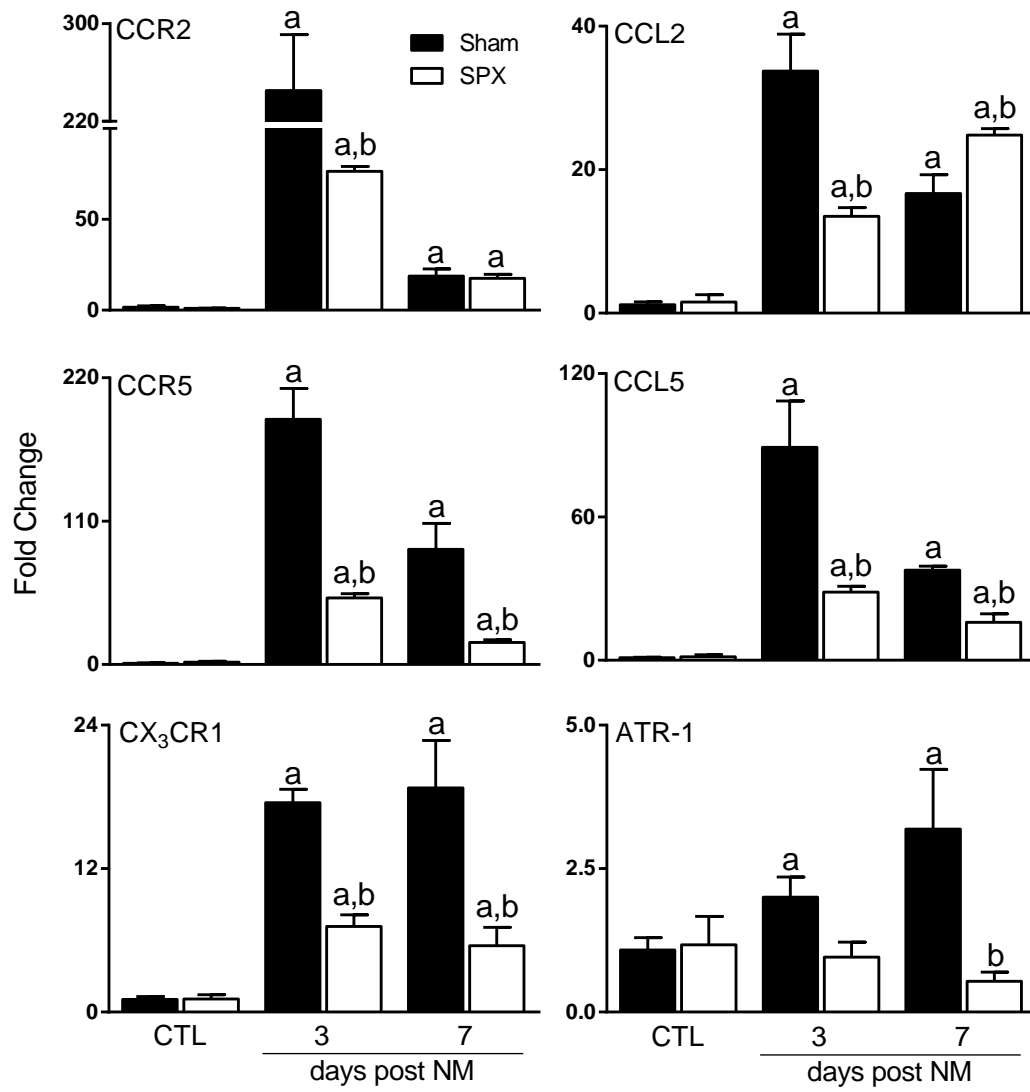


Fig. 16. Effects of splenectomy on NM-induced expression of macrophage chemokine and chemokine receptor genes. Macrophages, isolated 3 d and 7 d after exposure of sham and SPX rats to PBS control (CTL) or NM, were analyzed by RT-PCR. Data were normalized relative to GAPDH. Bars, mean + SE (n = 3–5 rats). ^aSignificantly different (p < 0.05) from CTL. ^bSignificantly different (p < 0.05) from sham group.

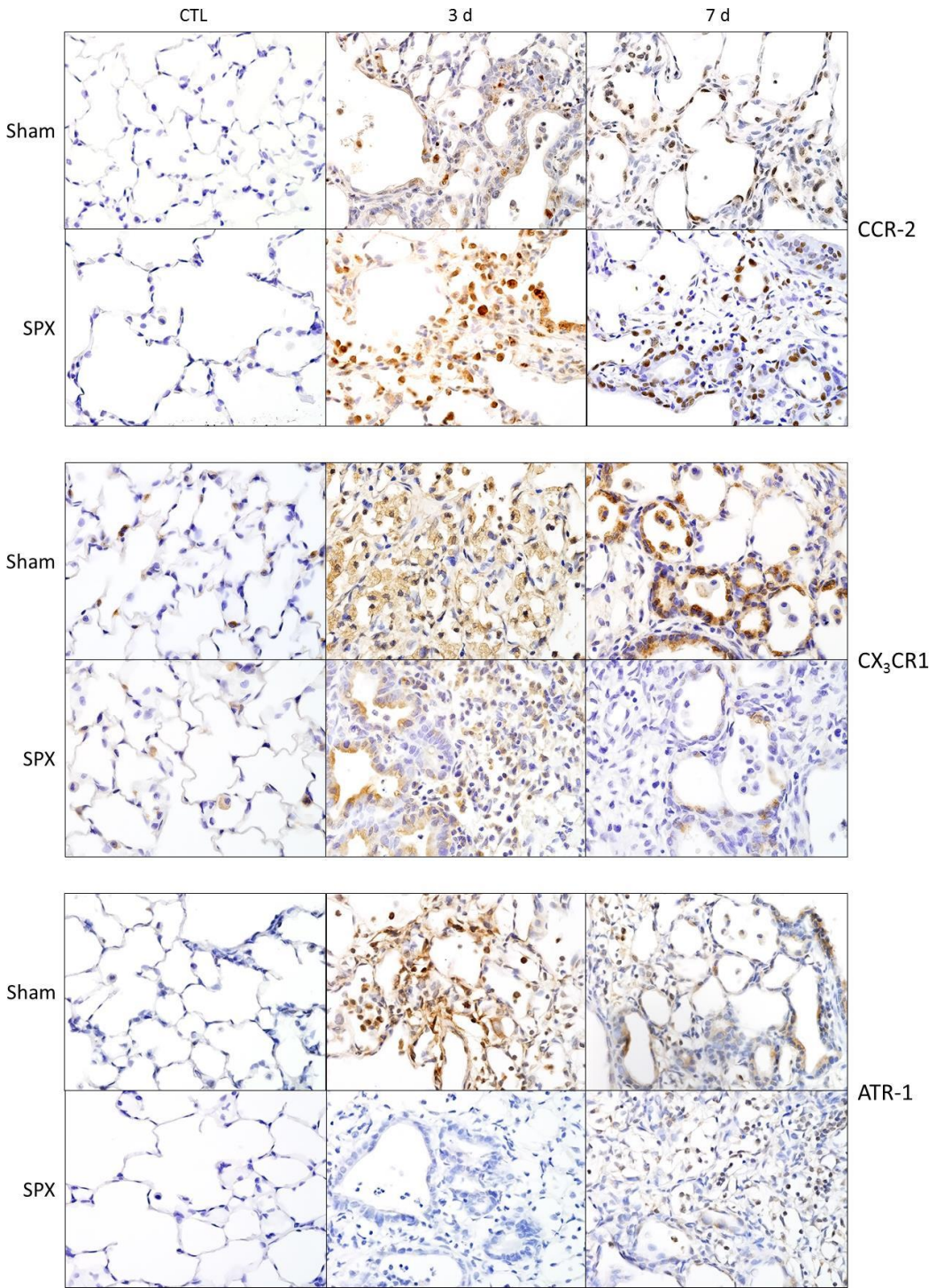


Fig. 17. Effects of splenectomy on NM-induced expression of CCR2⁺, CX₃CR1⁺ and ATR-1⁺ macrophages in the lung. Sections, prepared 3 d and 7 d after exposure of sham and SPX rats to PBS control (CTL) or NM, were stained with antibody to CCR2 (upper panels), CX₃CR1 (middle panels), or ATR-1 (lower panels). Binding was visualized using a Vectastain kit. Original magnification, 600x. Representative sections from 3 rats/treatment group are shown.

Fig. 18. Flow cytometric analysis of lung macrophages. Cells isolated 1 d, 3 d and 7 d after exposure of sham and SPX rats to PBS control (CTL) or NM were immunostained with antibody to CD11b and CD43 or the appropriate isotype controls, as described in the *Materials and Methods*, and then analyzed by flow cytometry. Upper panels: Representative histograms from 3-5 rats/treatment group. Lower panels: The absolute number of resident alveolar macrophages (pop. A, CD11b⁻CD43⁻), infiltrating immature macrophages (pop. B, CD11b⁺CD43⁺), and infiltrating mature macrophages (pop. C, CD11b⁺CD43⁻) was calculated from the total number of cells collected and forward/side scatter gate. Data are represented as mean + SE (n = 3–5 rats). ^aSignificantly different (p < 0.05) from CTL. ^bSignificantly different (p < 0.05) from sham group.

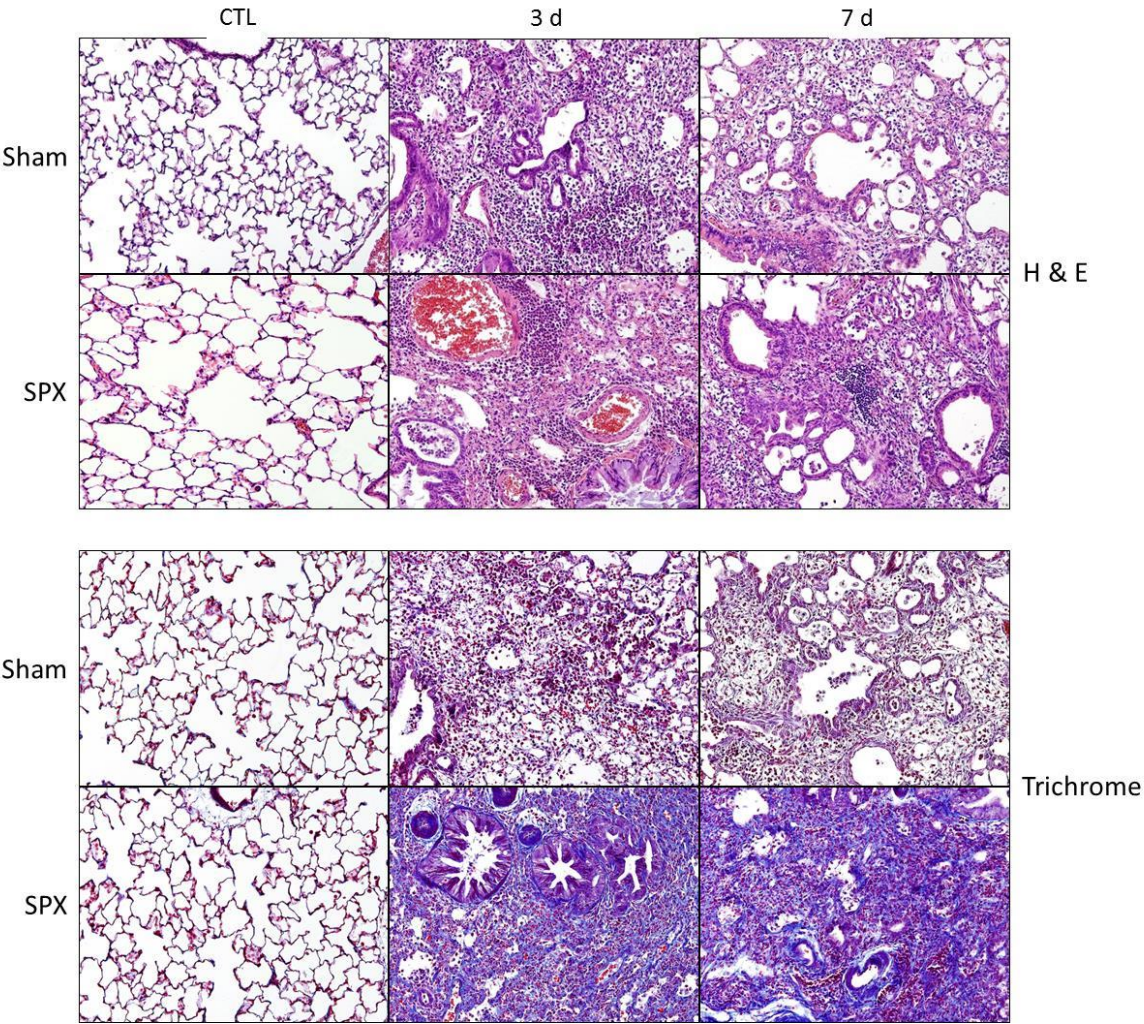


Fig. 19. Effects of splenectomy on NM-induced lung pathology. Lung sections prepared 3 d and 7 d after exposure of sham and SPX rats to PBS control (CTL) or NM, were stained with H&E (upper panels) or Gomori's trichrome (lower panels). Original magnification, 200x. Representative sections from 3 rats/treatment

P-H2A.X(S139)

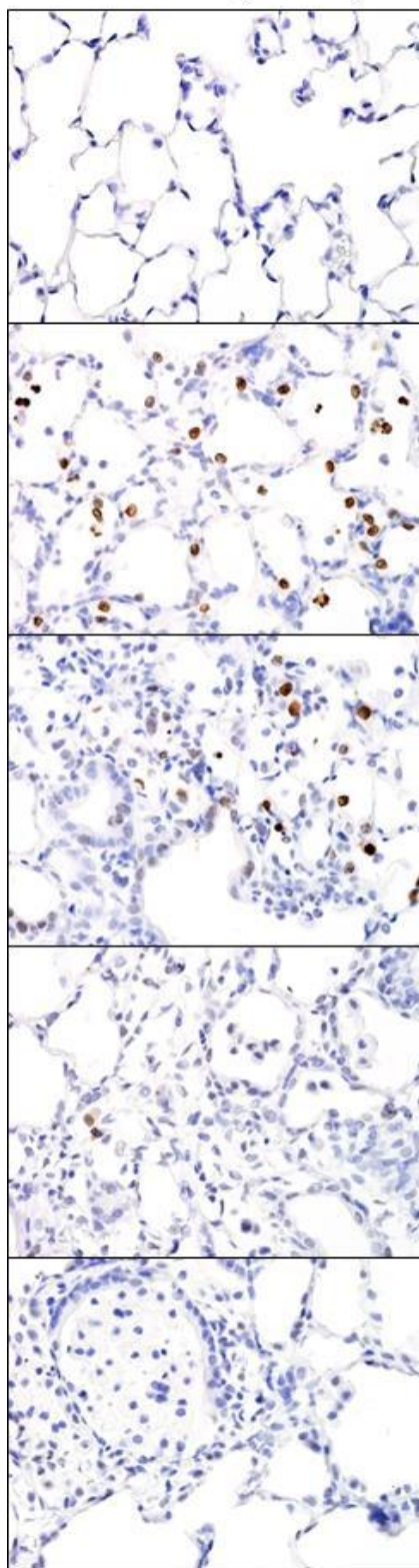


Fig. 20. Effects of NM on expression of histone H2A.X phosphorylation. Lung sections, prepared 1 d, 3 d, 7 d and 28 d after exposure of rats to PBS control (CTL) or NM, were immunostained with antibody to γ -H2A.X. Binding was visualized using a Vectastain kit. Original magnification, 600x. Representative sections from 3 rats/treatment group are shown.

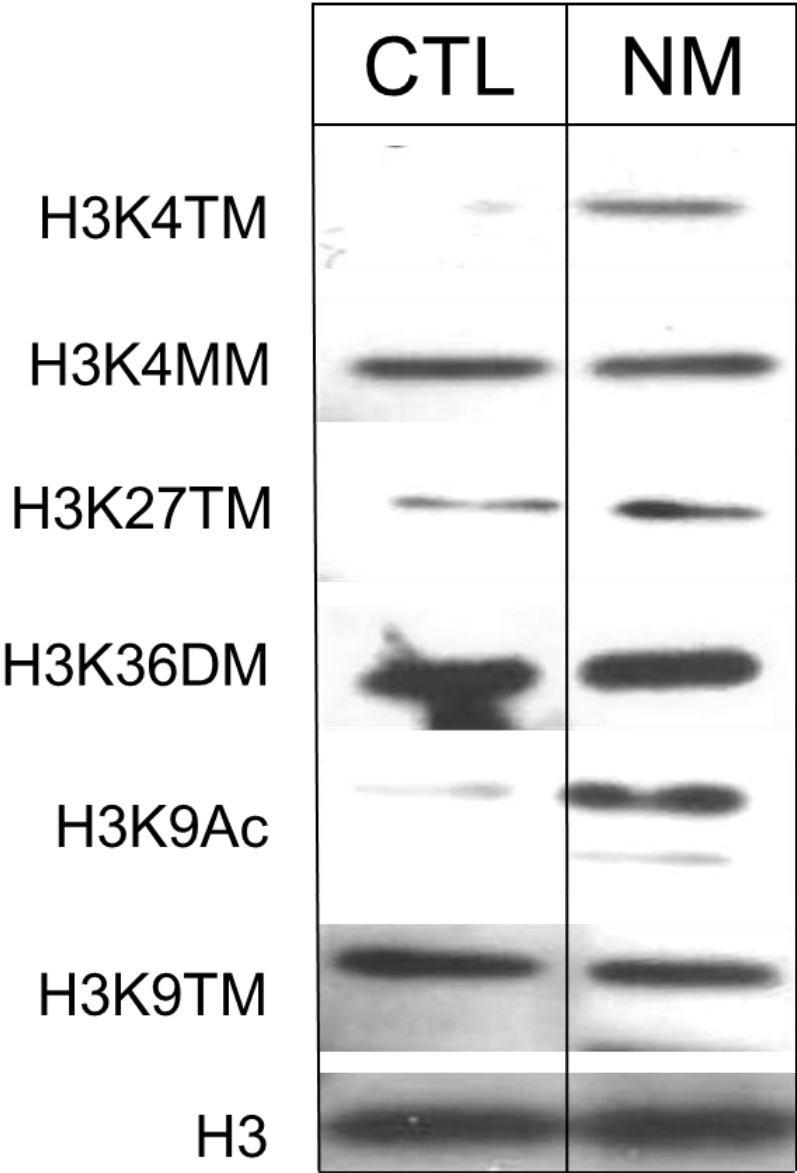


Fig. 21. Effects of NM on modified histone expression. Lung cell nuclear extracts, prepared 1 d after exposure of rats to PBS control (CTL) or NM, were immunostained with antibody to H3K4MM and TM, H3K9Ac and TM and H3K36DM. Binding was visualized using a ECL chemiluminescence kit. Representative blot from 3 extracts/treatment group are shown.

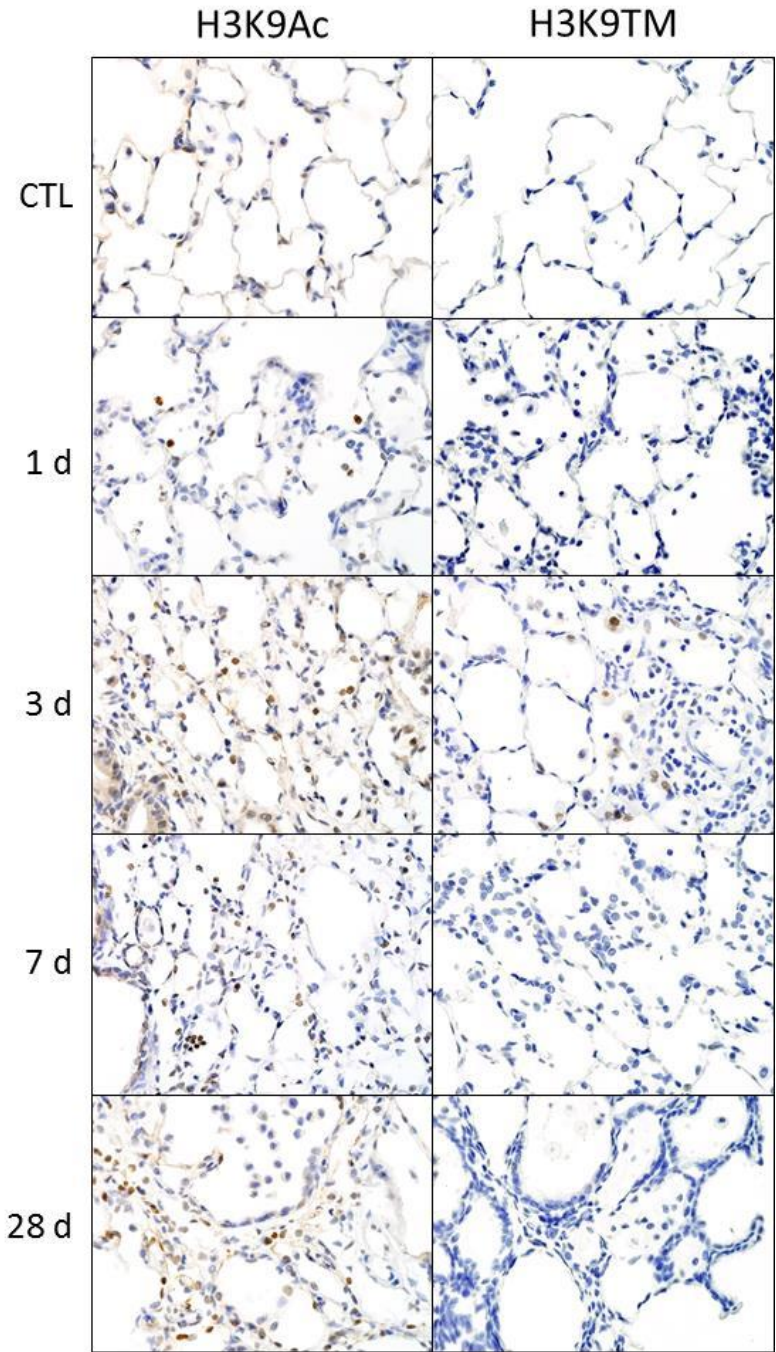


Fig. 22. Effects of NM on H3K9Ac and H3K9TM expression. Lung sections, prepared 1 d, 3 d, 7 d and 28 d after exposure of rats to PBS control (CTL) or NM, were immunostained with antibody to H3K9Ac (left panels) and H3K9TM (right panels). Binding was visualized using a Vectastain kit. Original magnification, 600x. Representative sections from 3 rats/treatment group are shown.

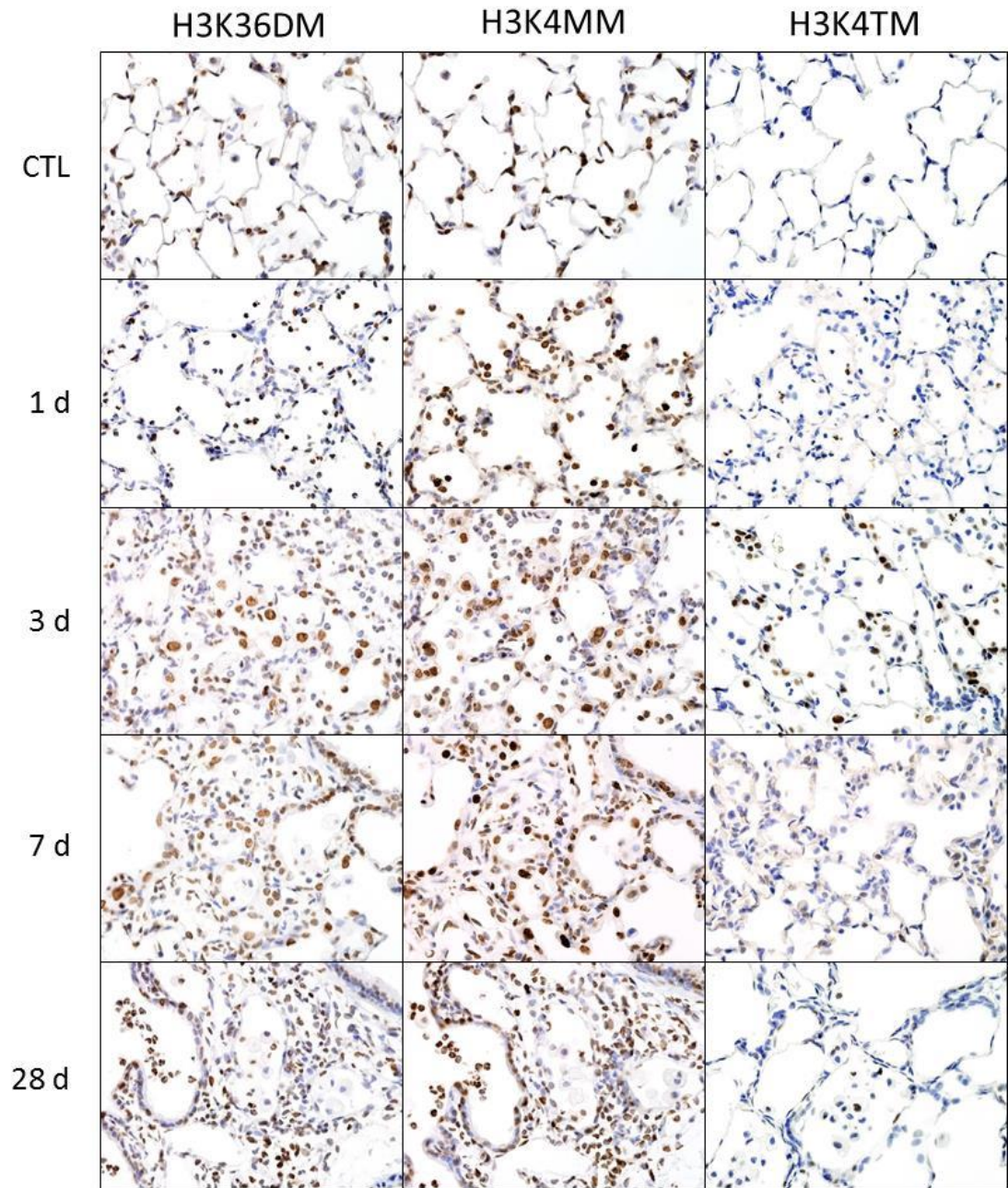


Fig. 23. Effects of NM on H3K36DM, H3K4MM and H3K4TM expression. Lung sections, prepared 1 d, 3 d, 7 d and 28 d after exposure of rats to PBS control (CTL) or NM, were immunostained with antibody to H3K36DM (left panels), H3K4MM (center panels) and H3K4MM (right panels). Binding was visualized using a Vectastain kit. Original magnification, 600x. Representative sections from 3 rats/treatment group are shown.

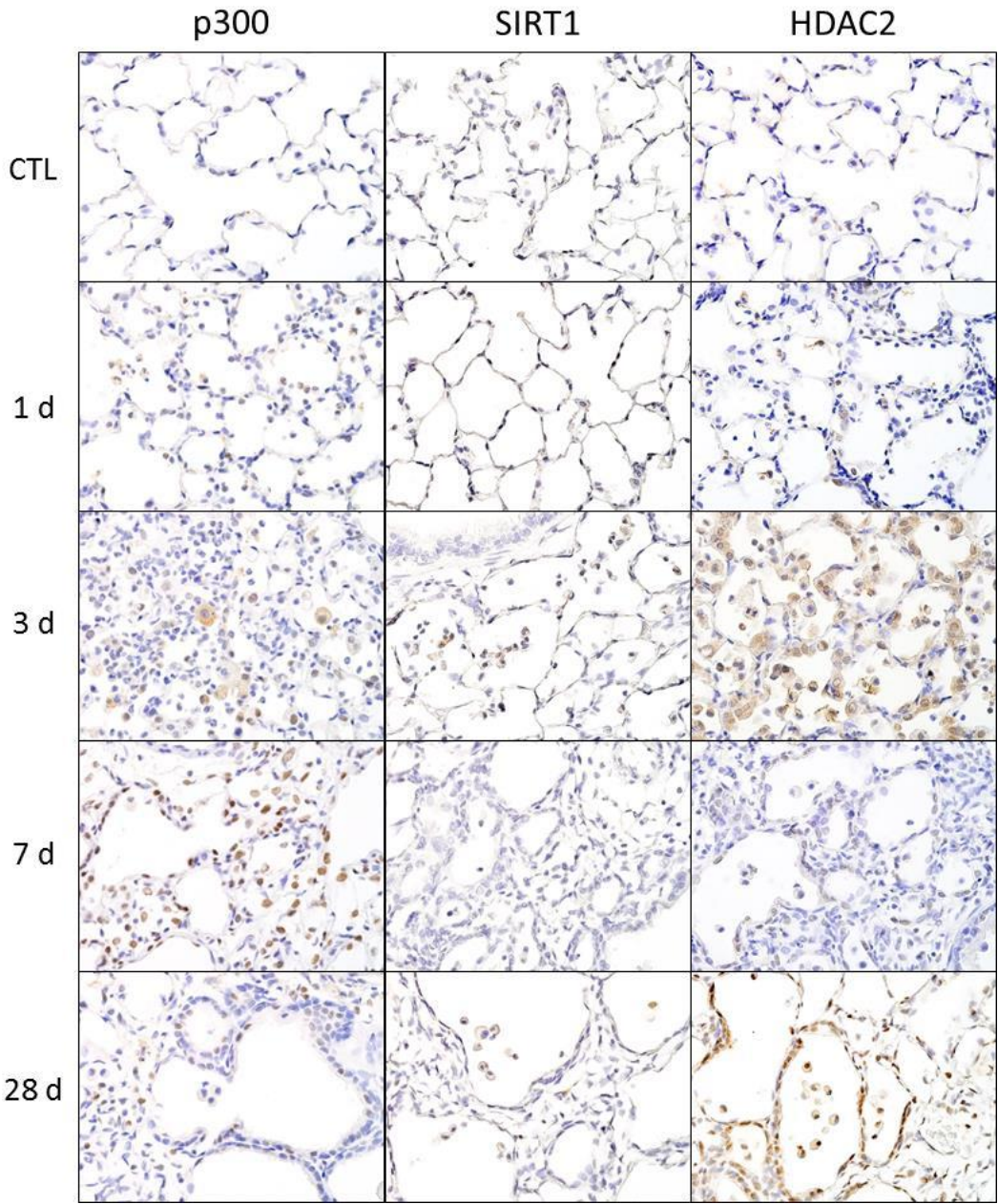


Fig. 24. Effects of NM on p300, SIRT1 and HDAC2 expression. Lung sections, prepared 1 d, 3 d, 7 d and 28 d after exposure of rats to PBS control (CTL) or NM, were immunostained with antibody to p300 (left panels), SIRT1 (center panels) and HDAC2 (right panels). Binding was visualized using a Vectastain kit. Original magnification, 600x. Representative sections from 3 rats/treatment group are shown.

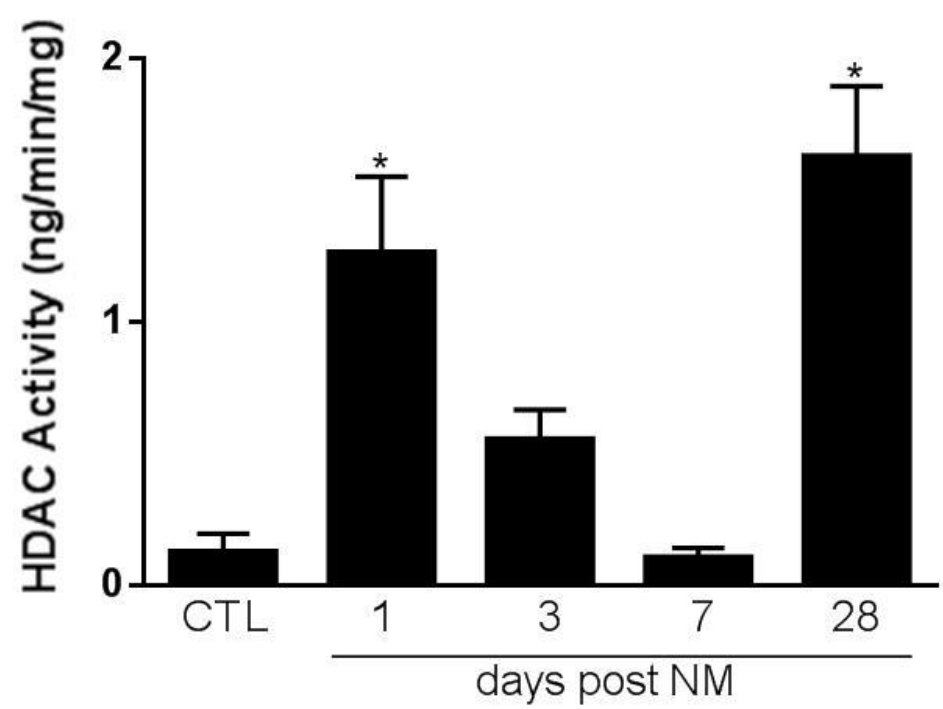
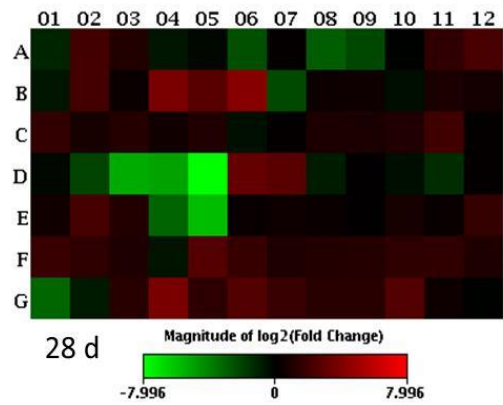
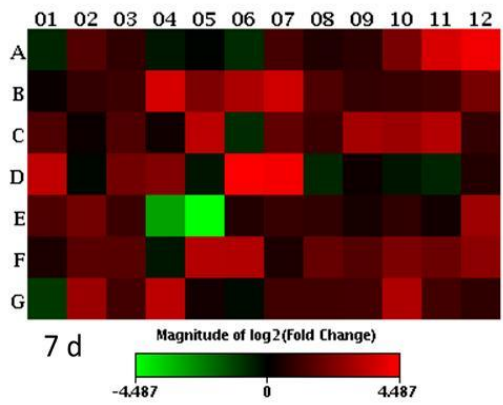
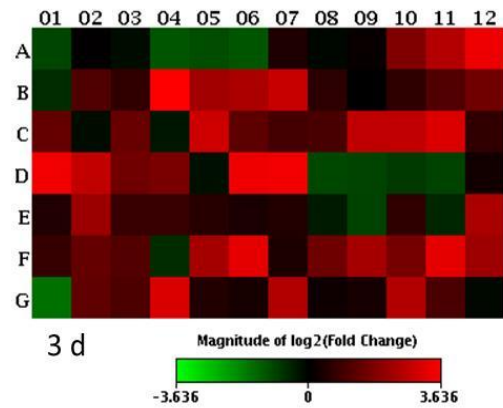
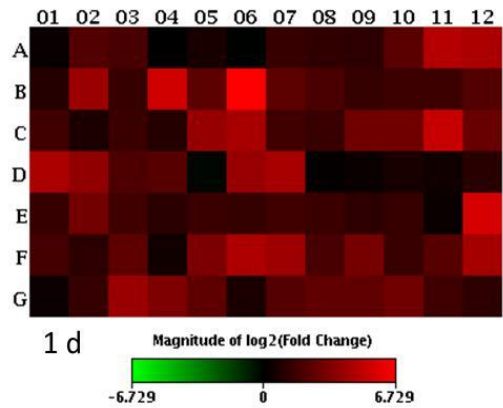


Fig. 25. Effects of NM on lung macrophage HDAC activity. Macrophage nuclear extracts, isolated 1 d, 3 d, 7 d, and 28 d after exposure of rats to PBS control (CTL) or NM, were analyzed for total HDAC activity. Bars, mean \pm SE (n = 3–5 rats). *Significantly different ($p \leq 0.05$) from CTL.

	1	2	3	4	5	6	7	8	9	10	11	12
A	let-7a-5p	let-7b-5p	let-7c-5p	let-7d-5p	let-7e-5p	let-7f-5p	let-7i-5p	101a-3p	101b-3p	106b-3p	125a-5p	125b-5p
B	128-3p	136-5p	140-5p	141-3p	142-3p	144-3p	145-5p	148b-3p	152-3p	15b-5p	16-5p	17-5p
C	181a-5p	181b-5p	181c-5p	181d-5p	182	183-5p	186-5p	195-5p	19a-3p	19b-3p	200a-3p	200c-3p
D	203a-3p	205	20a-5p	20b-5p	21-5p	221-3p	222-3p	23a-5p	23b-3p	26a-5p	26b-5p	27a-3p
E	27b-3p	291a-3p	29a-3p	29b-3p	29c-3p	30a-5p	30b-5p	30c-5p	30d-5p	30e-5p	320-3p	322-5p
F	323-3p	325-3p	327	34a-5p	34c-5p	351-5p	369-3p	374-5p	381-5p	384-5p	410-3p	429
G	448-3p	449a-5p	495	497-5p	539-5p	664-3p	673-5p	743b-5p	878	9a-5p	93-5p	98-5p



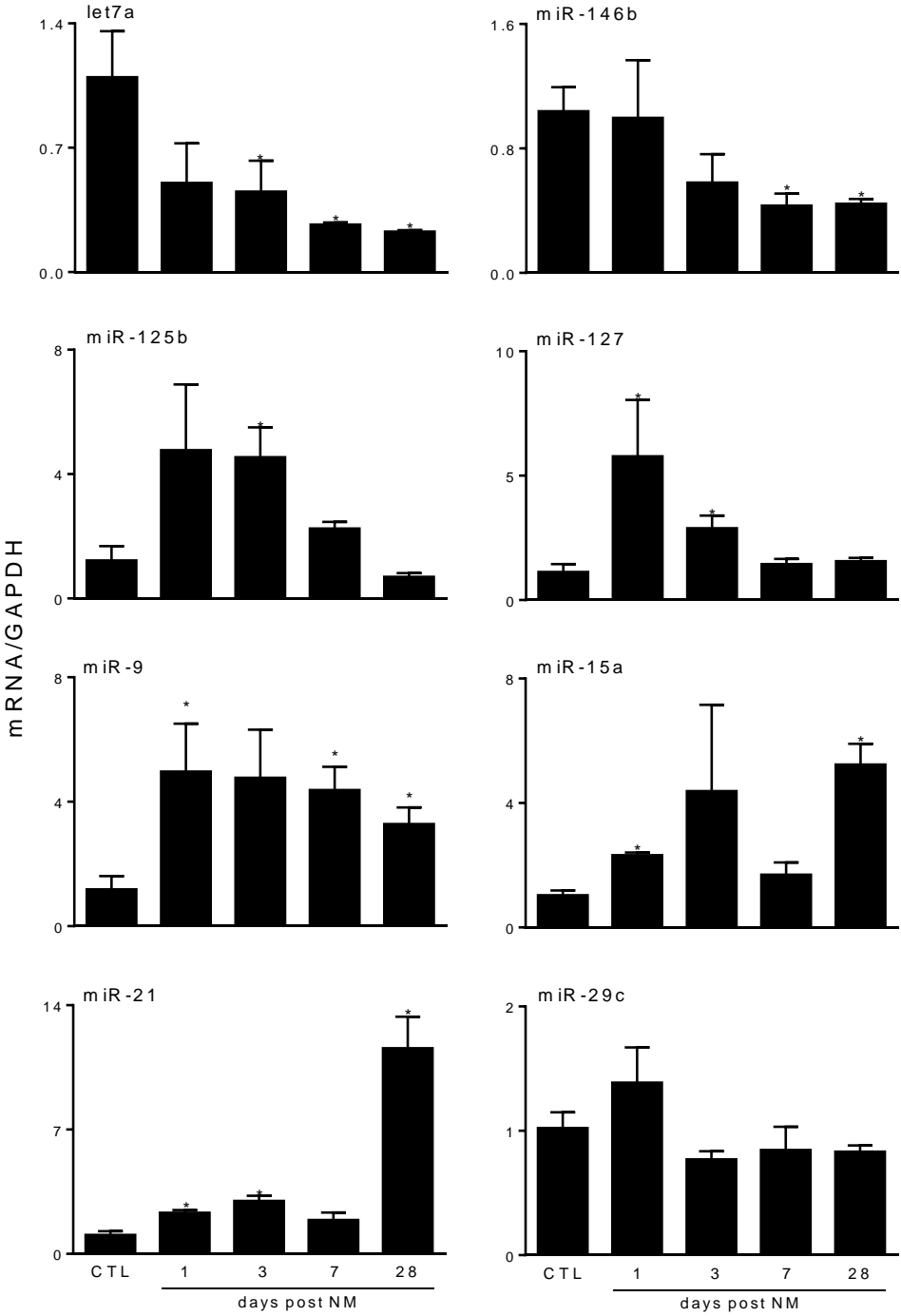


Fig. 26. Effects of NM on miRNA expression. Upper panel: alveolar macrophages, isolated 1 d, 3 d, 7 d, and 28 d after exposure of rats to PBS control (CTL) or NM, were analyzed for miRNA expression by RT-PCR. Lower panel: validation of miRNA expression by RT-PCR. Data were normalized relative to GAPDH. Bars, mean \pm SE (n = 3–5 rats). *Significantly different ($p \leq 0.05$) from CTL.

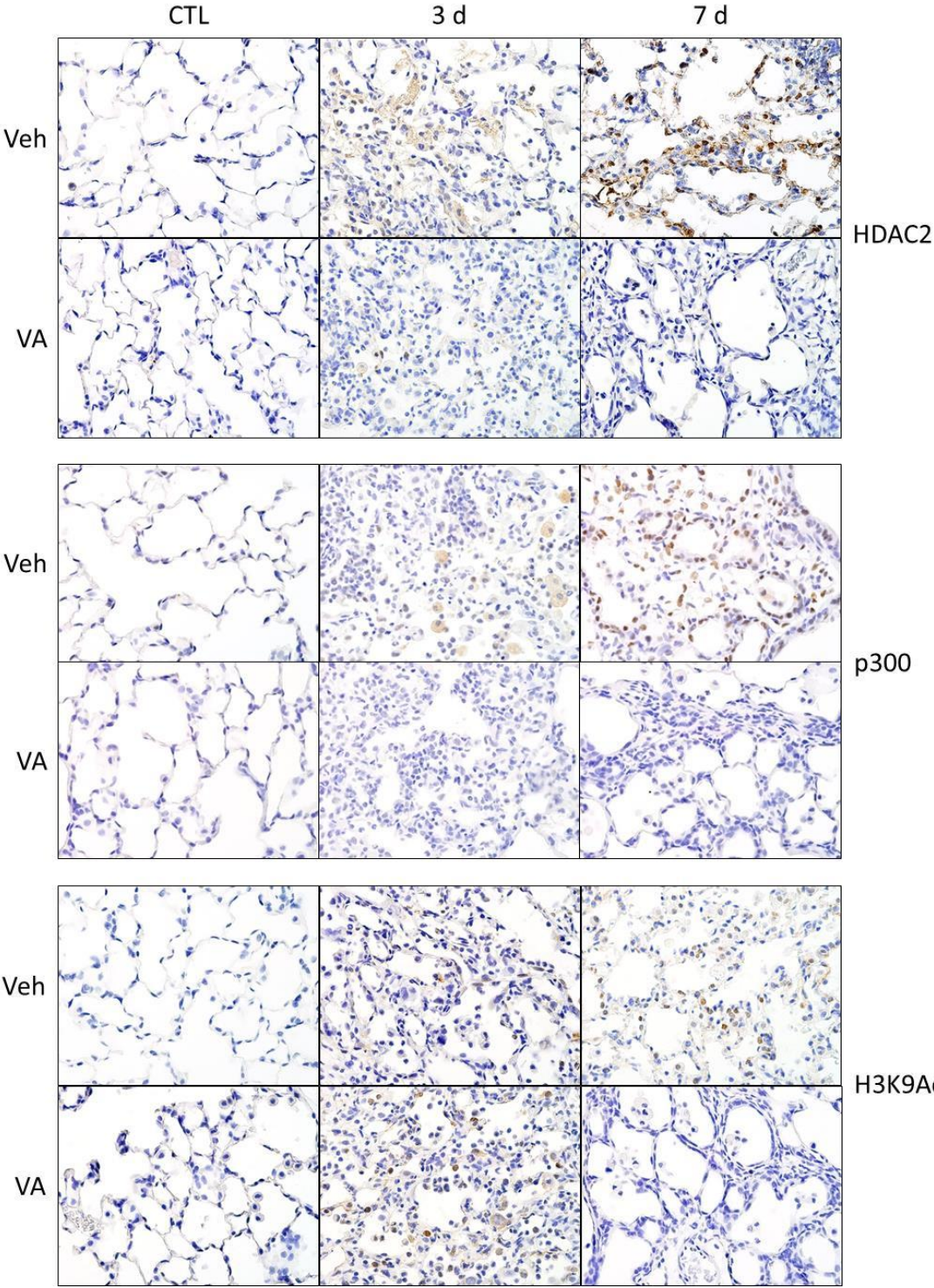


Fig. 27. Effects of valproic acid (VPA) on NM-induced HDAC2, p300 and H3K9Ac expression. Lung sections from rats treated with vehicle (Veh) or VA, were prepared 3 d or 7 d after exposure to PBS control (CTL) or NM and immunostained with antibody to HDAC2 (upper panels), p300 (center panels) or H3K9Ac (lower panels). Binding was visualized using a Vectastain kit. Original magnification, 600x. Representative sections from at least 3 rats/treatment group are shown.

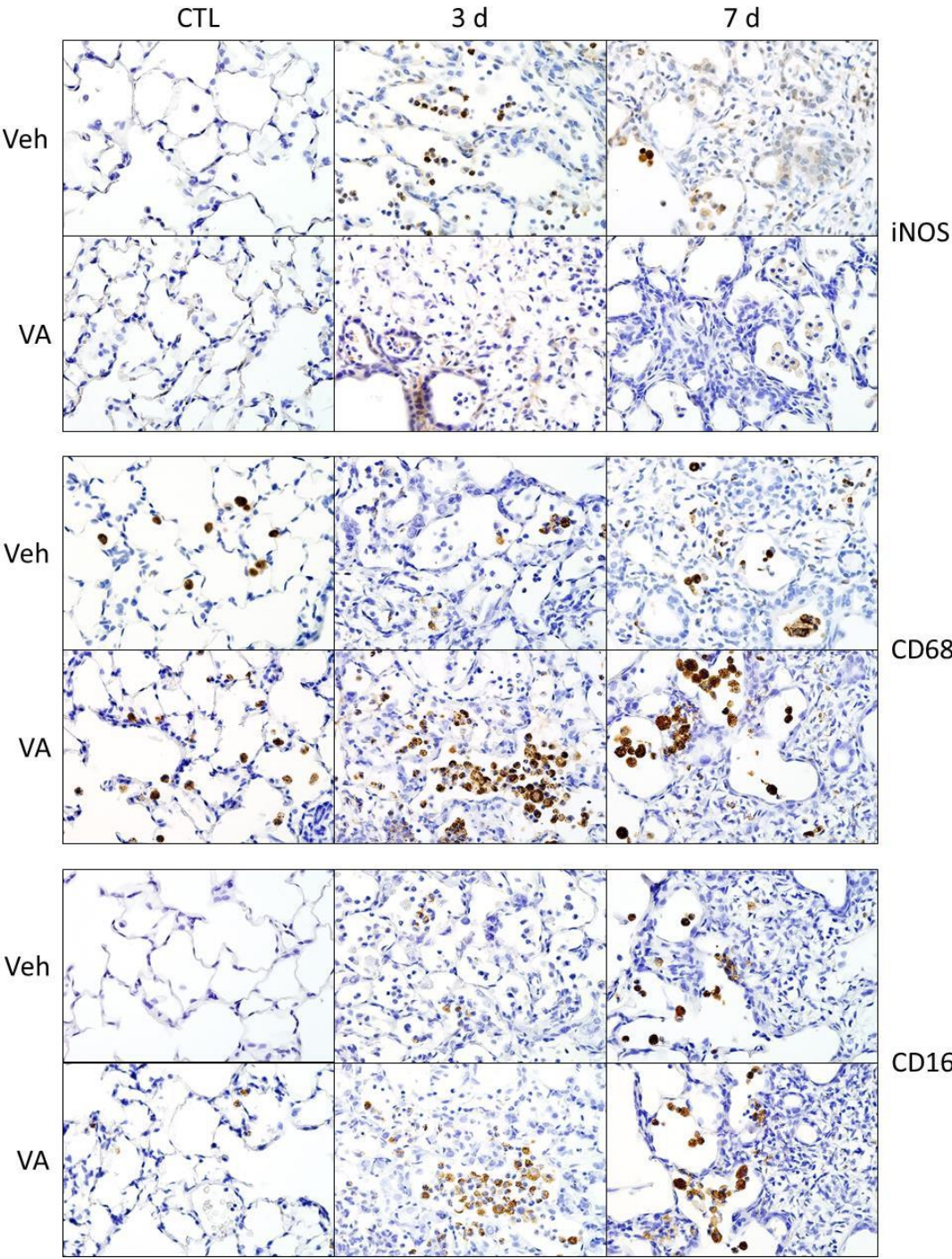


Fig. 28. Effects of valproic acid (VPA) on NM-induced pro- and antiinflammatory expression. Lung sections from rats treated with vehicle (Veh) or VA, prepared 3 d or 7 d after exposure to PBS control (CTL) or NM, were immunostained with antibodies to iNOS (upper panels), CD68 (center panels) or CD163 (lower panels). Binding was visualized using a Vectastain kit. Original magnification, 600x. Representative sections from at least 3 rats/treatment group are shown.

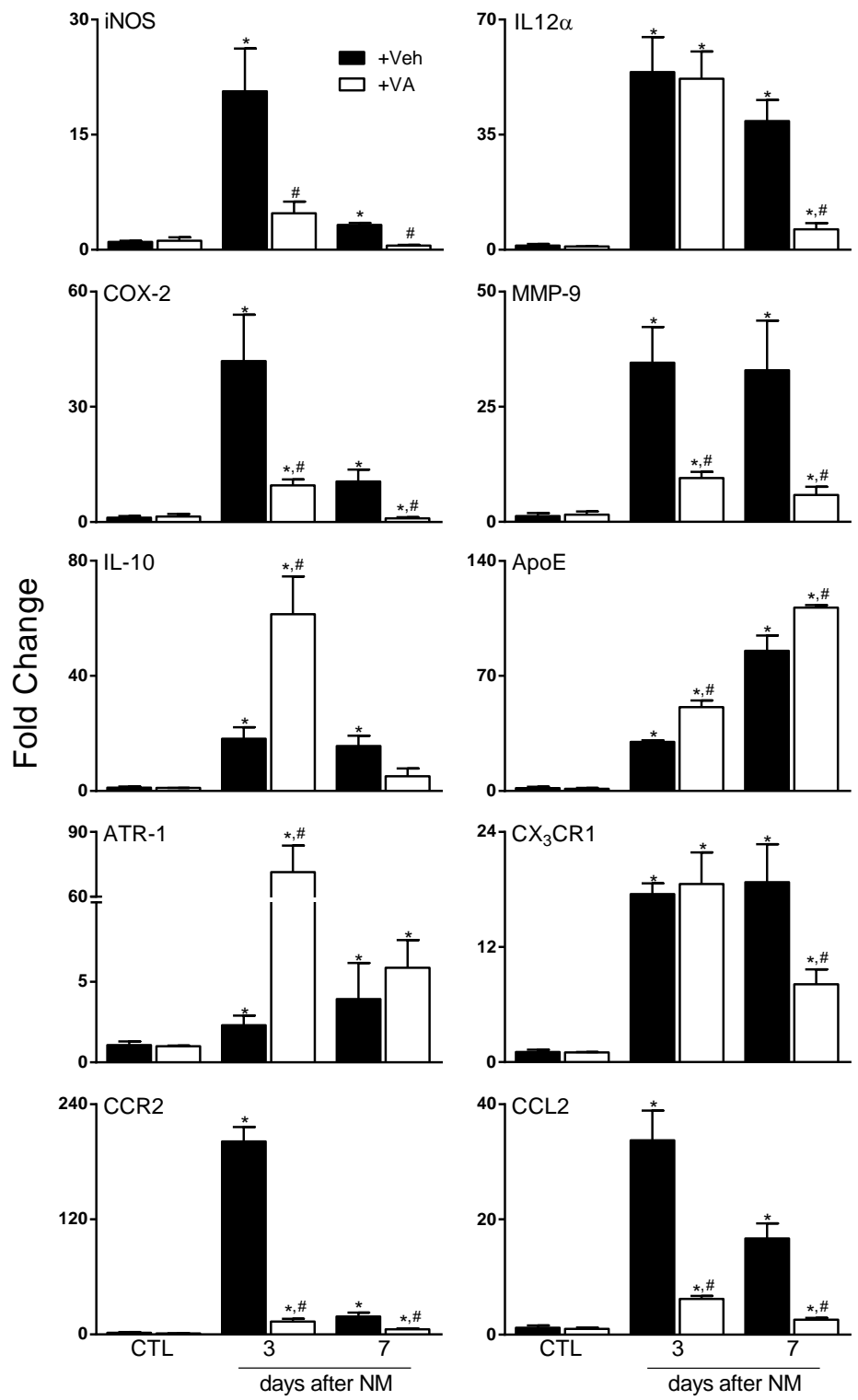


Fig. 29. Effects of valproic acid (VPA) on NM-induced macrophage gene expression. Cells, isolated from rats treated with vehicle (Veh) or VA, 3 d or 7 d after exposure to PBS control (CTL) or NM, were analyzed for gene expression by RT-PCR. Data were normalized relative to GAPDH. Bars, mean \pm SE (n = 3–7 rats). *Significantly different ($p \leq 0.05$) from CTL.

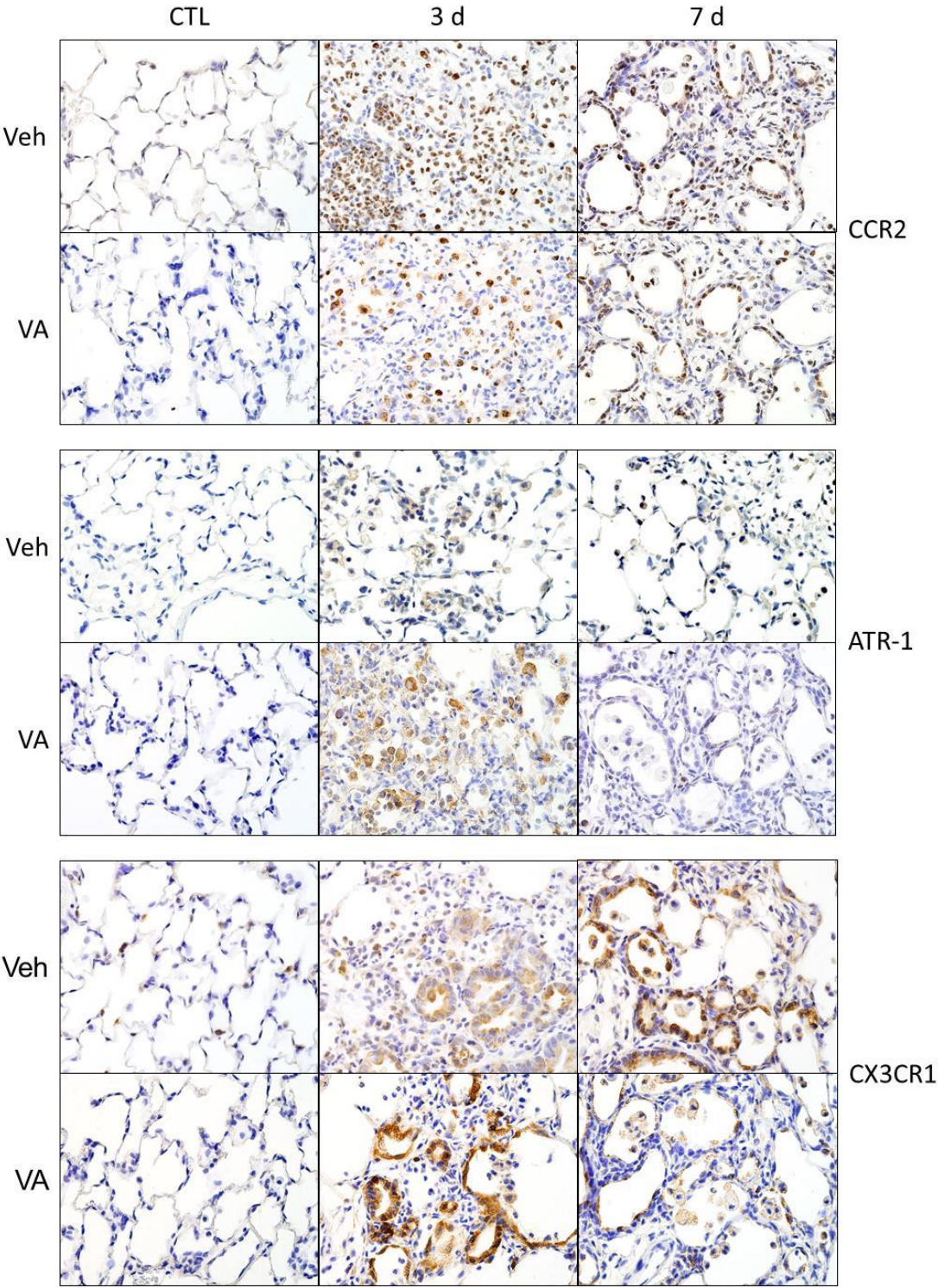


Fig. 30. Effects of valproic acid (VPA) on NM-induced CCR2, ATR-1 α and CX₃CR1 expression. Lung sections from rats treated with vehicle (Veh) or VA, prepared 3 d or 7 d after exposure to PBS control (CTL) or NM, were immunostained with antibody to CCR2 (upper panels) or ATR-1 (lower panels). Binding was visualized using a Vectastain kit. Original magnification, 600x. Representative sections from at least 3 rats/treatment group are shown.

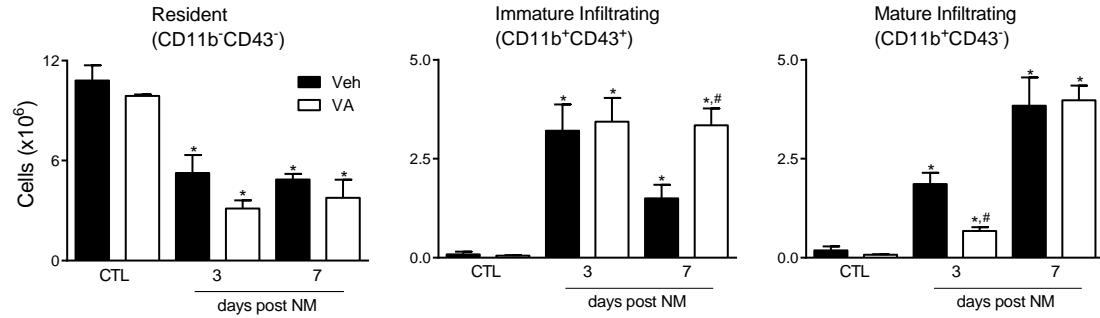
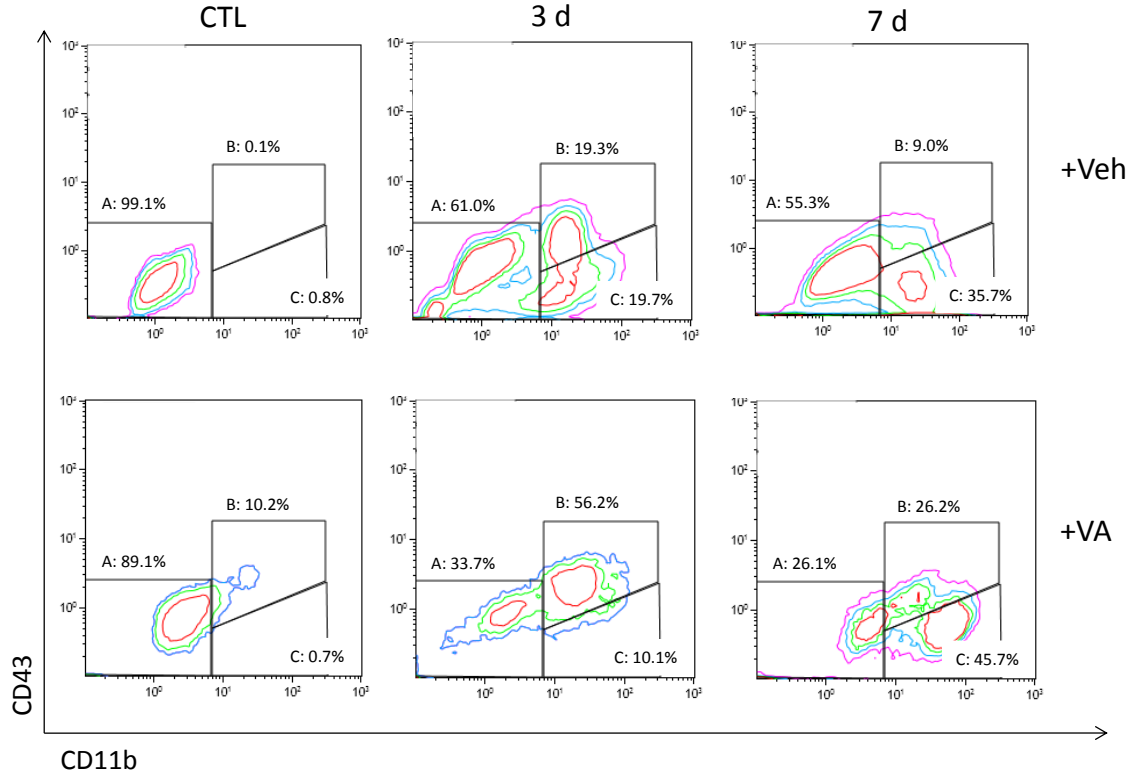


Fig. 31. Flow cytometric analysis of lung macrophages. Cells, isolated 3 d and 7 d after exposure of rats to PBS control (CTL) or NM, were immunostained with antibody to CD11b and CD43 or the appropriate isotype controls and then analyzed by flow cytometry. Pop. A: resident alveolar macrophages (CD11b⁻CD43⁻); Pop. B: infiltrating immature macrophages (CD11b⁺CD43⁺); and Pop. C: infiltrating mature macrophages (CD11b⁺CD43⁻). One representative analysis from 3-5 rats/treatment group is shown.

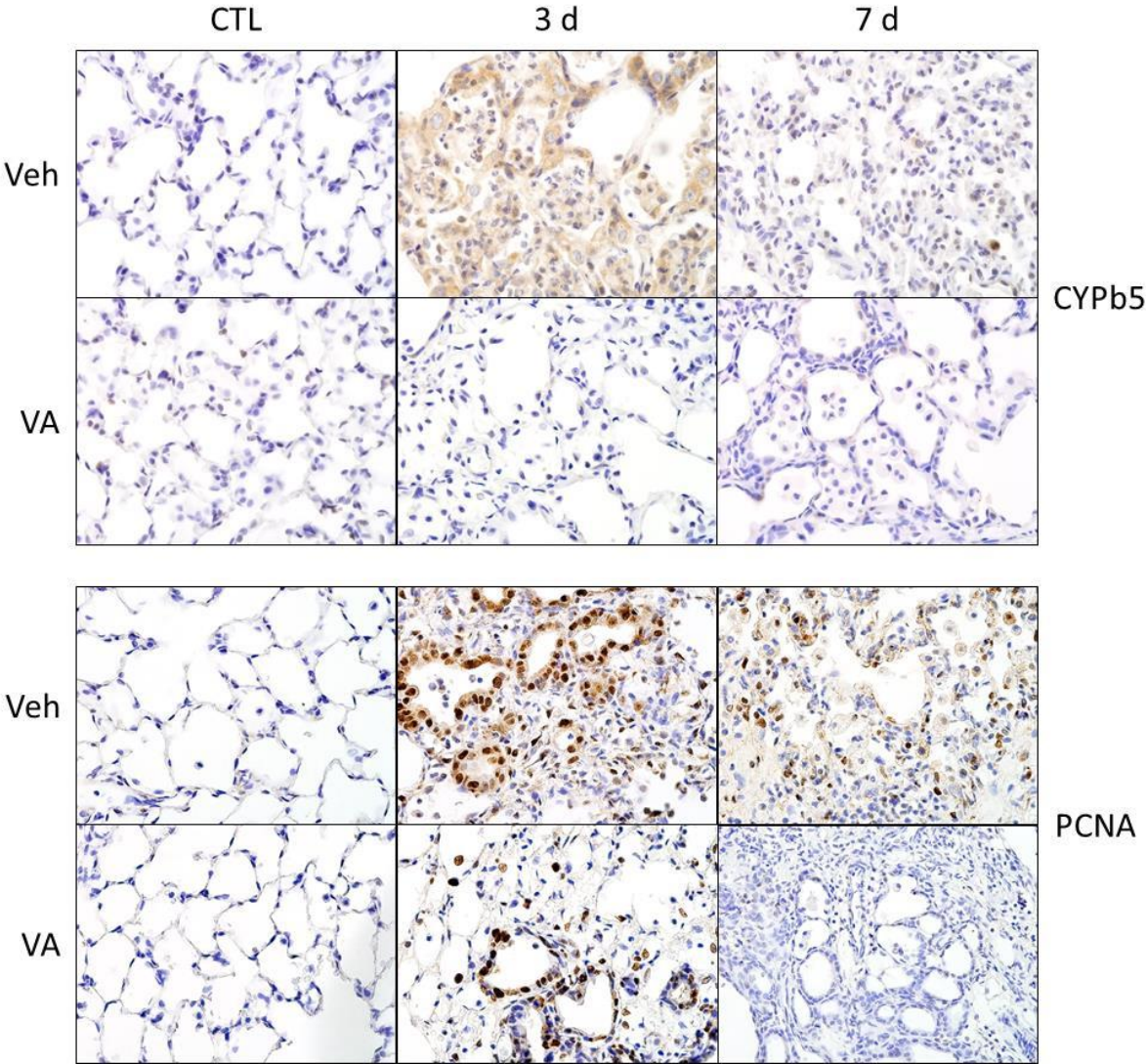


Fig. 32. Effects of valproic acid (VPA) on NM-induced oxidative stress, proliferation and DNA damage. Lung sections from rats treated with vehicle (Veh) or VA, were prepared 3 d or 7 d after exposure to PBS control (CTL) or NM and immunostained with antibody to CYPb5 (upper panels), PCNA (center panels) or γ H2A.X (lower panels). Binding was visualized using a Vectastain kit. Original magnification, 600x. Representative sections from at least 3 rats/treatment group are shown.

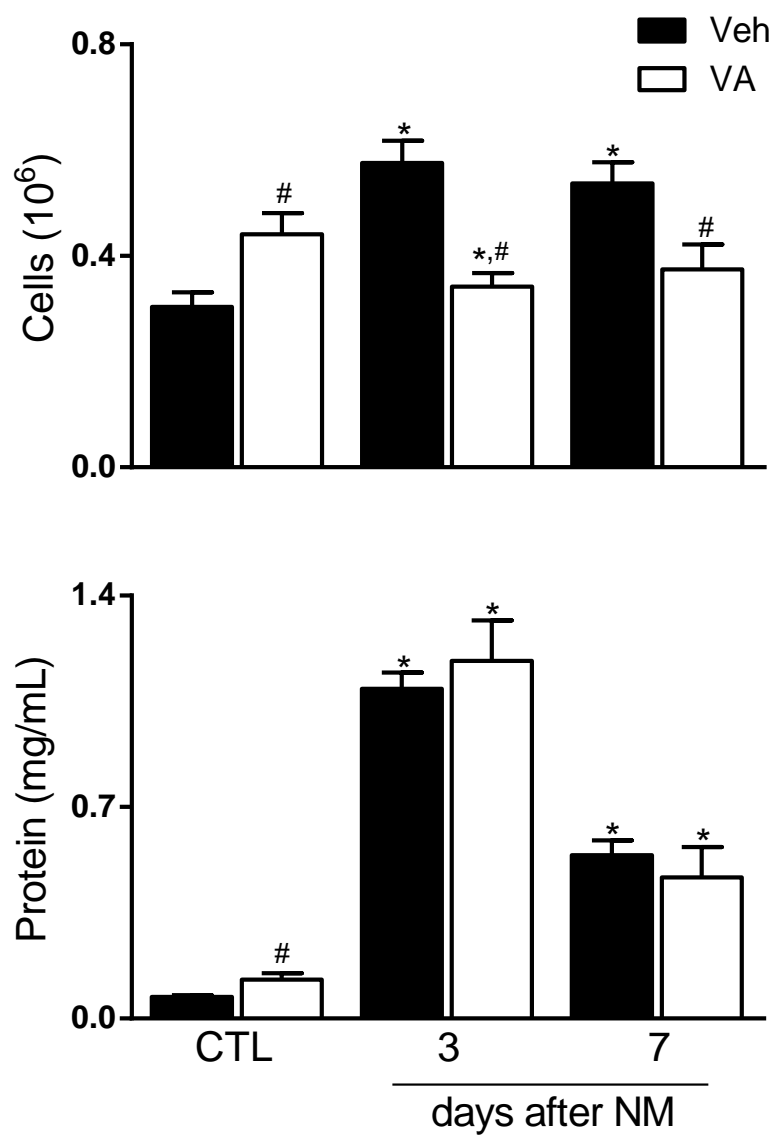


Fig. 33. Effects of valproic acid (VPA) on NM-induced lung injury and inflammation. BAL fluid, isolated from rats treated with vehicle (Veh) or VA, 3 d or 7 d after exposure to PBS control (CTL) or NM, was analyzed for cell infiltration (upper panel) and protein content (lower panel). Bars, mean \pm SE (n = 5-9 rats). *Significantly different ($p \leq 0.05$) from CTL. #Significantly different ($p \leq 0.05$) from Veh treated rats.

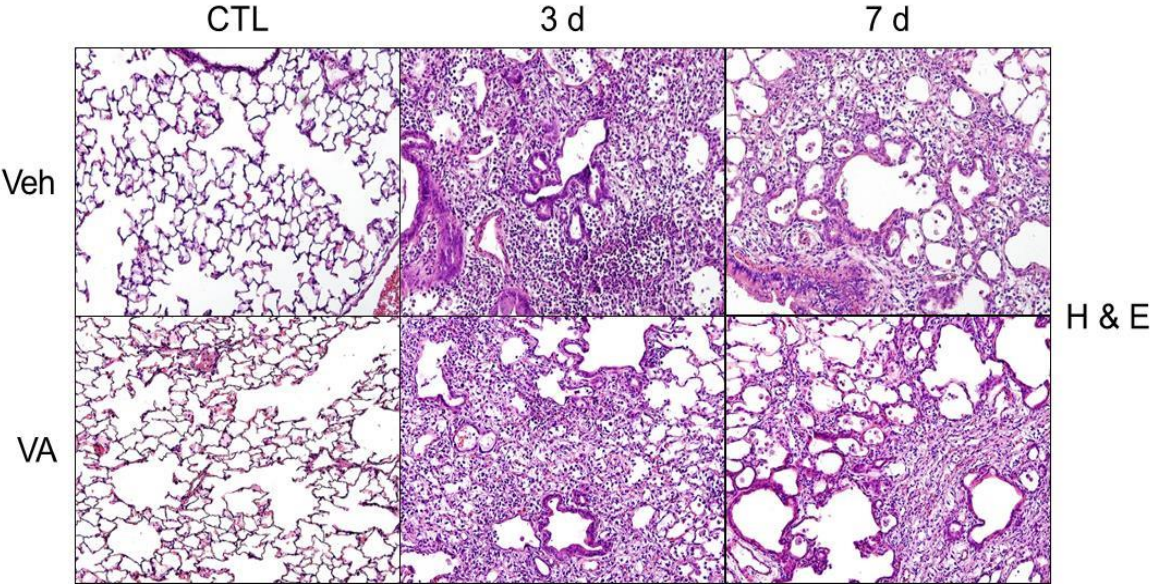


Fig. 34. Effects of valproic acid (VPA) on NM-induced lung pathology. Lung sections from rats treated with vehicle (Veh) or VPA, prepared 3 d or 7 d after exposure to PBS control (CTL) or NM, were stained with H&E. Original magnification, 200x. Representative sections from at least 3 rats/treatment group are shown

SUPPLEMENTAL FIGURES

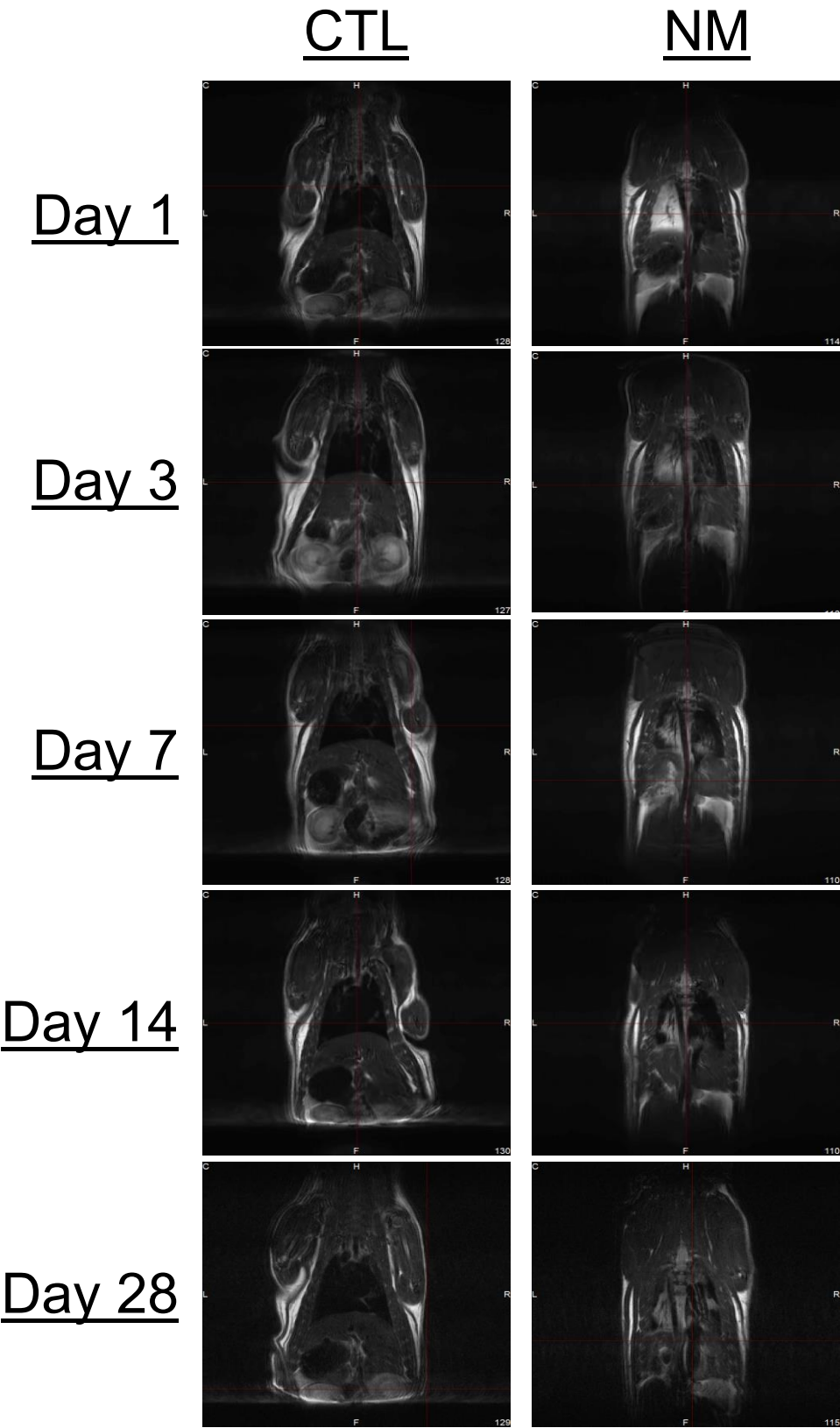


Fig. 1S. MRI analysis of rats exposed to NM. Rats were imaged 1 d, 3 d, 7 d, 14 d and 28 d after exposure to NM. One representative image is shown.

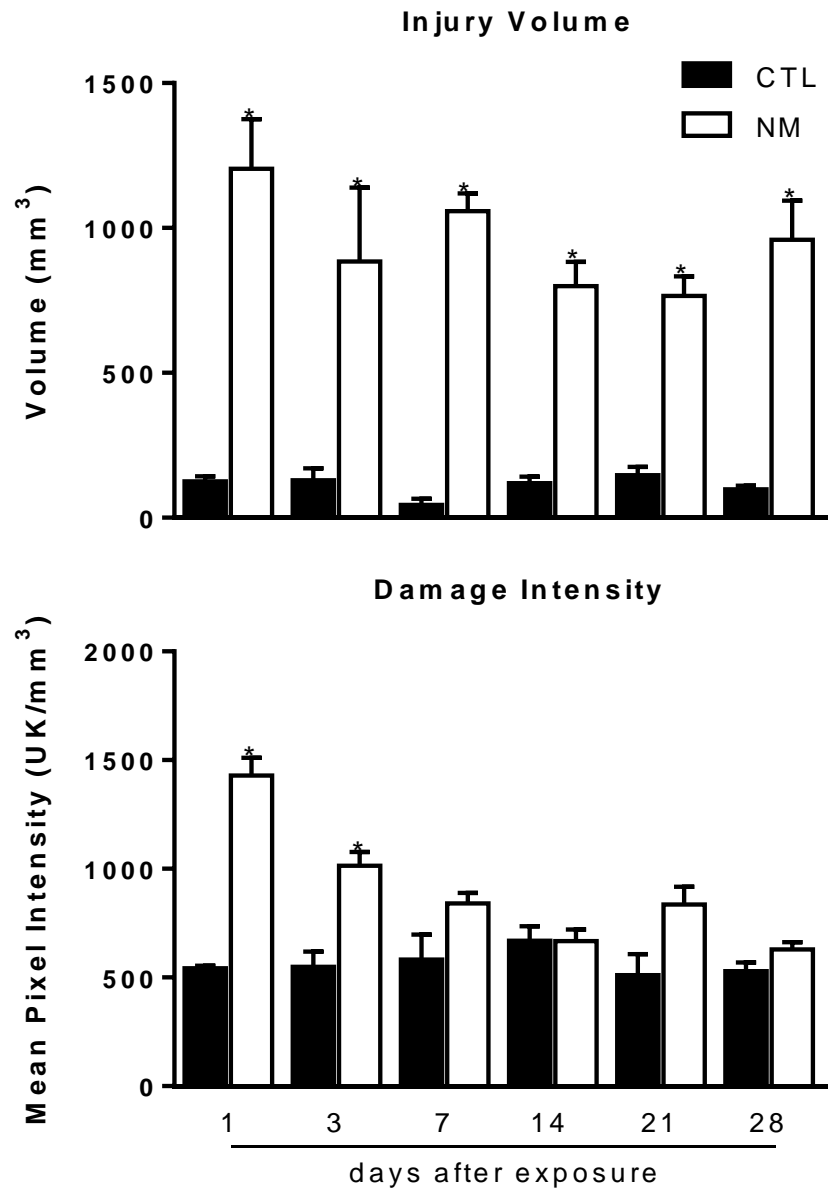


Fig.2S. Quantitation of NM-induced lung injury. Rats were imaged at 1 d, 3 d, 7 d, 14 d, 21 d and 28 d after exposure to PBS CTL or NM and analyzed for injury volume and extent of damage using VivoQuant software. Bars, mean \pm SEM (n=4-6). *Significantly different from rats treated with CTL ($p \leq 0.05$)

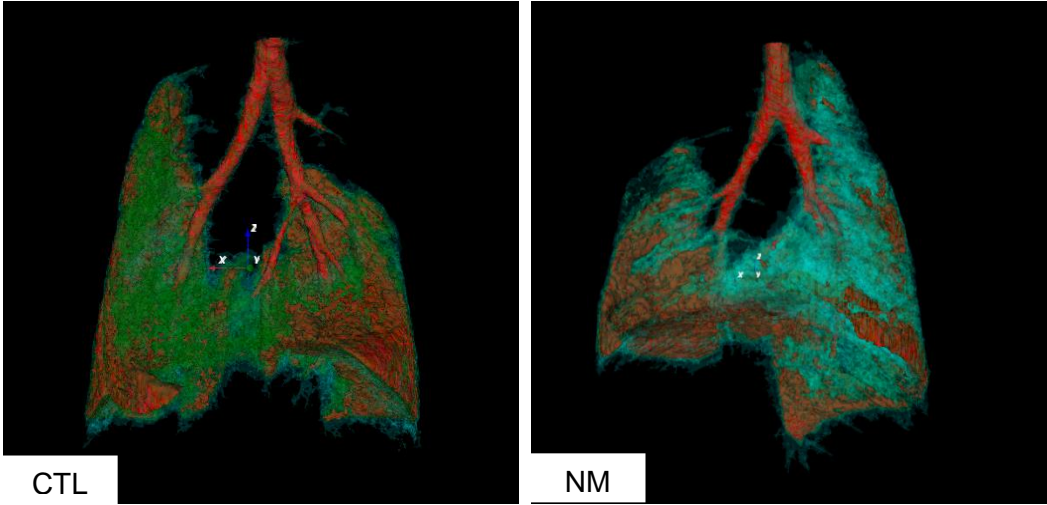


Fig. 3S. 3D tissue rendering of lung after exposure to PBS control (CTL) or NM. Lungs were analyzed 1 d, 3 d, 7 d, 14 d, 21 d and 28 d after exposure of rats to CTL or NM with Albira PET/SPECT/CT scan (Bruker Co., Villerica, MA). Representative image of lung 28 d following NM is shown.

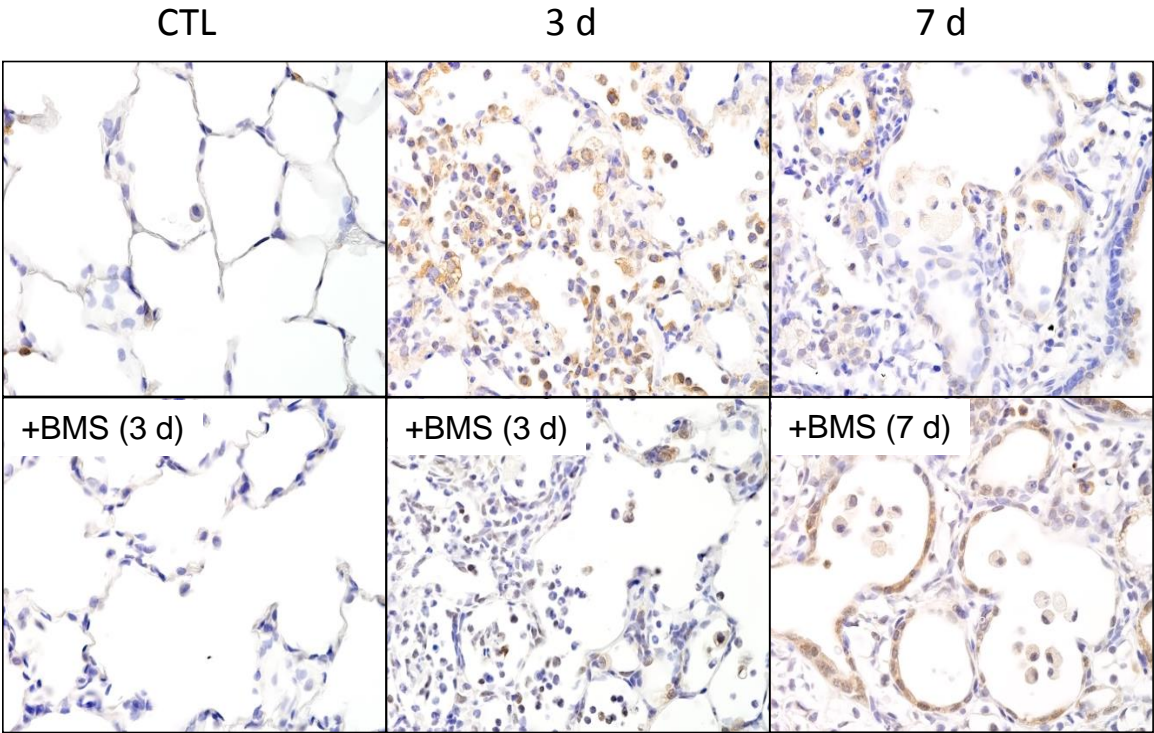


Fig. 4S. Effects of CCR2 inhibition on NM-induced CCR2 expression. Lung sections from rats treated with vehicle (Veh) or the CCR2 inhibitor (BMS), prepared 3 d or 7 d after exposure to PBS control (CTL) or NM were immunostained with antibody to CCR2. Binding was visualized using a Vectastain kit. Original magnification, 600x. Representative sections from at least 3 rats/treatment group are shown.

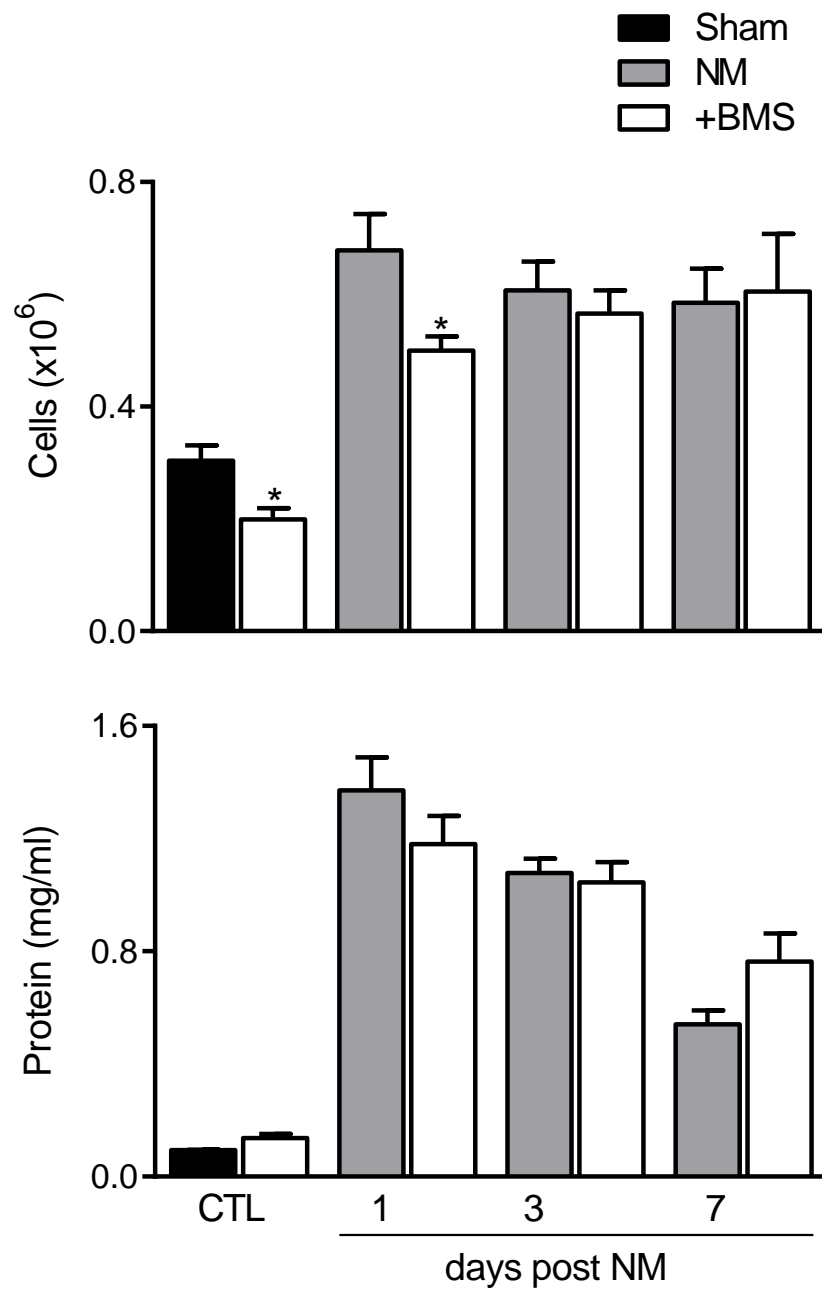


Fig. 5S. Effects of CCR2 inhibition on lung injury and inflammation. BAL fluid, collected from rats treated with the CCR2 inhibitor (BMS), prepared 3 d and 7 d after exposure of mice to PBS control (CTL) or NM, were analyzed for cell (upper panel) and protein content (lower panel). Bars, mean \pm SE (n = 3-5 rats). *Significantly different ($p \leq 0.05$) from CTL.

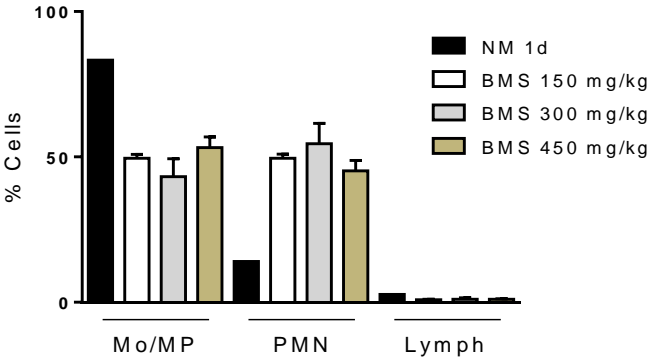
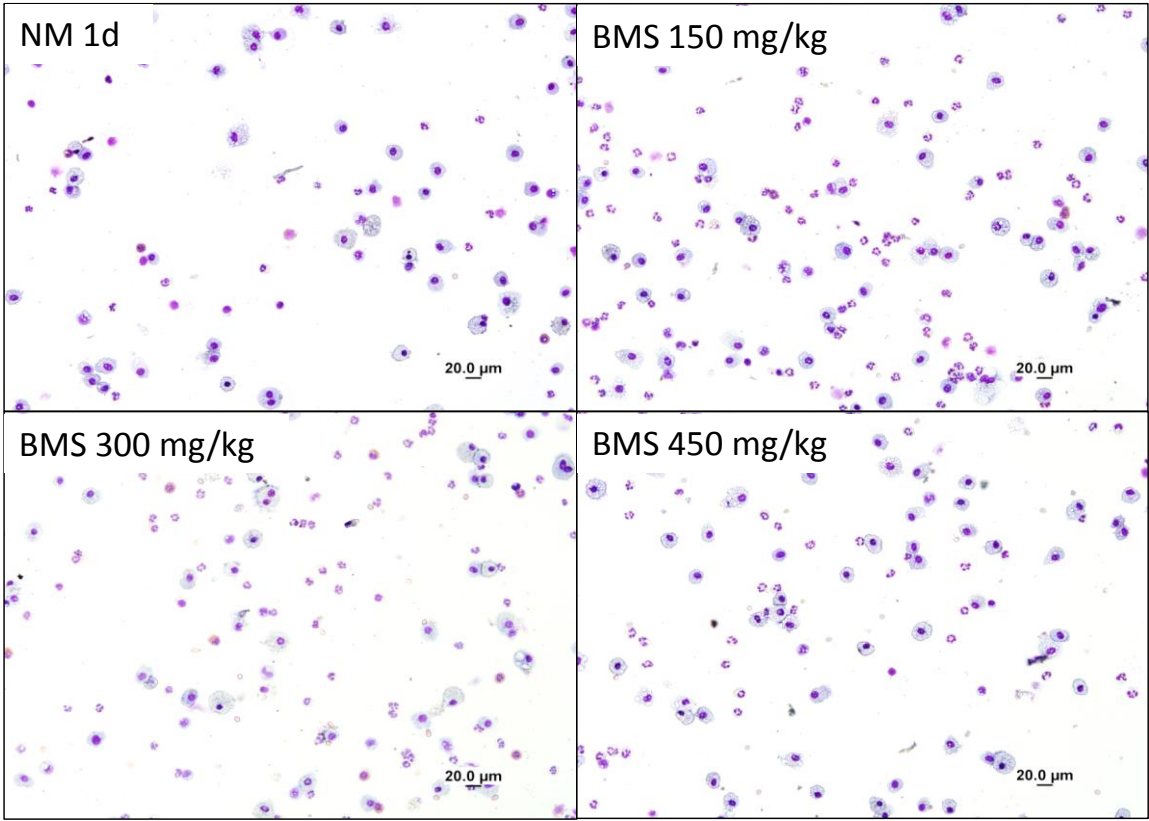


Fig. 6S. Effects of CCR2 inhibition on cellular infiltration. Top panels: Cytospin differential analysis of BAL cells collected from rats treated with the CCR2 inhibitor (BMS) 1 d after exposure of rats to NM. Cytospins showed >98% macrophages (not shown). Lower panels: Quantification of leukocytes accumulating in the lung after NM exposure. Bars, mean \pm SE (n = 3-5 rats). *Significantly different ($p \leq 0.05$) from CTL.

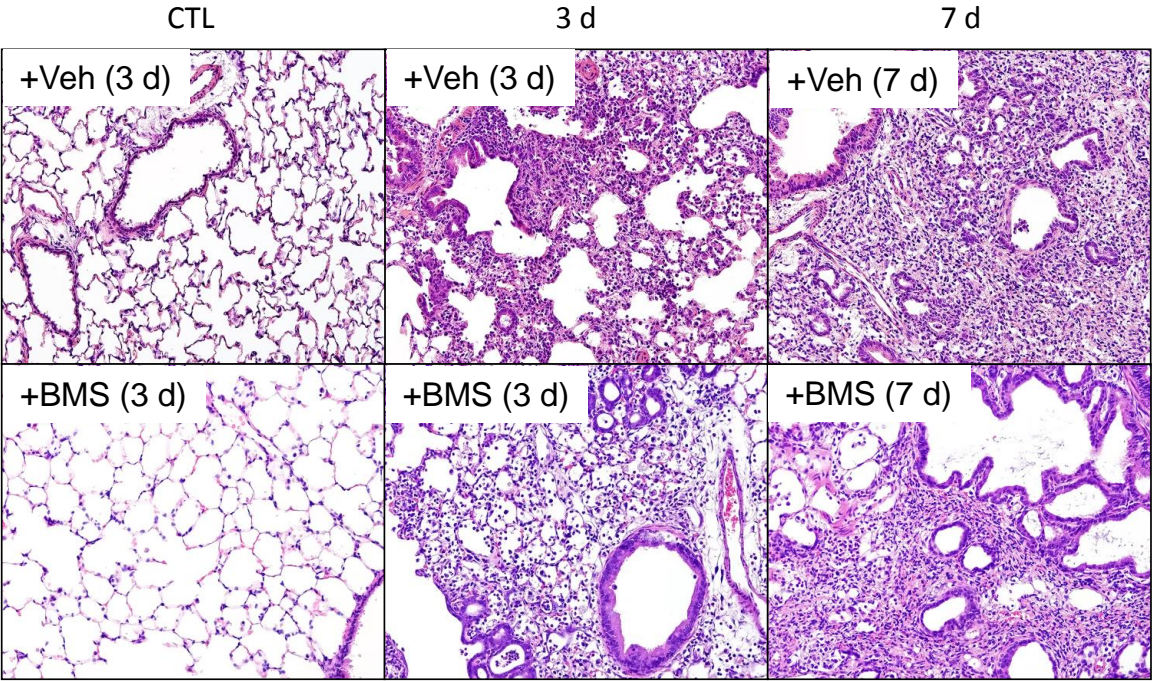


Fig. 7S. Effects of CCR2 inhibition on NM-induced lung pathology. Lung sections from rats treated with vehicle (Veh) or the CCR2 inhibitor (BMS), prepared 3 d or 7 d after exposure to PBS control (CTL) or NM, were stained with H&E. Original magnification, 200x. Representative sections from at least 3 rats/treatment group are shown

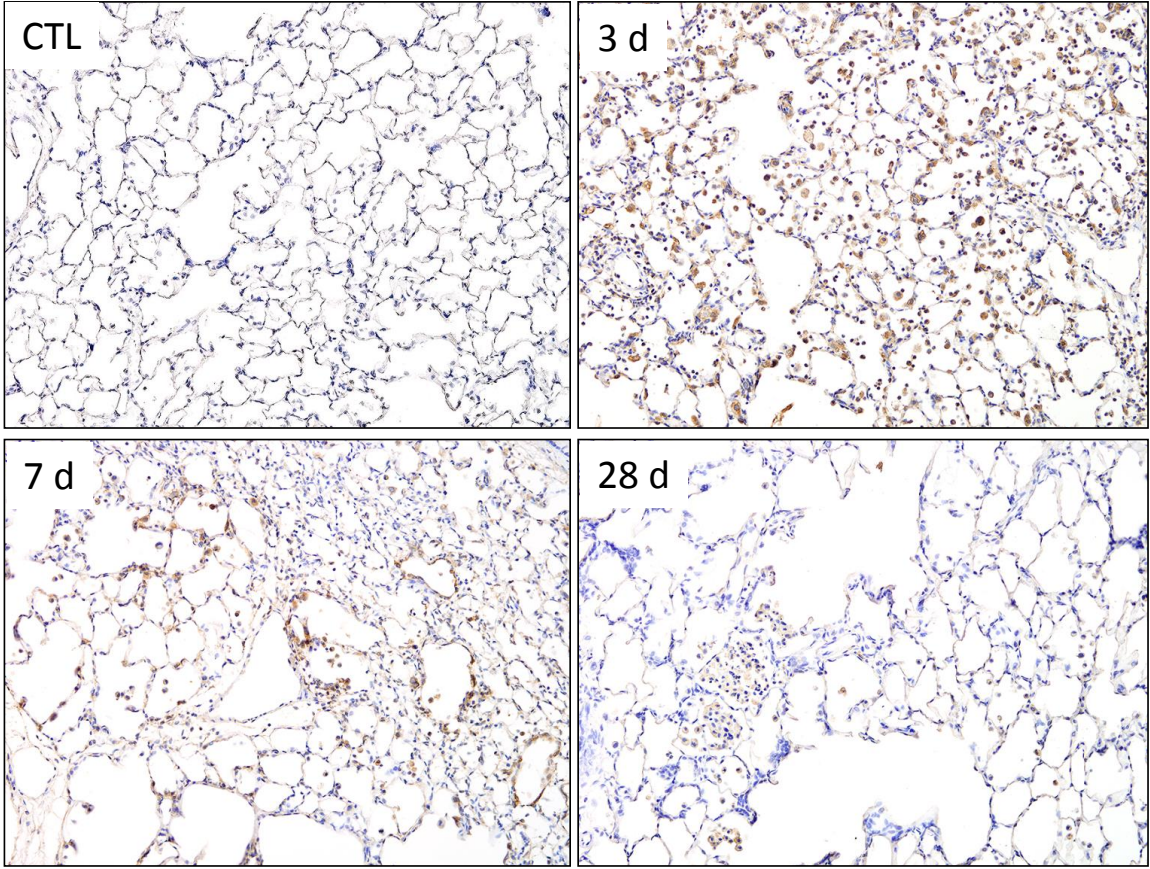


Fig. 8S. Effects of NM oxidized-LDL uptake. Lung sections, prepared 3 d, 7 d or 28 d after exposure of rats to PBS control (CTL) or NM, were immunostained with antibody to ox-LDL. Binding was visualized using a Vectastain kit. Original magnification, 600x. Representative sections from at least 3 rats/treatment group are shown.

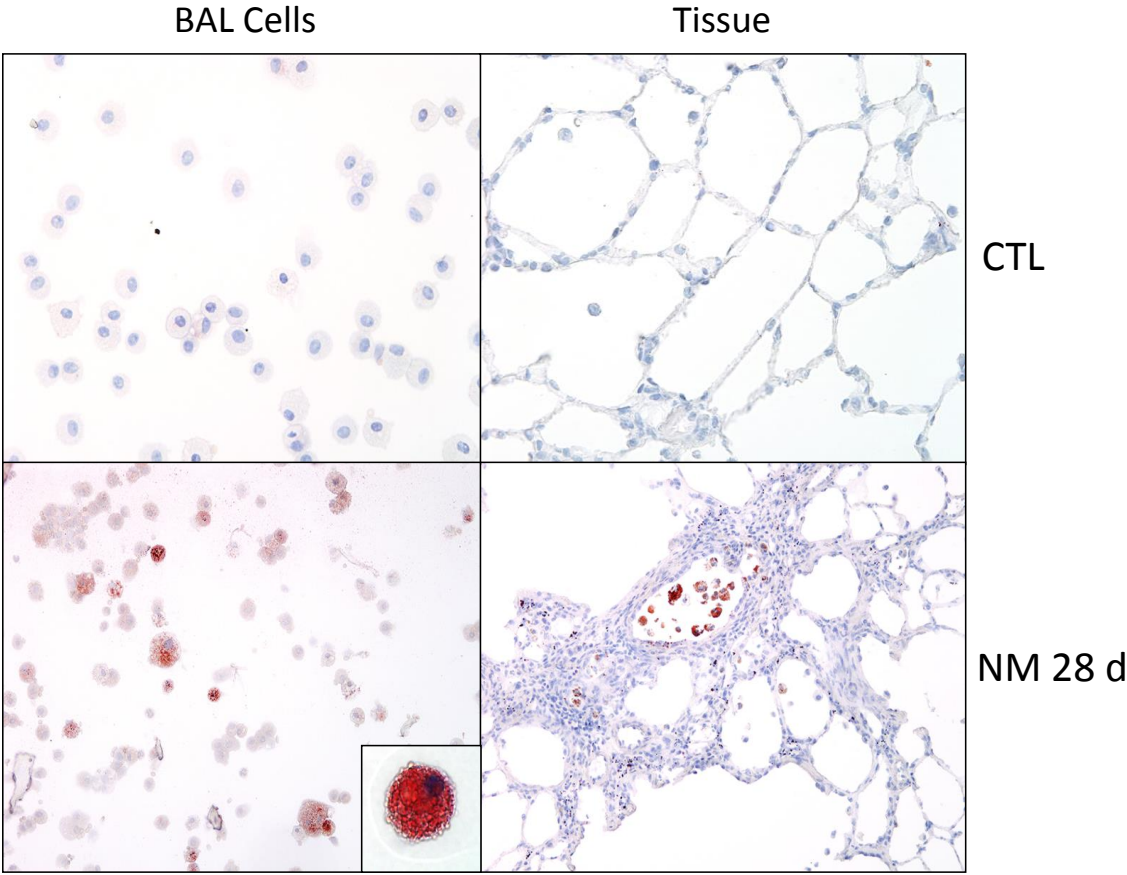


Fig. 9S. Effects of NM on macrophage lipid content. BAL cells and lung tissue, collected 28 d after exposure of rats to PBS control (CTL) or NM, were stained with Oil Red O. Original magnification, 200x. Representative sections from at least 3 rats/treatment group are shown

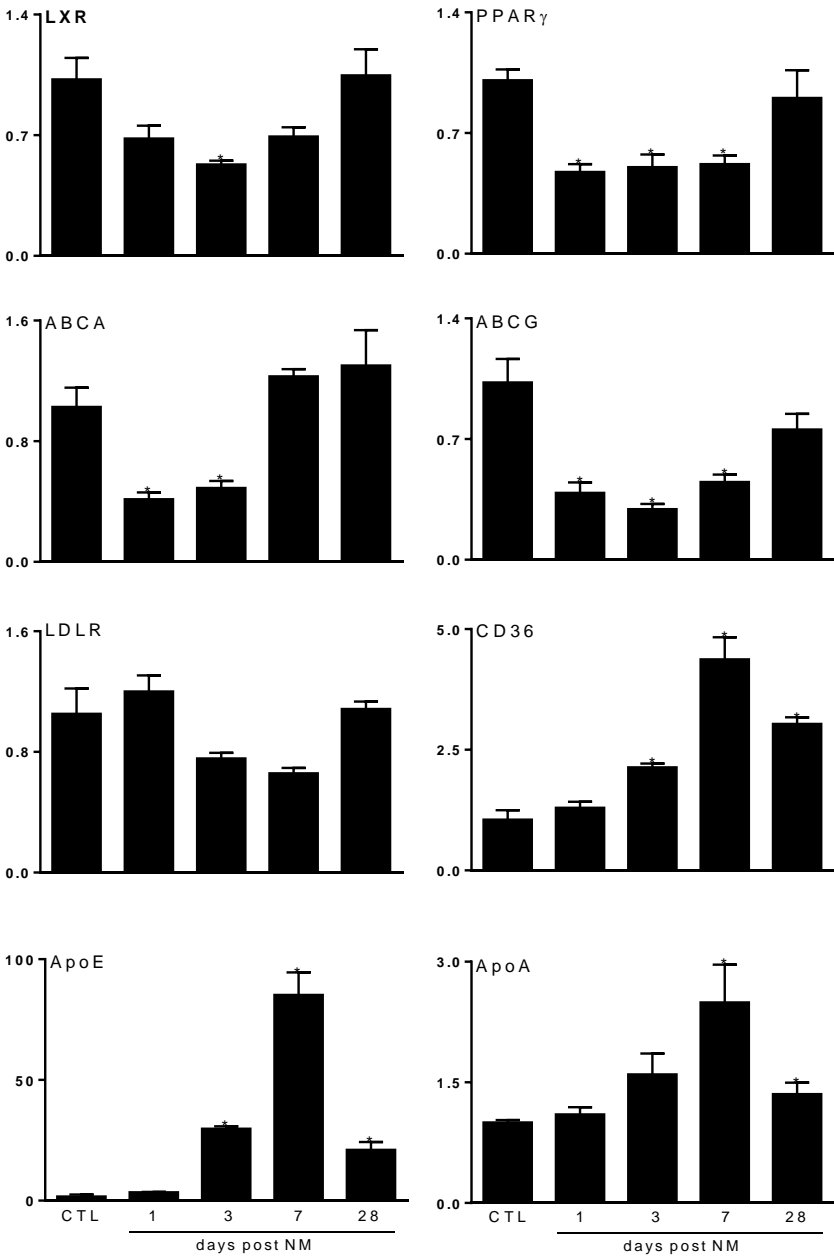


Fig. 10S. Effects of NM on gene expression associated with lipid regulation. Lung cells, isolated 1 d, 3 d, 7 d or 28 d after exposure of rats to PBS control (CTL) or NM, were analyzed by RT-PCR. Data were normalized relative to GAPDH. Bars, mean \pm SE (n = 3–7 rats). *Significantly different ($p \leq 0.05$) from CTL.

TABLES

Table 1. Semi-quantitative IHC scoring

		Staining Intensity	Positive Cells (%)
CD11b	CTL	0	0 ± 2
	1 d	3*	92 ± 4*
	3 d	2*	86 ± 11*
	7 d	2*	80 ± 18*
	28 d	1	65 ± 21*
iNOS	CTL	0	0 ± 1
	1 d	3*	72 ± 11*
	3 d	2*	59 ± 16*
	7 d	1	35 ± 14*
	28 d	0	22 ± 12
CD68	CTL	2	84 ± 6
	1 d	2	55 ± 17*
	3 d	2	77 ± 10
	7 d	3	85 ± 5
	28 d	2	92 ± 6
CD163	CTL	0	0 ± 0
	1 d	1	3 ± 3
	3 d	2	21 ± 13
	7 d	2*	82 ± 6*
	28 d	3*	85 ± 6*
CD206	CTL	1	35 ± 11
	1 d	1	39 ± 10
	3 d	2	65 ± 26
	7 d	3	90 ± 6*
	28 d	3*	85 ± 8*
ARG-II	CTL	0	0 ± 0
	1 d	2	82 ± 14*
	3 d	3*	93 ± 6*
	7 d	2	90 ± 4*
	28 d	1	79 ± 12*
YM-1	CTL	0	0 ± 0
	1 d	0	5 ± 5
	3 d	2	32 ± 12*
	7 d	4*	77 ± 8*
	28 d	4*	85 ± 7*
CCR2	CTL	0	5 ± 5
	1 d	1	50 ± 21*
	3 d	2*	68 ± 6*
	7 d	1	46 ± 12*
	28 d	0	25 ± 10
CX ₃ CR1	CTL	1	45 ± 13
	1 d	2	24 ± 17
	3 d	2*	92 ± 2*
	7 d	1	33 ± 30
	28 d	1	70 ± 19

Lung sections, stained for markers involved in macrophage activation and trafficking were scored for intensity and number (%) of positive macrophages present in the injured areas 1 d, 3 d, 7 d and 28 d after NM exposure. Intensity is represented as median using 0-4 scoring system. GRADE 0 = no staining; GRADE 1 = weak; GRADE 2 = moderate; GRADE 3 = strong; GRADE 4 = very strong staining. Number (%) of positive cells is represented as mean \pm SE (n = 3–5 rats). *Significantly different ($p \leq 0.05$) from CTL rats. Intensity staining was analyzed using Kruskal-Wallis non parametric one-way ANOVA

Table 2. Expression of CD43 and CD68 by lung macrophages

Macrophages	Phenotype	Cells (x10 ⁶)	
		CTL	NM
Resident (CD11b ⁻)	CD43 ⁻	10.8±0.9	5.2±1.2*
	CD43 ⁺	N.D.	N.D.
	CD68 ⁻	0.5±0.1	1.0±0.1*
	CD68 ⁺	9.9±0.1	3.0±0.6*
Infiltrating (CD11b ⁺)	CD43 ⁻	0.2±0.1	2.1±0.4*
	CD43 ⁺	0.1±0.1	2.7±0.6*
	CD68 ⁻	N.D.	1.0±0.4*
	CD68 ⁺	0.1±0.01	2.5±0.5*

Resident (CD11b⁻) and infiltrating (CD11b⁺) cells isolated

3 d after exposure of rats to PBS control (CTL) or NM,

were stained with antibody to CD43 or CD68 and

analyzed by flow cytometry. Data are mean \pm SE (n = 3–

4 rats). *Significantly different ($p \leq 0.05$) from CTL rats.

N.D., not detectable.

Table 3. Effects of splenectomy on NM-induced sorted macrophage gene expression.

Time after NM	MPs subpopulation	mRNA (fold change)							
		CCR2		iNOS		IL-10		ApoE	
		Sham	SPX	Sham	SPX	Sham	SPX	Sham	SPX
3 d	Resident (CD11b ⁻ CD43 ⁻)	6.6±2.8	50.3±15.3 ^c	0.9±0.5	3.3±1.2	1.2±0.4	0.9±0.3	34.8±5.2	16.9±3.5 ^c
	Immature Infiltrating (CD11b ⁺ CD43 ⁺)	16.7±3.5	15.2±5.0	121±44.2 ^a	49.1±12.5 ^a	1.1±0.2	0.3±0.1	28.4±6.7	19.3±3.9
	Mature Infiltrating (CD11b ⁺ CD43 ⁻)	10.7±1.6	16.9±6.2	1.5±0.8 ^b	2.0±0.2 ^b	5.3±1.4 ^{a,b}	1.4±0.3 ^c	78.5±9.1 ^{a,b}	20.4±2.1 ^c
7 d	Resident (CD11b ⁻ CD43 ⁻)	3.7±0.8	5.0±1.5	0.8±0.4	2.7±1.4	1.2±0.3	0.6±0.03	10.9±5.2	12.4±0.9
	Immature Infiltrating (CD11b ⁺ CD43 ⁺)	8.7±2.6	2.8±0.3	159.7±53.5 ^a	55.3±9.8 ^a	1.9±0.3	0.6±0.4	96.6±2.8 ^a	22.7±2.5 ^c
	Mature Infiltrating (CD11b ⁺ CD43 ⁻)	3.7±0.7	8.3±2.1	0.9±0.1 ^b	0.8±0.1 ^b	6.0±0.5 ^{a,b}	0.7±0.2 ^c	119.5±14.9 ^a	27.7±1.9 ^{a,c}

Cells isolated 3 d and 7 d after exposure of SPX rats to PBS control (CTL) or NM, were stained with antibody to CD11b and CD43 as described in the *Materials and Methods*.

Resident (CD11b⁻CD43⁻), immature infiltrating (CD11b⁺CD43⁺), and mature infiltrating (CD11b⁺CD43⁻) macrophage subpopulations were assayed by RT-PCR for expression of pro- (iNOS, and CCR2) and anti-inflammatory (IL-10 and ApoE) genes. Data were normalized to GAPDH and presented as fold change relative to resident CD11b⁻CD43⁻ macrophages from CTL rats. Bars, mean ± SE (n = 3–4 rats). ^a Significantly different ($p \leq 0.05$) from resident (CD11b⁻CD43⁻). ^b Significantly different ($p \leq 0.05$) from immature (CD11b⁺CD43⁺). ^c Significantly different ($p \leq 0.05$) from Sham group.

Table 4. Effects of splenectomy on NM-induced lung injury and inflammation.

	Cells ($\times 10^5$)		Protein ($\mu\text{g/ml}$)	
	Sham	SPX	Sham	SPX
CTL	3.1 \pm 0.1	3.3 \pm 0.0	94.6 \pm 1.6	136.3 \pm 48.6
1 d	7.2 \pm 0.1 ^a	4.0 \pm 0.1 ^{a,b}	1372.0 \pm 117.4 ^a	1369.5 \pm 111.6 ^a
3 d	6.4 \pm 0.1 ^a	7.2 \pm 0.1 ^a	994.4 \pm 82.0 ^a	1098.7 \pm 158.2 ^a
7 d	6.7 \pm 0.1 ^a	8.0 \pm 0.1 ^a	592.4 \pm 47.3 ^a	936.7 \pm 23.1 ^{a,b}

BAL fluid, collected 1 d, 3 d and 7 d after exposure of sham and SPX rats to PBS control (CTL) or NM, was analyzed for cell and protein content. Data are mean \pm SE (n = 5-9 rats). ^aSignificantly different ($p \leq 0.05$) from CTL. ^bSignificantly different ($p \leq 0.05$) from sham rats.

Table 5. Effects of splenectomy on NM-induced lung pathology

Histopathological Scores	CTL		NM (3 d)		NM (7 d)	
	Sham	SPX	Sham	SPX	Sham	SPX
Mixed Cell Infiltration	0	0	3 ^a	4 ^{a,b}	2	3 ^a
Edema	0	0	2	2	2	3
Bronchio-alveolar Hyperplasia	0	0	2	3 ^a	3 ^a	3 ^a
Mesothelial Proliferation	0	0	0	2	0	0
Bronchioectasis	0	0	0	0	3 ^a	4 ^a
Emphysema	0	0	1	3 ^{a,b}	2	4 ^a
Metaplasia	0	0	0	3 ^{a,b}	1	3 ^a
Fibroplasia	0	0	2	3 ^a	2	4 ^a
Fibrosis	0	0	0	2 ^{a,b}	0	2 ^{a,b}

Lung sections, collected 3 d and 7 d after exposure of sham and SPX rats to PBS control (CTL) or NM, were stained with H&E and Gomori's trichrome and scored for histopathologic changes. GRADE 0 = no injury; GRADE 1 = minimal /very small; GRADE 2 = slight/small; GRADE 3 = moderate; GRADE 4 = extensive. Bars, median (n= 3-4 rats).

^aStatistically significant from CTL. ^bStatistically significant from Sham rats. Data were analyzed using Kruskal-Wallis non parametric one-way ANOVA followed by Mann-Whitney Rank Sum post-hoc test.

Table 6. Splenectomy semi-quantitative IHC scoring

		Staining Intensity		Positive Cells (%)	
Gene	Time	Sham	SPX	Sham	SPX
CD11b	PBS	0	0	0 ± 0	0 ± 0
	NM 3d	3 ^a	3 ^a	86 ± 11 ^a	91 ± 7 ^a
	NM 7d	3 ^a	3 ^a	90 ± 8 ^a	92 ± 4 ^a
iNOS	PBS	0	0	0 ± 0	2 ± 1
	NM 3d	1	2 ^a	59 ± 16 ^a	48 ± 12 ^a
	NM 7d	1	4 ^{a,b}	35 ± 14 ^a	93 ± 4 ^{a,b}
CD68	PBS	2	2	84 ± 6	78 ± 8
	NM 3d	2	2	64 ± 10	69 ± 11
	NM 7d	3	3	85 ± 5	88 ± 12
CD163	PBS	0	0	0 ± 0	0 ± 0
	NM 3d	2	2	21 ± 13	31 ± 23
	NM 7d	2 ^a	2 ^a	82 ± 6 ^a	70 ± 22 ^a
CD206	PBS	1	1	35 ± 11	27 ± 13
	NM 3d	2	2	65 ± 26	56 ± 14
	NM 7d	2 ^a	3 ^a	85 ± 6 ^a	90 ± 7 ^a
YM-1	PBS	0	0	0 ± 0	0 ± 0
	NM 3d	0	2	32 ± 12 ^a	21 ± 8 ^a
	NM 7d	3 ^a	3 ^a	77 ± 8 ^a	87 ± 4 ^a
CCR2	PBS	0	0	5 ± 5	0 ± 0
	NM 3d	1	3 ^{a,b}	48 ± 12 ^a	79 ± 14 ^{a,b}
	NM 7d	1	2	40 ± 9 ^a	41 ± 13 ^a
CX3CR1	PBS	1	1	45 ± 13	65 ± 15
	NM 3d	2 ^a	1	92 ± 2 ^a	63 ± 8 ^b
	NM 7d	2	0 ^b	48 ± 15	8 ± 4 ^b
ATR-1α	PBS	0	0	0 ± 0	0 ± 0
	NM 3d	3 ^a	0 ^b	79 ± 11 ^a	4 ± 2 ^b
	NM 7d	1	0	15 ± 4	18 ± 2

Lung sections from sham and SPX rats stained for markers involved in macrophage activation and trafficking were scored for intensity and number (%) of positive macrophages present in injured areas 3 d and 7 d after NM exposure. Intensity is represented as median using 0-4 scoring system. GRADE 0 = no staining; GRADE 1 = weak; GRADE 2 = moderate; GRADE 3 = strong; GRADE 4 = very strong staining. Number (%) of positive cells is represented as mean ± SE (n = 3–5 rats).

*Significantly different ($p \leq 0.05$) from CTL rats. Intensity staining was analyzed using Kruskal-Wallis non parametric one-way ANOVA followed by Mann-Whitney Rank Sum post-hoc test; number of positive cells was analyzed using one-way ANOVA followed by unpaired t-test.

Table 7. Effects of VPA on NM-induced lung pathology

Histopathological Scores	CTL		NM (3 d)		NM (7 d)	
	Veh	VPA	Veh	VPA	Veh	VPA
Mixed Cell Infiltration	0	0	3 ^a	4 ^{a,b}	2	3 ^a
Edema	0	0	2	2	2	2
Bronchio-alveolar Hyperplasia	0	0	2	3 ^a	3 ^a	3 ^a
Mesothelial Proliferation	0	0	2	1	1	1
Bronchioectasis	0	0	1	1	3 ^a	2 ^a
Emphysema	0	0	1	1	2 ^a	2 ^a
Metaplasia	0	0	1	1	1	1
Fibroplasia	0	0	2 ^a	2 ^a	2 ^a	2 ^a

Lung sections, collected 3 d and 7 d after exposure of rats to PBS (CTL) or NM followed by vehicle (Veh) or VPA were stained with H&E and scored for histopathologic changes.

GRADE 0 = no injury; GRADE 1 = minimal /very small; GRADE 2 = slight/small; GRADE 3 = moderate; GRADE 4 = extensive. Bars, median (n= 3-4 rats). ^aStatistically significant from CTL. ^bStatistically significant from Sham rats. Data were analyzed using Kruskal-Wallis non parametric one-way ANOVA followed by Mann-Whitney Rank Sum post-hoc test.

Table 8. Valproic acid semi-quantitative IHC scoring

		Staining Intensity		Positive Cells (%)	
Gene	Time	Veh	VPA	Veh	VPA
HDAC2	CTL	0	0	3 ± 3	2 ± 1
	NM 3d	2 ^a	0 ^b	54 ± 12 ^a	10 ± 5 ^b
	NM 7d	3 ^a	0 ^b	65 ± 14 ^a	5 ± 5 ^b
p300	CTL	0	0	0 ± 0	0 ± 0
	NM 3d	2 ^a	0 ^b	44 ± 10 ^a	8 ± 4 ^b
	NM 7d	2 ^a	0 ^b	75 ± 15 ^a	5 ± 5 ^b
H3K9Ac	CTL	0	0	5 ± 2	0 ± 0
	NM 3d	1	2 ^a	15 ± 3	61 ± 13 ^{a,b}
	NM 7d	1	0	82 ± 6 ^a	10 ± 5 ^b
iNOS	CTL	0	0	0 ± 0	0 ± 0
	NM 3d	2 ^a	1	59 ± 16 ^a	28 ± 12 ^{a,b}
	NM 7d	2	1	65 ± 12 ^a	33 ± 8 ^{a,b}
CD68	CTL	2	2	84 ± 6	88 ± 5
	NM 3d	2	2	55 ± 10 ^a	79 ± 11 ^b
	NM 7d	3	3	85 ± 5	92 ± 6
CD163	CTL	0	0	0 ± 0	0 ± 0
	NM 3d	2	2	21 ± 13	61 ± 15 ^{a,b}
	NM 7d	2 ^a	2 ^a	82 ± 6 ^a	85 ± 12 ^a
CCR2	CTL	0	0	5 ± 5	2 ± 1
	NM 3d	2 ^a	2 ^a	78 ± 12 ^a	69 ± 14 ^a
	NM 7d	1	1	46 ± 9 ^a	40 ± 13 ^a
CX ₃ CR1	CTL	1	0	55 ± 8	25 ± 15 ^b
	NM 3d	2 ^a	2 ^a	76 ± 6 ^a	53 ± 8 ^b
	NM 7d	1	1	48 ± 15	74 ± 10 ^{a,b}
ATR-1α	CTL	0	0	0 ± 0	0 ± 0
	NM 3d	1 ^a	3 ^{a,b}	69 ± 11 ^a	87 ± 9 ^{a,b}
	NM 7d	1	0	34 ± 11 ^a	8 ± 2 ^b
CYPb5	CTL	0	0	0 ± 0	0 ± 0
	NM 3d	2 ^a	0	95 ± 5 ^a	5 ± 5 ^b
	NM 7d	1	0	28 ± 7 ^a	5 ± 5 ^b
PCNA	CTL	0	0	0 ± 0	0 ± 0
	NM 3d	1	2 ^a	29 ± 11 ^a	37 ± 9 ^a
	NM 7d	1	0	44 ± 6 ^a	5 ± 2 ^b
γ-H2A.X.	CTL	0	0	0 ± 0	0 ± 0
	NM 3d	2 ^a	2 ^a	9 ± 6	32 ± 5 ^{a,b}
	NM 7d	0	0	4 ± 2	5 ± 3

Lung sections, collected 3 d and 7 d after exposure of rats to PBS (CTL) or NM followed by vehicle (Veh) or VPA were stained for markers involved in macrophage activation and trafficking and scored for intensity and number (%) of positive macrophages present in injured areas. Intensity is represented as median using 0-4 scoring system. GRADE 0 = no staining; GRADE 1 = weak; GRADE 2 = moderate; GRADE 3 = strong; GRADE 4 = very strong staining. Number (%) of positive cells is represented as mean \pm SE (n = 3–5 rats). ^aStatistically significant from CTL. ^bStatistically significant from Sham rats. Intensity staining was analyzed using Kruskal-Wallis non parametric one-way ANOVA followed by Mann-Whitney Rank Sum post-hoc test; number of positive cells was analyzed using one-way ANOVA followed by unpaired t-test.

REFERENCES:

- Ajami, B., et al. (2007). Local self-renewal can sustain CNS microglia maintenance and function throughout adult life. *Nat Neurosci* 10(12), 1538-43, 10.1038/nn2014.
- Alessandri, A. L., et al. (2013). Resolution of inflammation: mechanisms and opportunity for drug development. *Pharmacol Ther* 139(2), 189-212, 10.1016/j.pharmthera.2013.04.006.
- Alvarez-Breckenridge, C. A., et al. (2012). The histone deacetylase inhibitor valproic acid lessens NK cell action against oncolytic virus-infected glioblastoma cells by inhibition of STAT5/T-BET signaling and generation of gamma interferon. *J Virol* 86(8), 4566-77, 10.1128/jvi.05545-11.
- Amendola, M., et al. (2009). Regulated and multiple miRNA and siRNA delivery into primary cells by a lentiviral platform. *Mol Ther* 17(6), 1039-52, 10.1038/mt.2009.48.
- Anilkumar, T. V., et al. (1992). The nature of cytotoxic drug-induced cell death in murine intestinal crypts. *Br J Cancer* 65(4), 552-8.
- Annunziato, F., et al. (1999). Assessment of chemokine receptor expression by human Th1 and Th2 cells in vitro and in vivo. *J Leukoc Biol* 65(5), 691-9.
- Arai, M., et al. (2013). Chemokine receptors CCR2 and CX3CR1 regulate skin fibrosis in the mouse model of cytokine-induced systemic sclerosis. *J Dermatol Sci* 69(3), 250-8, 10.1016/j.jdermsci.2012.10.010.
- Arndt, P. G., et al. (2006). Systemic inhibition of the angiotensin-converting enzyme limits lipopolysaccharide-induced lung neutrophil recruitment through both bradykinin and angiotensin II-regulated pathways. *J Immunol* 177(10), 7233-41.
- Arnold, L., et al. (2007). Inflammatory monocytes recruited after skeletal muscle injury switch into antiinflammatory macrophages to support myogenesis. *J Exp Med* 204(5), 1057-69, 10.1084/jem.20070075.
- Auffray, C., et al. (2007). Monitoring of blood vessels and tissues by a population of monocytes with patrolling behavior. *Science* 317(5838), 666-70, 10.1126/science.1142883.
- Baitsch, D., et al. (2011). Apolipoprotein E induces antiinflammatory phenotype in macrophages. *Arterioscler Thromb Vasc Biol* 31(5), 1160-8, 10.1161/atvbaha.111.222745.
- Balali-Mood, M., and Hefazi, M. (2006). Comparison of early and late toxic effects of sulfur mustard in Iranian veterans. *Basic Clin Pharmacol Toxicol* 99(4), 273-82, 10.1111/j.1742-7843.2006.pto_429.x.
- Banerjee, S., et al. (2013). miR-125a-5p regulates differential activation of macrophages and inflammation. *J Biol Chem* 288(49), 35428-36, 10.1074/jbc.M112.426866.
- Barnes, P. J., et al. (2005). Histone acetylation and deacetylation: importance in inflammatory lung diseases. *Eur Respir J* 25(3), 552-63, 10.1183/09031936.05.00117504.
- Barnes, P. J., et al. (2006). Pulmonary biomarkers in chronic obstructive pulmonary disease. *Am J Respir Crit Care Med* 174(1), 6-14, 10.1164/rccm.200510-1659PP.
- Barth, M. W., et al. (1995). Review of the macrophage disappearance reaction. *J Leukoc Biol* 57(3), 361-7.
- Bayarsaihan, D. (2011). Epigenetic mechanisms in inflammation. *J Dent Res* 90(1), 9-17, 10.1177/0022034510378683.
- Baylin, S. B. (2005). DNA methylation and gene silencing in cancer. *Nat Clin Pract Oncol* 2 Suppl 1, S4-11, 10.1038/ncponc0354.
- Berger, S. L. (2007). The complex language of chromatin regulation during transcription. *Nature* 447(7143), 407-12, 10.1038/nature05915.

- Bhalla, D. K. (1999). Ozone-induced lung inflammation and mucosal barrier disruption: toxicology, mechanisms, and implications. *J Toxicol Environ Health B Crit Rev* 2(1), 31-86, 10.1080/109374099281232.
- Billiar, T. R., et al. (1988). Splenectomy alters Kupffer cell response to endotoxin. *Arch Surg* 123(3), 327-32.
- Blom, I. E., et al. (2002). Gene regulation of connective tissue growth factor: new targets for antifibrotic therapy? *Matrix Biol* 21(6), 473-82.
- Boldogh, I., et al. (2003). Reduced DNA double strand breaks in chlorambucil resistant cells are related to high DNA-PKcs activity and low oxidative stress. *Toxicology* 193(1-2), 137-52.
- Boring, L., et al. (1997). Impaired monocyte migration and reduced type 1 (Th1) cytokine responses in C-C chemokine receptor 2 knockout mice. *J Clin Invest* 100(10), 2552-61, 10.1172/jci119798.
- Boven, L. A., et al. (2006). Myelin-laden macrophages are anti-inflammatory, consistent with foam cells in multiple sclerosis. *Brain* 129(Pt 2), 517-26, 10.1093/brain/awh707.
- Brogdon, J. L., et al. (2007). Histone deacetylase activities are required for innate immune cell control of Th1 but not Th2 effector cell function. *Blood* 109(3), 1123-30, 10.1182/blood-2006-04-019711.
- Brulikova, L., et al. (2012). DNA interstrand cross-linking agents and their chemotherapeutic potential. *Curr Med Chem* 19(3), 364-85.
- Bruniquel, D., and Schwartz, R. H. (2003). Selective, stable demethylation of the interleukin-2 gene enhances transcription by an active process. *Nat Immunol* 4(3), 235-40, 10.1038/ni887.
- Buckley, C. D., et al. (2014). Proresolving lipid mediators and mechanisms in the resolution of acute inflammation. *Immunity* 40(3), 315-27, 10.1016/j.immuni.2014.02.009.
- Butovsky, O., et al. (2012). Modulating inflammatory monocytes with a unique microRNA gene signature ameliorates murine ALS. *J Clin Invest* 122(9), 3063-87, 10.1172/jci62636.
- Cao, Q., et al. (2014). Failed renoprotection by alternatively activated bone marrow macrophages is due to a proliferation-dependent phenotype switch in vivo. *Kidney Int* 85(4), 794-806, 10.1038/ki.2013.341.
- Castano, A. P., et al. (2009). Serum amyloid P inhibits fibrosis through Fc gamma R-dependent monocyte-macrophage regulation in vivo. *Sci Transl Med* 1(5), 5ra13, 10.1126/scitranslmed.3000111.
- Chakrabarty, A., et al. (2007). MicroRNA regulation of cyclooxygenase-2 during embryo implantation. *Proc Natl Acad Sci U S A* 104(38), 15144-9, 10.1073/pnas.0705917104.
- Chamoto, K., et al. (2013). Migration of CD11b+ accessory cells during murine lung regeneration. *Stem Cell Res* 10(3), 267-77, 10.1016/j.scr.2012.12.006.
- Chaudhuri, A. A., et al. (2011). MicroRNA-125b potentiates macrophage activation. *J Immunol* 187(10), 5062-8, 10.4049/jimmunol.1102001.
- Chen, J., et al. (2005). B56 regulatory subunit of protein phosphatase 2A mediates valproic acid-induced p300 degradation. *Mol Cell Biol* 25(2), 525-32, 10.1128/mcb.25.2.525-532.2005.
- Chinetti-Gbaguidi, G., et al. (2015). Macrophage subsets in atherosclerosis. *Nat Rev Cardiol* 12(1), 10-7, 10.1038/nrcardio.2014.173.
- Chou, R. C., et al. (2010). Lipid-cytokine-chemokine cascade drives neutrophil recruitment in a murine model of inflammatory arthritis. *Immunity* 33(2), 266-78, 10.1016/j.immuni.2010.07.018.
- Chow, C. W., et al. (2003). Oxidative stress and acute lung injury. *Am J Respir Cell Mol Biol* 29(4), 427-31, 10.1165/rcmb.F278.

- Clingen, P. H., et al. (2008). Histone H2AX phosphorylation as a molecular pharmacological marker for DNA interstrand crosslink cancer chemotherapy. *Biochem Pharmacol* 76(1), 19-27, 10.1016/j.bcp.2008.03.025.
- Colasurdo G.N., et al. (1995). Human respiratory syncytial virus affects nonadrenergic noncholinergic inhibition in cotton rat airways. *Am J Physiol*. 268(6 Pt 1):L1006-11.
- Coley, W., et al. (2010). Absence of DICER in monocytes and its regulation by HIV-1. *J Biol Chem* 285(42), 31930-43, 10.1074/jbc.M110.101709.
- Colonna M, Trinchieri G, Liu YJ. Plasmacytoid dendritic cells in immunity. *Nat Immunol*. 2004;5:1219–26
- Correa, F., et al. (2011). Activated microglia decrease histone acetylation and Nrf2-inducible anti-oxidant defence in astrocytes: restoring effects of inhibitors of HDACs, p38 MAPK and GSK3beta. *Neurobiol Dis* 44(1), 142-51, 10.1016/j.nbd.2011.06.016.
- Cosio, B. G., et al. (2004). Histone acetylase and deacetylase activity in alveolar macrophages and blood mononocytes in asthma. *Am J Respir Crit Care Med* 170(2), 141-7, 10.1164/rccm.200305-659OC.
- Cote, C. H., et al. (2013). Monocyte depletion increases local proliferation of macrophage subsets after skeletal muscle injury. *BMC Musculoskelet Disord* 14, 359, 10.1186/1471-2474-14-359.
- Dacre, J. C., and Goldman, M. (1996). Toxicology and pharmacology of the chemical warfare agent sulfur mustard. *Pharmacol Rev* 48(2), 289-326.
- Davies, L. C., et al. (2013a). Tissue-resident macrophages. *Nat Immunol* 14(10), 986-95, 10.1038/ni.2705.
- Davies, L. C., et al. (2013b). Distinct bone marrow-derived and tissue-resident macrophage lineages proliferate at key stages during inflammation. *Nat Commun* 4, 1886, 10.1038/ncomms2877.
- Davies, L. C., et al. (2011). A quantifiable proliferative burst of tissue macrophages restores homeostatic macrophage populations after acute inflammation. *Eur J Immunol* 41(8), 2155-64, 10.1002/eji.201141817.
- de las Casas-Engel, M., et al. (2013). Serotonin skews human macrophage polarization through HTR2B and HTR7. *J Immunol* 190(5), 2301-10, 10.4049/jimmunol.1201133.
- De Silva, I. U., et al. (2000). Defining the Roles of Nucleotide Excision Repair and Recombination in the Repair of DNA Interstrand Cross-Links in Mammalian Cells. *Mol Cell Biol* 20(21), 7980-90.
- Descamps, D., et al. (2012). Toll-like receptor 5 (TLR5), IL-1beta secretion, and asparagine endopeptidase are critical factors for alveolar macrophage phagocytosis and bacterial killing. *Proc Natl Acad Sci U S A* 109(5), 1619-24, 10.1073/pnas.1108464109.
- Dokmanovic, M., et al. (2007). Histone deacetylase inhibitors: overview and perspectives. *Mol Cancer Res* 5(10), 981-9, 10.1158/1541-7786.mcr-07-0324.
- Donaldson, K., et al. (2010). Asbestos, carbon nanotubes and the pleural mesothelium: a review of the hypothesis regarding the role of long fibre retention in the parietal pleura, inflammation and mesothelioma. *Part Fibre Toxicol* 22;(7):5. doi:10.1186/1743-8977-7-5.
- Egger, C., et al. (2013) Administration of bleomycin via the oropharyngeal aspiration route leads to sustained lung fibrosis in mice and rats as quantified by UTE-MRI and histology. *PLoS One*. 7;8(5):e63432. doi: 10.1371/journal.pone.0063432.
- Epelman, S., et al. (2014). Embryonic and adult-derived resident cardiac macrophages are maintained through distinct mechanisms at steady state and during inflammation. *Immunity* 40, 91–104.
- Falvo, J. V., et al. (2013). Epigenetic control of cytokine gene expression: regulation of the TNF/LT locus and T helper cell differentiation. *Adv Immunol* 118, 37-128, 10.1016/b978-0-12-407708-9.00002-9.

- Filippatos, G., et al. (2001). Regulation of apoptosis by angiotensin II in the heart and lungs (Review). *Int J Mol Med* 7(3), 273-80.
- Finn, R. D., et al. (2011). Cytochrome b5 null mouse: a new model for studying inherited skin disorders and the role of unsaturated fatty acids in normal homeostasis. *Transgenic Res* 20(3), 491-502, 10.1007/s11248-010-9426-1.
- Foster, S. L., et al. (2007). Gene-specific control of inflammation by TLR-induced chromatin modifications. *Nature* 447(7147), 972-8, 10.1038/nature05836.
- Fragkos, M., et al. (2009). H2AX is required for cell cycle arrest via the p53/p21 pathway. *Mol Cell Biol* 29(10), 2828-40, 10.1128/mcb.01830-08.
- Galvan-Pena, S., and O'Neill, L. A. J. (2014). Metabolic Reprograming in Macrophage Polarization. *Frontiers in Immunology*, 5, 420. doi:10.3389/fimmu.2014.00420
- Garchow, B. G., et al. (2011). Silencing of microRNA-21 in vivo ameliorates autoimmune splenomegaly in lupus mice. *EMBO Mol Med* 3(10), 605-15, 10.1002/emmm.201100171.
- Geering, B., and Simon, H. U. (2011). Peculiarities of cell death mechanisms in neutrophils. *Cell Death Differ* 18(9), 1457-69, 10.1038/cdd.2011.75.
- Ghabili, K., et al. (2011). Sulfur mustard toxicity: history, chemistry, pharmacokinetics, and pharmacodynamics. *Crit Rev Toxicol* 41(5), 384-403, 10.3109/10408444.2010.541224.
- Ghanei, M., and Harandi, A. A. (2007). Long term consequences from exposure to sulfur mustard: a review. *Inhal Toxicol* 19(5), 451-6, 10.1080/08958370601174990.
- Ghanei, M., et al. (2010). Long-term pulmonary complications of chemical warfare agent exposure in Iraqi Kurdish civilians. *Inhal Toxicol* 22(9), 719-24, 10.3109/08958371003686016.
- Ghasemi, H., et al. (2008). Long-term ocular complications of sulfur mustard in the civilian victims of Sardasht, Iran. *Cutan Ocul Toxicol* 27(4), 317-26, 10.1080/15569520802404382.
- Gleissner, C. A. (2012). Macrophage Phenotype Modulation by CXCL4 in Atherosclerosis. *Front Physiol* 3, 1, 10.3389/fphys.2012.00001.
- Goldberg, A. D., et al. (2007). Epigenetics: a landscape takes shape. *Cell* 128(4), 635-8, 10.1016/j.cell.2007.02.006.
- Gordon, S. (2003). Alternative activation of macrophages. *Nat Rev Immunol* 3(1), 23-35, 10.1038/nri978.
- Gordon, S., and Taylor, P. R. (2005). Monocyte and macrophage heterogeneity. *Nat Rev Immunol* 5(12), 953-64, 10.1038/nri1733.
- Gotoh, K., et al. (2012). Spleen-derived interleukin-10 downregulates the severity of high-fat diet-induced non-alcoholic fatty pancreas disease. *PLoS One* 7(12), e53154, 10.1371/journal.pone.0053154.
- Grabiec, A. M., et al. (2010). Histone deacetylase inhibitors suppress inflammatory activation of rheumatoid arthritis patient synovial macrophages and tissue. *J Immunol* 184(5), 2718-28, 10.4049/jimmunol.0901467.
- Groves, A. G., et al. (2012). Prolonged injury and altered lung function after ozone inhalation in mice with chronic lung inflammation. *Am J Respir Cell Mol Biol* 47(6), 776-83. 10.1165/rcmb.2011-0433OC.
- Guenther, M. G., et al. (2007). A chromatin landmark and transcription initiation at most promoters in human cells. *Cell* 130(1), 77-88, 10.1016/j.cell.2007.05.042.
- Guilliams M., et al. (2013). Alveolar macrophages develop from fetal monocytes that differentiate into long-lived cells in the first week of life via GM-CSF. *J Exp Med* 23;210(10):1977-92.
- Halili, M. A., et al. (2010). Differential effects of selective HDAC inhibitors on macrophage inflammatory responses to the Toll-like receptor 4 agonist LPS. *J Leukoc Biol* 87(6), 1103-14, 10.1189/jlb.0509363.

- Hashimoto, D., et al. (2013). Tissue-resident macrophages self-maintain locally throughout adult life with minimal contribution from circulating monocytes. *Immunity* 38(4), 792-804, 10.1016/j.immuni.2013.04.004.
- He, L., and Hannon, G. J. (2004). MicroRNAs: small RNAs with a big role in gene regulation. *Nat Rev Genet* 5(7), 522-31, 10.1038/nrg1379.
- He, X., et al. (2007). Angiotensin-converting enzyme inhibitor captopril prevents oleic acid-induced severe acute lung injury in rats. *Shock* 28(1), 106-11, 10.1097/SHK.0b013e3180310f3a.
- Heintzman, N. D., et al. (2009). Histone modifications at human enhancers reflect global cell-type-specific gene expression. *Nature* 459(7243), 108-12, 10.1038/nature07829.
- Herzog, E. L., et al. (2008). Knowns and Unknowns of the Alveolus. *Proc Am Thorac Soc* 5(7), 778-82, 10.1513/pats.200803-028HR.
- Hiroyoshi, T., et al. (2012). Splenectomy protects the kidneys against ischemic reperfusion injury in the rat. *Transpl Immunol* 27(1), 8-11, 10.1016/j.trim.2012.03.005.
- Howell, D. N., et al. (1994). Differential expression of CD43 (leukosialin, sialophorin) by mononuclear phagocyte populations. *J Leukoc Biol* 55(4), 536-44.
- Huang, W. C., et al. (2012). Classical macrophage activation up-regulates several matrix metalloproteinases through mitogen activated protein kinases and nuclear factor-kappaB. *PLoS One* 7(8), e42507, 10.1371/journal.pone.0042507.
- Hulsmans, M., and Holvoet, P. (2013). MicroRNA-containing microvesicles regulating inflammation in association with atherosclerotic disease. *Cardiovasc Res* 100(1), 7-18, 10.1093/cvr/cvt161.
- Hume, D. A., and Freeman, T. C. (2014). Transcriptomic analysis of mononuclear phagocyte differentiation and activation. *Immunol Rev* 262(1), 74-84, 10.1111/imr.12211.
- Huston, J. M., et al. (2006). Splenectomy inactivates the cholinergic antiinflammatory pathway during lethal endotoxemia and polymicrobial sepsis. *J Exp Med* 203(7), 1623-8, 10.1084/jem.20052362.
- Iliopoulos, D., et al. (2009). An epigenetic switch involving NF-kappaB, Lin28, Let-7 MicroRNA, and IL6 links inflammation to cell transformation. *Cell* 139(4), 693-706, 10.1016/j.cell.2009.10.014.
- Iliopoulos, D., et al. (2010). STAT3 activation of miR-21 and miR-181b-1 via PTEN and CYLD are part of the epigenetic switch linking inflammation to cancer. *Mol Cell* 39(4), 493-506, 10.1016/j.molcel.2010.07.023.
- Ingersoll, M. A., et al. (2011). Monocyte trafficking in acute and chronic inflammation. *Trends Immunol* 32(10), 470-7, 10.1016/j.it.2011.05.001.
- Ishibashi, M., et al. (2004). Critical role of monocyte chemoattractant protein-1 receptor CCR2 on monocytes in hypertension-induced vascular inflammation and remodeling. *Circ Res* 94(9), 1203-10, 10.1161/01.res.0000126924.23467.a3.
- Ishii, M., et al. (2009). Epigenetic regulation of the alternatively activated macrophage phenotype. *Blood* 114(15), 3244-54, 10.1182/blood-2009-04-217620.
- Ishikawa, M., et al. (2014). MCP/CCR2 signaling is essential for recruitment of mesenchymal progenitor cells during the early phase of fracture healing. *PLoS One* 9(8), e104954, 10.1371/journal.pone.0104954.
- Ivashkiv, L. B. (2013). Epigenetic regulation of macrophage polarization and function. *Trends Immunol* 34(5), 216-23, 10.1016/j.it.2012.11.001.
- Iyer, A., et al. (2012). MicroRNA-146a: a key regulator of astrocyte-mediated inflammatory response. *PLoS One* 7(9), e44789, 10.1371/journal.pone.0044789.
- Jacquelin, S., et al. (2013). CX3CR1 reduces Ly6Chigh-monocyte motility within and release from the bone marrow after chemotherapy in mice. *Blood* 122(5), 674-83, 10.1182/blood-2013-01-480749.

- Jaenisch, R., and Bird, A. (2003). Epigenetic regulation of gene expression: how the genome integrates intrinsic and environmental signals. *Nat Genet* 33 Suppl, 245-54, 10.1038/ng1089.
- Janahi I.A., et al. (2000). Recurrent milk aspiration produces changes in airway mechanics, lung eosinophilia, and goblet cell hyperplasia in a murine model. *Pediatr Res*. 2000 Dec;48(6):776-81.
- Janssen, W. J., et al. (2008). Surfactant proteins A and D suppress alveolar macrophage phagocytosis via interaction with SIRP alpha. *Am J Respir Crit Care Med* 178(2), 158-67, 10.1164/rccm.200711-1661OC.
- Jenkins, S. J., et al. (2011). Local macrophage proliferation, rather than recruitment from the blood, is a signature of TH2 inflammation. *Science* 332(6035), 1284-8, 10.1126/science.1204351.
- Jiang, P., et al. (2012). MiR-34a inhibits lipopolysaccharide-induced inflammatory response through targeting Notch1 in murine macrophages. *Exp Cell Res* 318(10), 1175-84, 10.1016/j.yexcr.2012.03.018.
- Jiang, X., et al. (2010). microRNAs and the regulation of fibrosis. *Febs j* 277(9), 2015-21, 10.1111/j.1742-4658.2010.07632.x.
- Kawahara, Y., and Mieda-Sato, A. (2012). TDP-43 promotes microRNA biogenesis as a component of the Drosha and Dicer complexes. *Proc Natl Acad Sci U S A* 109(9), 3347-52, 10.1073/pnas.1112427109.
- Kawai, Y., and Arinze, I. J. (2006). Valproic acid-induced gene expression through production of reactive oxygen species. *Cancer Res* 66(13), 6563-9, 10.1158/0008-5472.can-06-0814.
- Kee, N., et al. (2002). The utility of Ki-67 and BrdU as proliferative markers of adult neurogenesis. *J Neurosci Methods* 115(1), 97-105.
- Kehe, K., and Szinicz, L. (2005). Medical aspects of sulphur mustard poisoning. *Toxicology* 214(3), 198-209, 10.1016/j.tox.2005.06.014.
- Kim, Y., et al. (2012). Histone Deacetylase 3 Mediates Allergic Skin Inflammation by Regulating Expression of MCP1 Protein. *J Biol Chem* 287(31), 25844-59, 10.1074/jbc.M112.348284.
- Kirby, A. C., et al. (2009). Alveolar macrophages transport pathogens to lung draining lymph nodes. *J Immunol* 183(3), 1983-9, 10.4049/jimmunol.0901089.
- Kirby, A. C., et al. (2006). CD11b regulates recruitment of alveolar macrophages but not pulmonary dendritic cells after pneumococcal challenge. *J Infect Dis* 193(2), 205-13, 10.1086/498874.
- Kittan, N. A., et al. (2013). Cytokine induced phenotypic and epigenetic signatures are key to establishing specific macrophage phenotypes. *PLoS One* 8(10), e78045, 10.1371/journal.pone.0078045.
- Kohn, K. W., et al. (1987). Mechanisms of DNA sequence selective alkylation of guanine-N7 positions by nitrogen mustards. *Nucleic Acids Res* 15(24), 10531-49.
- Kramer, O. H., et al. (2003). The histone deacetylase inhibitor valproic acid selectively induces proteasomal degradation of HDAC2. *Embo j* 22(13), 3411-20, 10.1093/emboj/cdg315.
- Kumar, M. S., et al. (2007). Impaired microRNA processing enhances cellular transformation and tumorigenesis. *Nat Genet* 39(5), 673-7, 10.1038/ng2003.
- Kuo, L. J., and Yang, L. X. (2008). Gamma-H2AX - a novel biomarker for DNA double-strand breaks. *In Vivo* 22(3), 305-9.
- Lane, A. A., and Chabner, B. A. (2009). Histone deacetylase inhibitors in cancer therapy. *J Clin Oncol* 27(32), 5459-68, 10.1200/jco.2009.22.1291.

- Laskin, D. L., et al. (2011). Macrophages and tissue injury: agents of defense or destruction? *Annu Rev Pharmacol Toxicol* 51, 267-88, 10.1146/annurev.pharmtox.010909.105812.
- Lauder, S. N., et al. (2011). Paracetamol reduces influenza-induced immunopathology in a mouse model of infection without compromising virus clearance or the generation of protective immunity. *Thorax* 66(5), 368-74, 10.1136/thx.2010.150318.
- Lee, J. H., et al. (2010). Histone deacetylase inhibitor induces DNA damage, which normal but not transformed cells can repair. *Proc Natl Acad Sci U S A* 107(33), 14639-44, 10.1073/pnas.1008522107.
- Lee, J. Y., et al. (2014). Valproic acid protects motor neuron death by inhibiting oxidative stress and endoplasmic reticulum stress-mediated cytochrome C release after spinal cord injury. *J Neurotrauma* 31(6), 582-94, 10.1089/neu.2013.3146.
- Leuschner, F., et al. (2010). Angiotensin-converting enzyme inhibition prevents the release of monocytes from their splenic reservoir in mice with myocardial infarction. *Circ Res* 107(11), 1364-73, 10.1161/circresaha.110.227454.
- Li, Q., et al. (2011). Involvement of NF- κ B/miR-448 regulatory feedback loop in chemotherapy-induced epithelial-mesenchymal transition of breast cancer cells. *Cell Death Differ* 18(1), 16-25, 10.1038/cdd.2010.103.
- Li, X., et al. (2006). Extravascular sources of lung angiotensin peptide synthesis in idiopathic pulmonary fibrosis. *Am J Physiol Lung Cell Mol Physiol* 291(5), L887-95, 10.1152/ajplung.00432.2005.
- Li, Y., and Alam, H. B. (2012). Creating a pro-survival and anti-inflammatory phenotype by modulation of acetylation in models of hemorrhagic and septic shock. *Adv Exp Med Biol* 710, 107-33, 10.1007/978-1-4419-5638-5_11.
- Lin, S. L., et al. (2009). Bone marrow Ly6Chigh monocytes are selectively recruited to injured kidney and differentiate into functionally distinct populations. *J Immunol* 183(10), 6733-43, 10.4049/jimmunol.0901473.
- Lino Cardenas, C. L., et al. (2013). miR-199a-5p is upregulated during fibrogenic response to tissue injury and mediates TGF β -induced lung fibroblast activation by targeting caveolin-1. *PLoS Genet* 9(2), e1003291, 10.1371/journal.pgen.1003291.
- Liu, C. C., et al. (2011a). Global DNA methylation, DNMT1, and MBD2 in patients with rheumatoid arthritis. *Immunol Lett* 135(1-2), 96-9, 10.1016/j.imlet.2010.10.003.
- Liu, G., et al. (2010). miR-21 mediates fibrogenic activation of pulmonary fibroblasts and lung fibrosis. *J Exp Med* 207(8), 1589-97, 10.1084/jem.20100035.
- Liu, G., et al. (2011b). Phenotypic and functional switch of macrophages induced by regulatory CD4⁺CD25⁺ T cells in mice. *Immunol Cell Biol* 89(1), 130-42, 10.1038/icb.2010.70.
- Liu, Y., et al. (2006). Suberoylanilide hydroxamic acid induces Akt-mediated phosphorylation of p300, which promotes acetylation and transcriptional activation of RelA/p65. *J Biol Chem* 281(42), 31359-68, 10.1074/jbc.M604478200.
- Liutkeviciute, Z., et al. (2009). Cytosine-5-methyltransferases add aldehydes to DNA. *Nat Chem Biol* 5(6), 400-2, 10.1038/nchembio.172.
- Lumeng, C. N. (2007). Obesity induces a phenotypic switch in adipose tissue macrophage polarization 117(1), 175-84, 10.1172/jci29881.
- Ma, Y., et al. (2014). Silencing miR-21 sensitizes non-small cell lung cancer A549 cells to ionizing radiation through inhibition of PI3K/Akt 2014, 617868, 10.1155/2014/617868.
- Mack, M., et al. (2001). Expression and characterization of the chemokine receptors CCR2 and CCR5 in mice. *J Immunol* 166(7), 4697-704.
- Malaviya, R., et al. (2010). Inflammatory effects of inhaled sulfur mustard in rat lung. *Toxicol Appl Pharmacol* 248(2), 89-99, 10.1016/j.taap.2010.07.018.

- Malaviya, R., et al. (2012). Attenuation of acute nitrogen mustard-induced lung injury, inflammation and fibrogenesis by a nitric oxide synthase inhibitor. *Toxicol Appl Pharmacol* 265(3), 279-91, 10.1016/j.taap.2012.08.027.
- Mantovani, A., et al. (2010). The chemokine system in cancer biology and therapy. *Cytokine Growth Factor Rev* 21(1), 27-39, 10.1016/j.cytogfr.2009.11.007.
- Mantovani, A., et al. (2004). The chemokine system in diverse forms of macrophage activation and polarization. *Trends Immunol* 25(12), 677-86, 10.1016/j.it.2004.09.015.
- Marks, P. A., and Breslow, R. (2007). Dimethyl sulfoxide to vorinostat: development of this histone deacetylase inhibitor as an anticancer drug. *Nat Biotechnol* 25(1), 84-90, 10.1038/nbt1272.
- Marr, A. K., et al. (2014). Leishmania donovani Infection Causes Distinct Epigenetic DNA Methylation Changes in Host Macrophages. *PLoS Pathog* 10(10), 10.1371/journal.ppat.1004419.
- Martin, T. R., et al. (1984). Leukotriene B₄ production by the human alveolar macrophage: a potential mechanism for amplifying inflammation in the lung. *Am Rev Respir Dis* 129(1), 106-11.
- Martinez, F. O., and Gordon, S. (2014). The M1 and M2 paradigm of macrophage activation: time for reassessment. *F1000Prime Rep* 6, 13, 10.12703/p6-13.
- Martinez, F. O., et al. (2008). Macrophage activation and polarization. *Front Biosci* 13, 453-61.
- Maskrey, B. H., et al. (2011). Mechanisms of resolution of inflammation: a focus on cardiovascular disease. *Arterioscler Thromb Vasc Biol* 31(5), 1001-6, 10.1161/atvbaha.110.213850.
- Maus, U. A., et al. (2006). Resident alveolar macrophages are replaced by recruited monocytes in response to endotoxin-induced lung inflammation. *Am J Respir Cell Mol Biol* 35(2), 227-35, 10.1165/rcmb.2005-0241OC.
- Medhora, M., et al. (2012). Radiation damage to the lung: mitigation by angiotensin-converting enzyme (ACE) inhibitors. *Respirology* 17(1), 66-71, 10.1111/j.1440-1843.2011.02092.x.
- Menoret, A., et al. (2012). Cytochrome b5 and cytokeratin 17 are biomarkers in bronchoalveolar fluid signifying onset of acute lung injury. *PLoS One* 7(7), e40184, 10.1371/journal.pone.0040184.
- Mercier, F. E., et al. (2012). The bone marrow at the crossroads of blood and immunity. *Nat Rev Immunol* 12(1), 49-60, 10.1038/nri3132.
- Merkerova, M., et al. (2008). Differential expression of microRNAs in hematopoietic cell lineages. *Eur J Haematol* 81(4), 304-10, 10.1111/j.1600-0609.2008.01111.x.
- Mills, C. D., and Ley, K. (2014). M1 and M2 Macrophages: The Chicken and the Egg of Immunity. *J Innate Immun* 6(6), 716-26, 10.1159/000364945.
- Moestrup, S. K., and Moller, H. J. (2004). CD163: a regulated hemoglobin scavenger receptor with a role in the anti-inflammatory response. *Ann Med* 36(5), 347-54.
- Moldoveanu, B., et al. (2009). Inflammatory mechanisms in the lung. *J Inflamm Res* 2, 1-11.
- Mosser, D. M., and Edwards, J. P. (2008). Exploring the full spectrum of macrophage activation. *Nat Rev Immunol* 8(12), 958-69, 10.1038/nri2448.
- Mullican, S. E., et al. (2011). Histone deacetylase 3 is an epigenomic brake in macrophage alternative activation. *Genes Dev* 25(23), 2480-8, 10.1101/gad.175950.111.
- Munder, M. (2009). Arginase: an emerging key player in the mammalian immune system. *Br J Pharmacol* 158(3), 638-51, 10.1111/j.1476-5381.2009.00291.x.
- Murphy, P. M., et al. (2000). International union of pharmacology. XXII. Nomenclature for chemokine receptors. *Pharmacol Rev* 52(1), 145-76.

- Murray, L. A., et al. (2011). TGF-beta driven lung fibrosis is macrophage dependent and blocked by Serum amyloid P. *Int J Biochem Cell Biol* 43(1), 154-62, 10.1016/j.biocel.2010.10.013.
- Murray, P. J. (2005). The primary mechanism of the IL-10-regulated antiinflammatory response is to selectively inhibit transcription. *Proc Natl Acad Sci U S A* 102(24), 8686-91, 10.1073/pnas.0500419102.
- Murray, P. J., and Wynn, T. A. (2011). Protective and pathogenic functions of macrophage subsets. *Nat Rev Immunol* 11(11), 723-37, 10.1038/nri3073.
- Nahrendorf, M., et al. (2007). The healing myocardium sequentially mobilizes two monocyte subsets with divergent and complementary functions. *J Exp Med* 204(12), 3037-47, 10.1084/jem.20070885.
- Natoli, G., et al. (2011). The genomic landscapes of inflammation. *Genes Dev* 25(2), 101-6, 10.1101/gad.2018811.
- Nile, C. J., et al. (2008). Methylation status of a single CpG site in the IL6 promoter is related to IL6 messenger RNA levels and rheumatoid arthritis. *Arthritis Rheum* 58(9), 2686-93, 10.1002/art.23758.
- Noll, D. M., et al. (2006). Formation and Repair of Interstrand Cross-Links in DNA. *Chem Rev* 106(2), 277-301, 10.1021/cr040478b.
- Oakes, J. M., et al. (2013). Regional distribution of aerosol deposition in rat lungs using magnetic resonance imaging. *Ann Biomed Eng.* 41(5):967-78. doi: 10.1007/s10439-013-0745-2.
- Odegaard and Chadwa (2011). Alternativemacrophageactivationandmetabolism. *AnnuRevPathol* 6:275–97.doi:10.1146/annurev-pathol-011110-130138
- Ogiwara, H., et al. (2011). Histone acetylation by CBP and p300 at double-strand break sites facilitates SWI/SNF chromatin remodeling and the recruitment of non-homologous end joining factors. *Oncogene* 30(18), 2135-46, 10.1038/onc.2010.592; 10.1038/onc.2010.592.
- Okuma, T., et al. (2004). C-C chemokine receptor 2 (CCR2) deficiency improves bleomycin-induced pulmonary fibrosis by attenuation of both macrophage infiltration and production of macrophage-derived matrix metalloproteinases. *J Pathol* 204(5), 594-604, 10.1002/path.1667.
- Olson, T. S., and Ley, K. (2002). Chemokines and chemokine receptors in leukocyte trafficking. *Am J Physiol Regul Integr Comp Physiol* 283(1), R7-28, 10.1152/ajpregu.00738.2001.
- Oo, Y. H., et al. (2010). The Role of Chemokines in the Recruitment of Lymphocytes to the Liver. *Dig Dis* 28(1), 31-44, 10.1159/000282062.
- Orkin, S.H., and Zon, L.I. (2008). Hematopoiesis: an evolving paradigm for stem cell biology. *Cell* 132, 631–644
- Orom, U. A., et al. (2008). MicroRNA-10a binds the 5'UTR of ribosomal protein mRNAs and enhances their translation. *Mol Cell* 30(4), 460-71, 10.1016/j.molcel.2008.05.001.
- Ostrand-Rosenberg S, Sinha P. (2009) Myeloid-Derived Suppressor Cells: Linking Inflammation and Cancer. *Journal of immunology*.182(8):4499-4506. doi:10.4049/jimmunol.0802740.
- Pandi, G., et al. (2013). MicroRNA miR-29c down-regulation leading to de-repression of its target DNA methyltransferase 3a promotes ischemic brain damage. *PLoS One* 8(3), e58039, 10.1371/journal.pone.0058039.
- Pang, M., and Zhuang, S. (2010). Histone Deacetylase: A Potential Therapeutic Target for Fibrotic Disorders. *J Pharmacol Exp Ther* 335(2), 266-72, 10.1124/jpet.110.168385.
- Park, J. S., et al. (2007). Anti-inflammatory effects of short chain fatty acids in IFN-gamma-stimulated RAW 264.7 murine macrophage cells: involvement of NF-kappaB

- and ERK signaling pathways. *Int Immunopharmacol* 7(1), 70-7, 10.1016/j.intimp.2006.08.015.
- Park, S. M., et al. (2008). The miR-200 family determines the epithelial phenotype of cancer cells by targeting the E-cadherin repressors ZEB1 and ZEB2. *Genes Dev* 22(7), 894-907, 10.1101/gad.1640608.
- Pencheva, N., et al. (2012). Convergent multi-miRNA targeting of ApoE drives LRP1/LRP8-dependent melanoma metastasis and angiogenesis. *Cell* 151(5), 1068-82, 10.1016/j.cell.2012.10.028.
- Peserico, A., and Simone, C. (2011). Physical and functional HAT/HDAC interplay regulates protein acetylation balance. *J Biomed Biotechnol* 2011, 371832, 10.1155/2011/371832.
- Pilling, D., and Gomer, R. H. (2014). Persistent lung inflammation and fibrosis in serum amyloid P component (APCs^{-/-}) knockout mice. *PLoS One* 9(4), e93730, 10.1371/journal.pone.0093730.
- Podhorecka, M., et al. (2010). H2AX Phosphorylation: Its Role in DNA Damage Response and Cancer Therapy. *J Nucleic Acids* 2010, 10.4061/2010/920161.
- Ponticos, M., et al. (2009). Pivotal role of connective tissue growth factor in lung fibrosis: MAPK-dependent transcriptional activation of type I collagen. *Arthritis Rheum* 60(7), 2142-55, 10.1002/art.24620.
- Porcheray, F., et al. (2005). Macrophage activation switching: an asset for the resolution of inflammation. *Clin Exp Immunol* 142(3), 481-9, 10.1111/j.1365-2249.2005.02934.x.
- Pufahl, L., et al. (2012). Trichostatin A induces 5-lipoxygenase promoter activity and mRNA expression via inhibition of histone deacetylase 2 and 3. *J Cell Mol Med* 16(7), 1461-73, 10.1111/j.1582-4934.2011.01420.x.
- Punjabi, C. J., et al. (1994). Production of nitric oxide by rat type II pneumocytes: increased expression of inducible nitric oxide synthase following inhalation of a pulmonary irritant. *Am J Respir Cell Mol Biol* 11(2), 165-72, 10.1165/ajrcmb.11.2.7519435.
- Qin, S., and Parthun, M. R. (2002). Histone H3 and the histone acetyltransferase Hat1p contribute to DNA double-strand break repair. *Mol Cell Biol* 22(23), 8353-65.
- Qin, W., et al. (2011). TGF- β /Smad3 Signaling Promotes Renal Fibrosis by Inhibiting miR-29. *J Am Soc Nephrol* 22(8), 1462-74, 10.1681/asn.2010121308.
- Quatromoni JG, Eruslanov E. (2012). Tumor-associated macrophages: function, phenotype, and link to prognosis in human lung cancer. *American Journal of Translational Research*. 4(4):376-389.
- Rae F., et al. (2007). Characterisation and trophic functions of murine embryonic macrophages based upon the use of a Csf1r-EGFP transgene reporter. *Dev Biol* 1;308(1):232-46.
- Rahman, I., et al. (2004). Redox modulation of chromatin remodeling: impact on histone acetylation and deacetylation, NF-kappaB and pro-inflammatory gene expression. *Biochem Pharmacol* 68(6), 1255-67, 10.1016/j.bcp.2004.05.042.
- Rappeneau, S., et al. (2000). Protection from cytotoxic effects induced by the nitrogen mustard mechlorethamine on human bronchial epithelial cells in vitro. *Toxicol Sci* 54(1), 212-21.
- Robbins, C. S., et al. (2012). Extramedullary hematopoiesis generates Ly-6C(high) monocytes that infiltrate atherosclerotic lesions. *Circulation* 125(2), 364-74, 10.1161/circulationaha.111.061986.
- Roderburg, C., et al. (2011). Micro-RNA profiling reveals a role for miR-29 in human and murine liver fibrosis. *Hepatology* 53(1), 209-18, 10.1002/hep.23922.

- Rodríguez-Prados et al. (2010). Substrate fate in activated macrophages: a comparison between innate, classic and alternative activation. *J Immunol* 185(1):605–14. doi:10.4049/jimmunol.0901698
- Roger, T., et al. (2011). Histone deacetylase inhibitors impair innate immune responses to Toll-like receptor agonists and to infection. *Blood* 117(4), 1205-17, 10.1182/blood-2010-05-284711.
- Roman, R. J. (2002). P-450 metabolites of arachidonic acid in the control of cardiovascular function. *Physiol Rev* 82(1), 131-85, 10.1152/physrev.00021.2001.
- Romero F., et al. (2015). A Pneumocyte-Macrophage Paracrine Lipid Axis Drives the Lung toward Fibrosis. *Am J Respir Cell Mol Biol*. 53(1):74-86. doi: 10.1165/rcmb.2014-0343OC.
- Rosa, A., et al. (2007). The interplay between the master transcription factor PU.1 and miR-424 regulates human monocyte/macrophage differentiation. *Proc Natl Acad Sci U S A* 104(50), 19849-54, 10.1073/pnas.0706963104.
- Rosas-Ballina, M., et al. (2008). Splenic nerve is required for cholinergic antiinflammatory pathway control of TNF in endotoxemia. *Proc Natl Acad Sci U S A* 105(31), 11008-13, 10.1073/pnas.0803237105.
- Rosborough, B. R., et al. (2012). Histone deacetylase inhibition facilitates GM-CSF-mediated expansion of myeloid-derived suppressor cells in vitro and in vivo. *J Leukoc Biol* 91(5), 701-9, 10.1189/jlb.0311119.
- Rossetto, D., et al. (2012). Histone phosphorylation: A chromatin modification involved in diverse nuclear events. *Epigenetics* 7(10), 1098-108, 10.4161/epi.21975.
- Roy, S., and Sen, C. K. (2012). miRNA in wound inflammation and angiogenesis. *Microcirculation* 19(3), 224-32, 10.1111/j.1549-8719.2011.00156.x.
- Sallusto, F., et al. (1999). Distinct patterns and kinetics of chemokine production regulate dendritic cell function. *Eur J Immunol* 29(5), 1617-25, 10.1002/(sici)1521-4141(199905)29:05<1617::aid-immu1617>3.0.co;2-3.
- Samokhvalov, I. M., (2014). Deconvoluting the ontogeny of hematopoietic stem cells. *Cell Mol Life Sci* 71(6):957-78. doi: 10.1007/s00018-013-1364-7.
- Schmall, A., et al. (2014). Macrophage and Cancer Cell Crosstalk via CCR2 and CX3CR1 is a Fundamental Mechanism Driving Lung Cancer. *Am J Respir Crit Care Med* doi: 10.1164/rccm.201406-1137OC, 10.1164/rccm.201406-1137OC.
- Shakespeare, M. R., et al. (2013). Histone deacetylase 7 promotes Toll-like receptor 4-dependent proinflammatory gene expression in macrophages. *J Biol Chem* 288(35), 25362-74, 10.1074/jbc.M113.496281.
- Shanmugam, M. K., and Sethi, G. (2013). Role of epigenetics in inflammation-associated diseases. *Subcell Biochem* 61, 627-57, 10.1007/978-94-007-4525-4_27.
- Shao D., et al. (2010). PGC-1 β -regulated mitochondrial biogenesis and function in myotubes is mediated by NRF-1 and ERR- α . *Mitochondrion* 10(5):516–27. doi:10.1016/j.mito.2010.05.012
- Sharma, A., et al. (2012). Histone H2AX phosphorylation: a marker for DNA damage. *Methods Mol Biol* 920, 613-26, 10.1007/978-1-61779-998-3_40.
- Shashkin, P., et al. (2005). Macrophage differentiation to foam cells. *Curr Pharm Des* 11(23), 3061-72.
- Sheedy, F. J., et al. (2010). Negative regulation of TLR4 via targeting of the proinflammatory tumor suppressor PDCD4 by the microRNA miR-21. *Nat Immunol* 11(2), 141-7, 10.1038/ni.1828.
- Shin, J., et al. (2013). MicroRNA-34a enhances T cell activation by targeting diacylglycerol kinase zeta. *PLoS One* 8(10), e77983, 10.1371/journal.pone.0077983.

- Schulz, C., et al. (2012). A lineage of myeloid cells independent of Myb and hematopoietic stem cells. *Science* 336, 86–90.
- Shuto, T., et al. (2006). Promoter hypomethylation of Toll-like receptor-2 gene is associated with increased proinflammatory response toward bacterial peptidoglycan in cystic fibrosis bronchial epithelial cells. *Faseb j* 20(6), 782-4, 10.1096/fj.05-4934fje.
- Sica, A., and Mantovani, A. (2012). Macrophage plasticity and polarization: in vivo veritas. *J Clin Invest* 122(3), 787-95, 10.1172/jci59643.
- Silkoff, P. E., et al. (2003). The relationship of induced-sputum inflammatory cells to BAL and biopsy. *Chest* 123(3 Suppl), 371s-2s.
- Sindrilaru, A., et al. (2011). An unrestrained proinflammatory M1 macrophage population induced by iron impairs wound healing in humans and mice. *J Clin Invest* 121(3), 985-97, 10.1172/jci44490.
- Smiley, R. K., et al. (1961). Effect of Autologous Bone Marrow on the Cytopenias Induced by Nitrogen Mustard. *Can Med Assoc J* 84(22), 1230-4.
- Smith, K. J., et al. (1998). Histopathologic and Immunohistochemical Features in Human Skin after Exposure to Nitrogen and Sulfur Mustard. *The American Journal of Dermatopathology* 20(1), 22-28.
- Sonkoly, E., and Pivarcsi, A. (2009). microRNAs in inflammation. *Int Rev Immunol* 28(6), 535-61, 10.3109/08830180903208303.
- Steeg P.S., M. R. N., and Oppenheim J. J. (1980). Regulation of murine macrophage Ia-antigen expression by products of activated spleen cells. *J Exp Med* 152(6), 1734-44.
- Stiehl, D. P., et al. (2007). Histone deacetylase inhibitors synergize p300 autoacetylation that regulates its transactivation activity and complex formation. *Cancer Res* 67(5), 2256-64, 10.1158/0008-5472.can-06-3985.
- Stout, R. D., et al. (2005). Macrophages Sequentially Change Their Functional Phenotype in Response to Changes in Microenvironmental Influences. *The Journal of Immunology* 175(1), 342-349, 10.4049/jimmunol.175.1.342.
- Stout, R. D., and Suttles, J. (2004). Functional plasticity of macrophages: reversible adaptation to changing microenvironments. *J Leukoc Biol* 76(3), 509-13, 10.1189/jlb.0504272.
- Strawn, W. B., et al. (2004). Renin-angiotensin system expression in rat bone marrow haematopoietic and stromal cells. *Br J Haematol* 126(1), 120-6, 10.1111/j.1365-2141.2004.04998.x.
- Sunil, V. R., et al. (2011a). Role of TNFR1 in lung injury and altered lung function induced by the model sulfur mustard vesicant, 2-chloroethyl ethyl sulfide. *Toxicol Appl Pharmacol* 250(3), 245-55, 10.1016/j.taap.2010.10.027.
- Sunil, V. R., et al. (2011b). Functional and inflammatory alterations in the lung following exposure of rats to nitrogen mustard. *Toxicol Appl Pharmacol* 250(1), 10-8, 10.1016/j.taap.2010.09.016.
- Sunil, V. R., et al. (2012). Role of reactive nitrogen species generated via inducible nitric oxide synthase in vesicant-induced lung injury, inflammation and altered lung functioning. *Toxicol Appl Pharmacol* 261(1), 22-30, 10.1016/j.taap.2012.03.004.
- Sunil, V. R., et al. (2014). Pentoxifylline attenuates nitrogen mustard-induced acute lung injury, oxidative stress and inflammation. *Exp Mol Pathol* 97(1), 89-98, 10.1016/j.yexmp.2014.05.009.
- Svensson, M., et al. (2004). Stromal cells direct local differentiation of regulatory dendritic cells. *Immunity* 21(6), 805-16, 10.1016/j.immuni.2004.10.012.
- Swirski, F. K., et al. (2009). Identification of splenic reservoir monocytes and their deployment to inflammatory sites. *Science* 325(5940), 612-6, 10.1126/science.1175202.

- Tacke, F., et al. (2007). Monocyte subsets differentially employ CCR2, CCR5, and CX3CR1 to accumulate within atherosclerotic plaques. *J Clin Invest* 117(1), 185-94, 10.1172/jci28549.
- Taganov, K. D., et al. (2006). NF- κ B-dependent induction of microRNA miR-146, an inhibitor targeted to signaling proteins of innate immune responses. *Proc Natl Acad Sci U S A* 103(33), 12481-6, 10.1073/pnas.0605298103.
- Tanabe, K., et al. (2015). Migration of splenic lymphocytes promotes liver fibrosis through modification of T helper cytokine balance in mice. *J Gastroenterol* doi: 10.1007/s00535-015-1054-3, 10.1007/s00535-015-1054-3.
- Tang, H., et al. (2006). Endothelial stroma programs hematopoietic stem cells to differentiate into regulatory dendritic cells through IL-10. *Blood* 108(4), 1189-97, 10.1182/blood-2006-01-007187.
- Thompson, V. R., and DeCaprio, A. P. (2013). Covalent adduction of nitrogen mustards to model protein nucleophiles. *Chem Res Toxicol* 26(8), 1263-71, 10.1021/tx400188w.
- Tighe, R. M., et al. (2011). Ozone inhalation promotes CX3CR1-dependent maturation of resident lung macrophages that limit oxidative stress and inflammation. *J Immunol* 187(9), 4800-8, 10.4049/jimmunol.1101312.
- Tong, V., et al. (2005). Valproic acid I: time course of lipid peroxidation biomarkers, liver toxicity, and valproic acid metabolite levels in rats. *Toxicol Sci* 86(2), 427-35, 10.1093/toxsci/kfi184.
- Torella, D., et al. (2011). MicroRNA-133 controls vascular smooth muscle cell phenotypic switch in vitro and vascular remodeling in vivo. *Circ Res* 109(8), 880-93, 10.1161/circresaha.111.240150.
- Tsaprouni, L. G., et al. (2011). Differential patterns of histone acetylation in inflammatory bowel diseases. *J Inflamm (Lond)* 8(1), 1, 10.1186/1476-9255-8-1.
- Tsou, C. L., et al. (2007). Critical roles for CCR2 and MCP-3 in monocyte mobilization from bone marrow and recruitment to inflammatory sites. *J Clin Invest* 117(4), 902-9, 10.1172/jci29919.
- Tsubakimoto, Y., et al. (2009). Bone marrow angiotensin AT1 receptor regulates differentiation of monocyte lineage progenitors from hematopoietic stem cells. *Arterioscler Thromb Vasc Biol* 29(10), 1529-36, 10.1161/atvbaha.109.187732.
- Ueda, Y., and Willmore, L. J. (2000). Molecular regulation of glutamate and GABA transporter proteins by valproic acid in rat hippocampus during epileptogenesis. *Exp Brain Res* 133(3), 334-9.
- Vaissiere, T., et al. (2008). Epigenetic interplay between histone modifications and DNA methylation in gene silencing. *Mutat Res* 659(1-2), 40-8, 10.1016/j.mrrev.2008.02.004.
- Van Furth, R., et al. (1972). The Mononuclear Phagocyte System: A New Classification of Macrophages, Monocytes, and Their Precursor Cells. *Bulletin of the World Health Organization* 46.6: 845-852. Print.
- van Tits, L. J., et al. (2011). Oxidized LDL enhances pro-inflammatory responses of alternatively activated M2 macrophages: a crucial role for Kruppel-like factor 2. *Atherosclerosis* 214(2), 345-9, 10.1016/j.atherosclerosis.2010.11.018.
- Vats et al.(2006). Oxidative metabolism and PGC-1 α attenuate macrophage-mediated inflammation. *Cell Metab* 4(1):13-4.doi:10.1016/j.cmet.2006.08.006
- Venosa, A. M., R.; Laskin, J.D.; Laskin, D.L. (2014). Accumulation of Distinct Macrophage (MP) Subpopulations in the Lung Following Nitrogen Mustard (NM) Exposure; Contribution of Splenic Monocytes. *The Toxicologist* doi: (1), 571.
- Vettori, S., et al. (2012). Role of MicroRNAs in Fibrosis. *Open Rheumatol J* 6, 130-9, 10.2174/1874312901206010130.
- Vilela, M. C., et al. (2013). Absence of CCR5 increases neutrophil recruitment in severe herpetic encephalitis. *BMC Neurosci* 14, 19, 10.1186/1471-2202-14-19.

- Vinolo, M. A. R., et al. (2011). Regulation of Inflammation by Short Chain Fatty Acids. *Nutrients* 3(10), 858-76, 10.3390/nu3100858.
- Wang, B., et al. (2012a). Histone deacetylase inhibition activates transcription factor Nrf2 and protects against cerebral ischemic damage. *Free Radic Biol Med* 52(5), 928-36, 10.1016/j.freeradbiomed.2011.12.006.
- Wang, C., et al. (2013). Characterization of murine macrophages from bone marrow, spleen and peritoneum. *BMC Immunol* 14, 6, 10.1186/1471-2172-14-6.
- Wang, G., et al. (2015). HDAC inhibition prevents white matter injury by modulating microglia/macrophage polarization through the GSK3beta/PTEN/Akt axis. *Proc Natl Acad Sci U S A* 112(9), 2853-8, 10.1073/pnas.1501441112.
- Wang, R., et al. (1999). Angiotensin II induces apoptosis in human and rat alveolar epithelial cells. *Am J Physiol* 276(5 Pt 1), L885-9.
- Wang, T., et al. (2012b). TGF-beta-induced miR-21 negatively regulates the antiproliferative activity but has no effect on EMT of TGF-beta in HaCaT cells. *Int J Biochem Cell Biol* 44(2), 366-76, 10.1016/j.biocel.2011.11.012.
- Wang, X., et al. (2014). Co-culture of spleen stromal cells with bone marrow mononuclear cells leads to the generation of a novel macrophage subset. *Scand J Immunol* 79(1), 27-36, 10.1111/sji.12133.
- Wang, X. Y., et al. (2009). Matrilysin-1 mediates bronchiolization of alveoli, a potential premalignant change in lung cancer. *Am J Pathol* 175(2), 592-604, 10.2353/ajpath.2009.080461.
- Wang, Y., et al. (2007). Ex vivo programmed macrophages ameliorate experimental chronic inflammatory renal disease. *Kidney Int* 72(3), 290-9, 10.1038/sj.ki.5002275.
- Wang, Z., et al. (2008). Combinatorial patterns of histone acetylations and methylations in the human genome. *Nat Genet* 40(7), 897-903, 10.1038/ng.154.
- Weinberger, B., et al. (2011). Sulfur mustard-induced pulmonary injury: therapeutic approaches to mitigating toxicity. *Pulm Pharmacol Ther* 24(1), 92-9, 10.1016/j.pupt.2010.09.004.
- Wen, H., et al. (2008). Epigenetic regulation of dendritic cell-derived interleukin-12 facilitates immunosuppression after a severe innate immune response. *Blood* 111(4), 1797-804, 10.1182/blood-2007-08-106443.
- Wendlandt, E. B. (2012). The role of MicroRNAs miR-200b and miR-200c in TLR4 signaling and NF- κ B activation 18(6), 846-55, 10.1177/1753425912443903.
- Williams, C. J., et al. (2004). The chromatin remodeler Mi-2beta is required for CD4 expression and T cell development. *Immunity* 20(6), 719-33, 10.1016/j.immuni.2004.05.005.
- Williams, O. W., et al. (2006). Airway Mucus: From Production to Secretion. *Am J Respir Cell Mol Biol* 34 (5), 527-536. 10.1165/rcmb.2005-0436SF
- Wu, C., et al. (2012). Histone deacetylase inhibition by sodium valproate regulates polarization of macrophage subsets. *DNA Cell Biol* 31(4), 592-9, 10.1089/dna.2011.1401.
- Wu, G., and Morris, S. M. (1998). Arginine metabolism: nitric oxide and beyond. *Biochem J* 336(Pt 1), 1-17.
- Wystrychowski, W., et al. (2014). Splenectomy attenuates the course of kidney ischemia-reperfusion injury in rats. *Transplant Proc* 46(8), 2558-61, 10.1016/j.transproceed.2014.09.056.
- Xiao, J., et al. (2012). miR-29 Inhibits Bleomycin-induced Pulmonary Fibrosis in Mice. *Mol Ther* 20(6), 1251-1260.
- Xie, W., et al. (2013). MiR-181a regulates inflammation responses in monocytes and macrophages. *PLoS One* 8(3), e58639, 10.1371/journal.pone.0058639.

- Ximenes, J. C., et al. (2013). Valproic acid: an anticonvulsant drug with potent antinociceptive and anti-inflammatory properties. *Naunyn Schmiedeberg's Arch Pharmacol* 386(7), 575-87, 10.1007/s00210-013-0853-4.
- Xu, J., et al. (2011). CCR2 mediates the uptake of bone marrow-derived fibroblast precursors in angiotensin II-induced cardiac fibrosis. *Am J Physiol Heart Circ Physiol* 301(2), H538-47, 10.1152/ajpheart.01114.2010.
- Yamamoto, K., et al. (2005). ACE inhibitor and angiotensin II type 1 receptor blocker differently regulate ventricular fibrosis in hypertensive diastolic heart failure. *J Hypertens* 23(2), 393-400.
- Yang, J. et al. (2014). Monocyte and Macrophage Differentiation: Circulation Inflammatory Monocyte as Biomarker for Inflammatory Diseases. *Biomarker Research* 2014;2:1
- Yang, X., et al. (2014). Epigenetic regulation of macrophage polarization by DNA methyltransferase 3b. *Mol Endocrinol* 28(4), 565-74, 10.1210/me.2013-1293.
- Ying, H., et al. (2015). MiR-127 Modulates Macrophage Polarization and Promotes Lung Inflammation and Injury by Activating the JNK Pathway. *J Immunol* 194(3), 1239-51, 10.4049/jimmunol.1402088.
- Yoshikawa, M., et al. (2007). Inhibition of Histone Deacetylase Activity Suppresses Epithelial-to-Mesenchymal Transition Induced by TGF- β 1 in Human Renal Epithelial Cells. *Journal of the American Society of Nephrology* 18(1), 58-65, 10.1681/asn.2005111187.
- Zain, J. (2012). Role of histone deacetylase inhibitors in the treatment of lymphomas and multiple myeloma. *Hematol Oncol Clin North Am* 26(3), 671-704, ix, 10.1016/j.hoc.2012.01.006.
- Zaynagetdinov, R., et al. (2013). Identification of myeloid cell subsets in murine lungs using flow cytometry. *Am J Respir Cell Mol Biol* 49(2), 180-9, 10.1165/rcmb.2012-0366MA.
- Zhang, X., et al. (2008a). The isolation and characterization of murine macrophages. *Curr Protoc Immunol* Chapter 14, Unit 14.1, 10.1002/0471142735.im1401s83.
- Zhang, X., et al. (2012). MicroRNA-21 Modulates the Levels of Reactive Oxygen Species Levels by Targeting SOD3 and TNF α . *Cancer Res* 72(18), 4707-13, 10.1158/0008-5472.can-12-0639.
- Zhang, Y., et al. (2013). Expression profiles of miRNAs in polarized macrophages. *Int J Mol Med* 31(4), 797-802, 10.3892/ijmm.2013.1260.
- Zhang, Z., et al. (2008b). Valproic acid attenuates inflammation in experimental autoimmune neuritis. *Cell Mol Life Sci* 65(24), 4055-65, 10.1007/s00018-008-8521-4.
- Zhang, Z. Y., et al. (2010). MS-275, an histone deacetylase inhibitor, reduces the inflammatory reaction in rat experimental autoimmune neuritis. *Neuroscience* 169(1), 370-7, 10.1016/j.neuroscience.2010.04.074.
- Zhao, H., and Chen, T. (2013). Tet family of 5-methylcytosine dioxygenases in mammalian development. *J Hum Genet* 58(7), 421-7, 10.1038/jhg.2013.63.
- Zheng, Q., et al. (2014). Valproic acid protects septic mice from renal injury by reducing the inflammatory response. *J Surg Res* 192(1), 163-9, 10.1016/j.jss.2014.05.030.
- Zhou, Y., et al. (2014). Chitinase 3-like 1 suppresses injury and promotes fibroproliferative responses in Mammalian lung fibrosis. *Sci Transl Med* 6(240), 240ra76, 10.1126/scitranslmed.3007096.
- Zhu, D., et al. (2013). MicroRNA-17/20a/106a modulate macrophage inflammatory responses through targeting signal-regulatory protein alpha. *J Allergy Clin Immunol* 132(2), 426-36.e8, 10.1016/j.jaci.2013.02.005.
- Zhu, Q., and Wani, A. A. (2010). Histone modifications: crucial elements for damage response and chromatin restoration. *J Cell Physiol* 223(2), 283-8, 10.1002/jcp.22060.